CHEMICAL REVIEWS

pubs.acs.org/CR

Review

Multicomponent Quantum Chemistry: Integrating Electronic and Nuclear−Electronic Orbital Method

Fabijan Pavošević, Tanner Culpitt, and Sharon Hammes-Schiffer*

Cite This: https://dx.doi.org/10.1021/acs.chemrev.9b00798

Read Online

ACCESS | Metrics & More | Article Recommendations

ABSTRACT: In multicomponent quantum chemistry, more than one type of particle is treated quantum mechanically with either density functional theory or wave function based methods. In particular, the nuclear-electronic orbital (NEO) approach treats specified nuclei, typically hydrogen nuclei, on the same level as the electrons. This approach enables the incorporation of nuclear quantum effects, such as nuclear delocalization, anharmonicity, zero-point energy, and tunneling, as well as non-Born−Oppenheimer effects directly into quantum chemistry calculations. Such effects impact optimized geometries, molecular vibrational frequencies, reaction paths, isotope effects, and dynamical simulations. Multicomponent density functional theory (NEO-DFT) and time-dependent DFT (NEO-TDDFT) achieve an optimal balance between computational efficiency and accuracy for computing ground and excited state properties, respectively. Multicomponent wave function based methods, such as the coupled cluster singles and doubles (NEO-CCSD) method for ground states and the equation-of-motion counterpart (NEO-EOM-CCSD) for excited states, attain similar accuracy without requiring any parametrization and can be systematically improved but are more computationally expensive. Variants of the orbital-optimized perturbation theory (NEO-OOMP2) method achieve nearly the accuracy of NEO-CCSD for ground states with significantly lower computational cost. Additional approaches for computing excited electronic, vibrational, and vibronic states include the delta self-consistent field (NEO-ΔSCF), complete active space SCF (NEO-CASSCF), and nonorthogonal configuration interaction methods. Multireference methods are particularly important for describing hydrogen tunneling processes. Other types of multicomponent systems, such as those containing electrons and positrons, have also been studied within the NEO framework. The NEO approach allows the incorporation of nuclear quantum effects and non-Born−Oppenheimer effects for specified nuclei into quantum chemistry calculations in an accessible and computationally efficient manner.

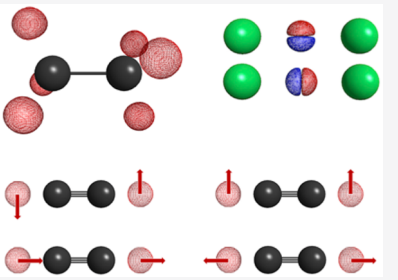

CONTENTS

Received: December 10, 2019

1. INTRODUCTION

Nuclear quantum effects play important roles in many aspects of chemistry, including zero-point energy, vibrationally excited states, hydrogen bonding interactions, proton transfer reactions, and hydrogen tunneling.[1−4] In addition, nonadiabatic effects between electrons and protons are known to be significant in proton-coupled electron transfer reactions,[5,6] which are essential for a wide range of chemical and biological processes.[7−9] In most quantum chemistry calculations, the Born−Oppenheimer separation is invoked between the electrons and the nuclei, and the electrons are assumed to respond instantaneously to the motions of the nuclei. In conventional Born−Oppenheimer methods, the nuclei move on the ground-state potential energy surface, which is generated by solving the electronic time-independent Schrödinger equation to obtain the energy at each nuclear configuration. In many cases, the nuclei are assumed to move classically on this potential energy surface, but the nuclei can also be propagated quantum mechanically on this potential energy surface using wave packet or path integral methods.

In the nuclear-electronic orbital (NEO) method,[10] specified nuclei are treated quantum mechanically on the same level as the electrons using molecular orbital techniques. In this case, the Born−Oppenheimer separation is invoked between the subsystem composed of the electrons and quantum nuclei and the subsystem composed of the other nuclei, which are referred to as "classical" for simplicity. Henceforth, we will not use quotation marks for the "classical" nuclei, with the understanding that they could also be treated quantum mechanically. The classical nuclei move on the potential energy surface obtained by solving the mixed nuclear-electronic time-independent Schrödinger equation. The NEO approach includes the nuclear delocalization and zero-point energy associated with the quantum nuclei during geometry optimizations, reaction paths, and dynamics. This approach also avoids the Born−Oppenheimer separation between the electrons and quantum nuclei. In addition, the NEO approach is useful for computing hydrogen/deuterium geometric and kinetic isotope effects. Both density functional theory (DFT)[11−21] and wave function based methods[10,22−26] have been developed within the NEO framework. Figure 1 depicts the protonic orbitals for the ethane molecule computed with the NEO-DFT method.

A variety of related multicomponent molecular orbital methods have been investigated. A fundamental non-Born−Oppenheimer molecular orbital theory was proposed by Thomas in 1969.[28] Significantly later, the nuclear orbital molecular orbital (NOMO)[29−35] and multicomponent molecular orbital (MCMO)[36−45] methods were developed by Tachikawa, Nakai, and co-workers independently and in parallel with the NEO method.[10] In many of these implementations, all nuclei, as well as all electrons, are treated quantum mechanically, requiring the removal of translations and rotations.[46,47] More recently, the NEO method was incorporated into the LOWDIN code as the any particle molecular orbital (APMO) method by Reyes.[48−50] The two-component quantum theory of atoms in molecules (TC-QTAIM) method[51] is also related to these other approaches. In addition to treating nuclei quantum mechanically, multicomponent molecular orbital methods have also been used to study systems containing positrons and muons.[24,52−61]

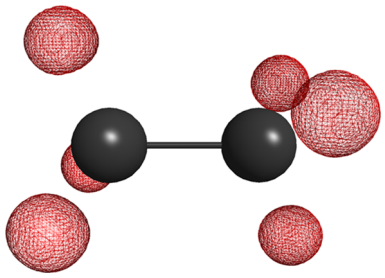

Figure 1. Protonic orbitals (red mesh) in ethane (C_2H_6) calculated with the NEO-DFT method. Reprinted with permission from ref 27. Copyright 2019 American Chemical Society.

A number of challenges arise with these types of multicomponent orbital methods. The multicomponent Hartree−Fock and second-order perturbation theory methods produce nonphysical, overlocalized proton densities[62,63] and thus are not reliable for computing molecular properties. Until recently, multicomponent configuration interaction and coupled cluster calculations have been limited to small systems,[31,37,46,64,65] no larger than diatomics, and have not been shown to provide accurate predictions of molecular properties depending on the proton densities. In an alternative approach, Adamowicz and co-workers have used explicitly correlated wave function methods to treat all electrons and all nuclei (or positrons) quantum mechanically on the same level.[66−76] These methods have been shown to be highly accurate for small molecular systems but are computationally expensive and therefore currently not easily applied to larger systems.

Various aspects of multicomponent DFT have also been explored over the past several decades. The Hohenberg−Kohn theorems[77] and the Kohn−Sham formalism[78] have been extended to multicomponent systems composed of two or more different types of particles.[47,79−81] Additional multicomponent DFT work has been conducted in the context of electron−positron systems.[82,83] Until recently, the multicomponent DFT methods have been limited by the lack of accurate electron−proton correlation functionals.[12,14,15,32,33,39,45] In terms of excited states, the multicomponent TDDFT formalism was developed by van Leeuwen and Gross to treat all electrons and nuclei quantum mechanically,[84,85] but such a fully quantum mechanical approach has not been applied to molecular systems.

This review summarizes the various NEO methods and their capabilities in describing ground and excited state properties of chemical systems. The other related multicomponent molec-

https://dx.doi.org/10.1021/acs.chemrev.9b00798
Chem. Rev. XXXX, XXX, XXX−XXX

ular orbital and DFT methods will be mentioned throughout this review to provide historical context and points of comparison as warranted. In addition to these approaches, alternative types of theoretical methods for describing nuclear quantum effects and nonadiabatic effects, such as path integral,[86−104] wavepacket,[105−109] multiconfigurational time-dependent Hartree (MCTDH),[110−112] and quantum Monte Carlo[113−117] methods, are also available. Given the vast literature associated with each of these methods, only brief summaries will be provided, with references to the relevant papers and reviews. A detailed discussion of each of these many methods is beyond the scope of this review, which by design is focused predominantly on the NEO approach.

The structure of this review is as follows. First the NEO Hamiltonian and the simplest form of the nuclear-electronic wave function, which is based on Hartree−Fock (HF) theory,[10] will be presented. Explicitly correlated wave function methods[62,63,118−120] lead to significant improvements over the NEO-HF method, which is not even qualitatively reasonable, but are significantly more computationally expensive. After this introductory material, the NEO-DFT[11−18,20] and multicomponent time-dependent DFT (TDDFT)[19,21] approaches for computing ground and excited state properties, respectively, will be discussed. The next section will illustrate the calculation of molecular vibrational frequencies[121,122] and diagonal Born−Oppenheimer corrections[27] within the NEO framework. Subsequently, the NEO coupled cluster,[23,25] orbital-optimized second-order perturbation theory,[26] and equation-of-motion[24] wave function based approaches, which also provide ground and excited state properties, will be presented. These approaches will be shown to be capable of providing accurate densities, energies, optimized geometries, and vibrational frequencies for chemical systems. In addition, an overview of other NEO approaches for computing excited states and hydrogen tunneling splittings,[123,124] including multireference methods,[10] will be provided for completeness.

Following this presentation of the underlying theories and capabilities, the NEO approach will be placed in the context of other types of theoretical methods for describing nuclear quantum effects and nonadiabatic effects, including path integral and wavepacket methods. In contrast to some of these alternative options, the NEO approach is designed to serve as a computationally practical method for incorporating nuclear quantum effects and non-Born−Oppenheimer effects for only specified nuclei. As for any computational method, the NEO methods will not be suitable for all applications, but they are particularly applicable to the wide range of important systems involving hydrogen bonding and hydrogen transfer. They are also easily applied to positronic systems, in which the positrons and electrons are treated quantum mechanically on the same level. The remaining challenges and future directions will be discussed at the end of this review.

2. FOUNDATIONS OF THE NUCLEAR-ELECTRONIC ORBITAL (NEO) METHOD

2.1. NEO Hamiltonian and Hartree−Fock Theory

In the NEO approach, the system is divided into N_e electrons, N_p quantum nuclei, and N_c classical nuclei.[10] Typically, at least two nuclei are treated classically to avoid complications with translations and rotations. For simplicity, here the quantum nuclei are assumed to be protons or deuterons, but the extension to other nuclei or to other quantum particles such as positrons is straightforward. The NEO Hamiltonian includes the standard electronic terms (i.e., the kinetic energy of the electrons, the attractive Coulomb interaction between the electrons and the classical nuclei, and the repulsive electron−electron Coulomb interaction), the analogous terms for the quantum nuclei, and the attractive Coulomb interaction between the electrons and the quantum nuclei. This Hamiltonian is expressed in atomic units as

$$H_{\mathrm{NEO}} = -\frac{1}{2}\sum_{i}^{N_e}\nabla_i^2 - \sum_{i}^{N_e}\sum_{A}^{N_c}\frac{Z_A}{|\mathbf{r}_i^e - \mathbf{r}_A^c|} + \sum_{i>j}^{N_e}\frac{1}{|\mathbf{r}_i^e - \mathbf{r}_j^e|} - \frac{1}{2m_p}\sum_{I}^{N_p}\nabla_I^2 + \sum_{I}^{N_p}\sum_{A}^{N_c}\frac{Z_A}{|\mathbf{r}_I^p - \mathbf{r}_A^c|} + \sum_{I>J}^{N_p}\frac{1}{|\mathbf{r}_I^p - \mathbf{r}_J^p|} - \sum_{I}^{N_p}\sum_{i}^{N_e}\frac{1}{|\mathbf{r}_i^e - \mathbf{r}_I^p|} \quad (1)$$

where $\mathbf{r}_i^e$ is the coordinate of electron i; $\mathbf{r}_I^p$ is the coordinate of proton I; $\mathbf{r}_A^c$ is the coordinate of the Ath classical nucleus; and m_p is the mass of a proton. The main goal of the NEO method is to solve the following mixed nuclear-electronic time-independent Schrödinger equation for fixed classical nuclei

$$H_{\mathrm{NEO}}\Psi(\mathbf{x}^e, \mathbf{x}^p; \mathbf{r}^c) = E_{\mathrm{NEO}}(\mathbf{r}^c)\Psi(\mathbf{x}^e, \mathbf{x}^p; \mathbf{r}^c) \quad (2)$$

where $\mathbf{x}^e$ and $\mathbf{x}^p$ are the collective spatial and spin coordinates of the electrons and quantum protons, respectively, and $\mathbf{r}^c$ is the collective spatial coordinate for the classical nuclei. The solution of the mixed nuclear-electronic time-dependent Schrödinger equation is another challenge that will be discussed later in this review.

The simplest NEO wave function is the NEO Hartree−Fock (NEO-HF) wave function,[10] which is expressed as

$$\Psi_{\mathrm{NEO\text{-}HF}}(\mathbf{x}^e, \mathbf{x}^p) = \Phi^e(\mathbf{x}^e)\Phi^p(\mathbf{x}^p) \quad (3)$$

Here $\Phi^e(\mathbf{x}^e)$ and $\Phi^p(\mathbf{x}^p)$ are Slater determinants composed of electronic and nuclear spin orbitals, respectively. In practice, the electronic and nuclear spatial orbitals are expanded in Gaussian basis sets. The NEO-HF energy is computed as the expectation value of H_{NEO} given in eq 1 with respect to the NEO-HF wave function given in eq 3 and can be expressed as

$$E_{\mathrm{NEO\text{-}HF}} = \sum_{i}^{N_e} h_i^e + \sum_{I}^{N_p} h_I^p + \frac{1}{2}\sum_{i}^{N_e}\sum_{j}^{N_e}(J_{ij}^e - K_{ij}^e) + \frac{1}{2}\sum_{I}^{N_p}\sum_{J}^{N_p}(J_{IJ}^p - K_{IJ}^p) - \sum_{I}^{N_p}\sum_{i}^{N_e}J_{iI}^{ep} \quad (4)$$

where h^e (h^p) denotes the electronic (protonic) contributions to the energy from the core Hamiltonian (i.e., the kinetic energy and interaction with the external potential); J^e (J^p) and K^e (K^p) are the electronic (protonic) Coulomb and exchange energies, respectively; and $-J^{ep}$ is the electron−proton Coulomb energy. These terms are defined according to standard quantum chemistry definitions, and the subscript indices denote the electronic and protonic spin orbitals.[125] Note that the repulsion term between classical nuclei is omitted from eq 4 for simplicity. Because the nuclear−nuclear exchange terms are negligible in molecular systems, and the lowest energy state corresponds to one nucleus per orbital,

https://dx.doi.org/10.1021/acs.chemrev.9b00798
Chem. Rev. XXXX, XXX, XXX−XXX

Table 1. Electronic and Protonic Coulomb and Exchange Energies and MP2 Correlation Energy Corrections for Acetylene, Ethylene, and Ethane[a]

	J^e	J^p	J^{ep}	K^e	K^p	$E^{ee(2)}$	$E^{pp(2)}$	$E^{ep(2)}$
C_2H_2	54.675	0.158	10.892	4.530	6.20×10^{-10}	−0.265	-1.37×10^{-09}	−0.0067
C_2H_4	63.785	1.333	24.371	5.166	$<1.0 \times 10^{-10}$	−0.288	-1.11×10^{-07}	−0.0136
C_2H_6	73.050	3.530	39.345	5.751	1.57×10^{-08}	−0.318	-4.03×10^{-07}	−0.0204

[a] $J^e = \frac{1}{2}\sum_{i\neq j}^{N_e} J_{ij}^e$, $K^e = \frac{1}{2}\sum_{i\neq j}^{N_e} K_{ij}^e$, $J^{ep} = \sum_i^{N_e}\sum_I^{N_p} J_{iI}^{ep}$, and J^p and K^p are defined analogously, as given in eq 4. The MP2 correlation energy corrections given in eq 6 are defined in ref 22. All energies are given in Hartree.

neglecting the effects of nuclear spin within the NEO framework is a well-justified approximation.

The NEO-HF energy is optimized variationally by varying the coefficients of the basis functions in the electronic and nuclear spatial orbitals, leading to Hartree−Fock−Roothaan equations for the electrons and quantum protons

$$\mathbf{F}^e\mathbf{C}^e = \mathbf{S}^e\mathbf{C}^e\boldsymbol{\varepsilon}^e$$
$$\mathbf{F}^p\mathbf{C}^p = \mathbf{S}^p\mathbf{C}^p\boldsymbol{\varepsilon}^p \quad (5)$$

Here $\mathbf{F}^e$, $\mathbf{C}^e$, $\mathbf{S}^e$, and $\boldsymbol{\varepsilon}^e$ are the electronic Fock matrix, orbital coefficient matrix, overlap matrix, and orbital energy matrix, respectively.[10,125] The protonic matrices are defined analogously. These equations are solved iteratively until self-consistency to produce the ground-state mixed nuclear-electronic wave function, which can be used to calculate the total NEO-HF energy in eq 4.

Over the past decade, even-tempered nuclear basis sets[16,17,21] have been developed for the quantum nuclei in terms of the traditional s, p, d, and higher angular momentum Gaussian basis functions used for electrons.[126] Most of the calculations presented in this review were performed with the 8s8p8d8f even-tempered nuclear basis set with exponents spanning the range from $2\sqrt{2}$ to 32. These Gaussian basis sets allow the usage of the efficient integral codes developed for electronic structure packages. Alternatively, more compact nuclear basis sets with exponents fit to relevant data sets can be used to optimize efficiency and accuracy.[10] Moreover, current applications assume that the electronic and nuclear basis functions associated with a given hydrogen atom are centered at the same position,[10] although this restriction could be removed. In general, the basis function centers for all quantum nuclei should be optimized variationally within the NEO framework. Typically, this optimization of the basis function centers occurs as part of the self-consistent field procedure (i.e., as an outer loop when solving eq 5). Alternative schemes are also possible, such as placing the basis function centers at the positions corresponding to the expectation values of the quantum protons.

Although the NEO-HF method is straightforward to implement, it does not provide even qualitatively reasonable proton densities and energies because of the inadequate treatment of electron−proton correlation, which is fundamentally different from electron−electron correlation.[118,120] Electron−proton correlation is particularly important because the electron−proton Coulomb interaction is attractive rather than repulsive. In contrast, proton−proton correlation is negligible in molecular systems because the protons are predominantly localized.[127] Because of the critical importance of electron−proton correlation, the proton densities are highly overlocalized, and other properties, such as vibrationally averaged geometries, energies, and frequencies are unreliable with the NEO-HF method. For this reason, methods that are effective in electronic structure are not always effective within the NEO framework.

Because the NEO-HF method does not produce accurate proton densities, the NEO-HF wave function is not a suitable reference for perturbative methods. In particular, the NEO-MP2 method,[22] which is based on second-order perturbation theory, does not lead to noticeable improvements in the proton densities. The NEO-MP2 energy has the form

$$E_{\text{NEO-MP2}} = E_{\text{NEO-HF}} + E^{pp(2)} + E^{ee(2)} + E^{ep(2)} \quad (6)$$

where $E^{pp(2)}$, $E^{ee(2)}$, and $E^{ep(2)}$ correspond to the second-order energy corrections for proton−proton, electron−electron, and electron−proton correlation, respectively.[22] These correlation energies are defined in more detail in Section 5. Several other methods[30,31,36,46,49] that are equivalent or nearly equivalent to NEO-HF and NEO-MP2 suffer from the same problems. Unfortunately, these methods do not yield accurate proton densities, rendering them unreliable for computing molecular properties. In particular, geometric isotope effects, which rely on a delicate balance between the hydrogen stretch and bend frequencies, cannot be reliably predicted with the NEO-HF or NEO-MP2 approaches.[38,39,48,49,128−131]

The proton−proton exchange and correlation energies are negligible in molecular systems because the protons are well-localized.[48,127] To illustrate this property, the electronic and protonic Coulomb and exchange contributions to the NEO-HF energy, as well as the MP2 electron−electron, proton−proton, and electron−proton correlation energy corrections,[22] have been calculated for a series of representative molecules. This series consists of acetylene, ethylene, and ethane, which include two, four, and six quantum protons, respectively. These molecules are considered to be representative because of the different spatial arrangements of the quantum protons in each system and the proximity of the quantum protons for ethylene and ethane (Figure 1). As shown in Table 1, the protonic exchange contributions to the energy, as well as the proton−proton MP2 energy corrections, are negligible for all three molecules. These results indicate that proton−proton exchange and correlation energies are many orders of magnitude smaller than electron−electron exchange and correlation and electron−proton correlation energies. Note that the NEO-MP2 method does not provide accurate proton densities, which would impact the quantitative proton−proton correlation contribution.

For predominantly electronically adiabatic systems, the standard grid-based approach provides accurate proton densities and energies. In the standard grid-based approach for a single quantum proton with all other nuclei fixed, the hydrogen is positioned at points comprising a three-dimensional grid, and the energy at each point is computed by solving the time-independent electronic Schrödinger equation at the appropriate level of theory. Subsequently, the proton

https://dx.doi.org/10.1021/acs.chemrev.9b00798
Chem. Rev. XXXX, XXX, XXX−XXX

vibrational wave functions and energies are determined by solving the three-dimensional time-independent Schrödinger equation for the proton moving on this potential energy surface using the Fourier grid Hamiltonian (FGH) method.[132,133] This type of grid-based calculation serves as a numerically accurate reference for testing the NEO methods for predominantly electronically adiabatic systems, where the electrons respond nearly instantaneously to the motion of the proton. The NEO-HF approach is much less accurate than this grid-based approach because the electronic and nuclear wave functions are determined within a mean field treatment for the NEO-HF approach, in contrast to the grid-based approach, where the electrons respond fully to the proton position at each grid point.

2.2. Explicitly Correlated Wave Functions for Quantum Protons and Positrons

Explicitly correlated methods using a wave function ansatz that includes Gaussian-type geminal functions[134] within the SCF procedure provide a much more accurate description of electron−proton correlation. The following explicitly correlated wave function ansatz has been investigated within the NEO framework[118,119]

$$\Psi_{\text{NEO-XCHF}}(\mathbf{x}^{\text{e}}, \mathbf{x}^{\text{p}}) = \Phi^{\text{e}}(\mathbf{x}^{\text{e}})\Phi^{\text{p}}(\mathbf{x}^{\text{p}})\left[1 + \sum_{i=1}^{N_{\text{e}}}\sum_{I=1}^{N_{\text{p}}}\sum_{k=1}^{N_{\text{gem}}} b_k e^{-\gamma_k|\mathbf{r}_i^{\text{e}}-\mathbf{r}_I^{\text{p}}|^2}\right] \quad (7)$$

Here the N_{gem} Gaussian-type geminal functions depend on the electron−proton distance, as well as the parameters b_k and γ_k, which are determined for small model systems and remain constant during the variational procedure.[62,63,118−120] In the NEO explicitly correlated Hartree−Fock (NEO-XCHF) approach,[118,119] the NEO-XCHF energy is computed as the expectation value of H_{NEO} given in eq 1 with respect to the NEO-XCHF wave function given in eq 7. This energy is optimized variationally with respect to the coefficients of the basis functions in the electronic and nuclear orbitals within the Slater determinants, leading to two sets of equations corresponding to the electrons and quantum protons that must be solved iteratively to self-consistency. In the reduced XCHF approach, denoted NEO-RXCHF,[57,62] only specified electronic orbitals are explicitly correlated to the nuclear orbitals to enhance the computational efficiency. Moreover, for the systems studied, the NEO-RXCHF method was found to be more accurate than the NEO-XCHF method, which correlates all electronic orbitals to the nuclear orbitals in the same manner using the same geminal parameters. By explicitly correlating only the relevant electronic orbitals to the nuclear orbitals, the RXCHF method ensures that the geminal parameters and explicitly correlated wave function are optimized to produce an accurate description of the key short-ranged electron−nucleus interactions.

Although the NEO-RXCHF approach is more accurate than the NEO-XCHF approach, the proton densities are still overlocalized, particularly for the off-axis bending modes.[62,63] Moreover, the NEO-XCHF and RXCHF approaches require the calculation of up to six-particle integrals for systems with multiple quantum protons and therefore are computationally prohibitive for large molecular systems. The accuracy of these approaches may be enhanced by allowing the electronic atomic basis functions or the geminal parameters to depend on the proton coordinate, thereby leading to more complex and expensive integrals that may not be analytically computable. Another option is to use a product rather than a sum of Gaussian-type geminals, which would lead to higher-dimensional integrals that would also be computationally expensive (i.e., the dimension of the integrals would be equivalent to the number of quantum particles). Other explicitly correlated methods have been applied to multicomponent systems in which all nuclei as well as all electrons are treated quantum mechanically.[66−76,117] In some cases, these methods produce accurate results for small systems, but typically they are not computationally tractable for larger molecular systems.

The NEO-XCHF approach was more successful in applications to positronic molecular systems because the electron and positron masses are identical, avoiding the substantial mass disparity inherent to treating electrons and protons on equal footing. In these applications, the electrons and positron are treated quantum mechanically on the same level, but the nuclei are fixed. Applications to positronium hydride (PsH), positron lithium (e^+Li), lithium positride (LiPs), and positron-lithium hydride (e^+LiH) illustrated that the NEO-XCHF approach provides accurate average contact densities, electron−positron contact densities, two-photon annihilation rates, and electronic and positronic single-particle densities.[54,55,57] Moreover, this approach predicts reasonably accurate binding energies of a positron to lithium, beryllium, sodium, and magnesium, as well as the electron−positron annihilation rates for these systems.[60] Several highly accurate but computationally expensive methods, such as the stochastic variational method, have been applied successfully to positronic systems.[68,71,73,135−141] However, these approaches are not easily extended to larger systems due to the computational expense. The NEO-XCHF approach offers a viable alternative.

3. MULTICOMPONENT DENSITY FUNCTIONAL THEORY (DFT) AND TIME-DEPENDENT DENSITY FUNCTIONAL THEORY (TDDFT)

3.1. NEO-DFT

Multicomponent DFT,[11,13,47,79−81,142] which refers to DFT with more than one type of quantum particle, has been found to achieve an especially effective balance between accuracy and computational tractability. Here the two types of particles are assumed to be electrons and protons, but the extension to other types of particles is straightforward. The Hohenberg−Kohn theorems[77] have been derived for multicomponent systems.[79] In this formulation, the total energy is a functional of the one-particle densities associated with the different types of quantum particles (i.e., the one-particle electron and proton densities). The Kohn−Sham formalism[78] has also been developed for multicomponent systems,[11,13,47,80] treating the reference system as the product of electronic and nuclear Slater determinants composed of Kohn−Sham orbitals. In this case, the total energy is expressed as

$$E[\rho^{\text{e}}, \rho^{\text{p}}] = E_{\text{ext}}[\rho^{\text{e}}, \rho^{\text{p}}] + E_{\text{ref}}[\rho^{\text{e}}, \rho^{\text{p}}] + E_{\text{exc}}[\rho^{\text{e}}] + E_{\text{pxc}}[\rho^{\text{p}}] + E_{\text{epc}}[\rho^{\text{e}}, \rho^{\text{p}}] \quad (8)$$

Here, $E_{\text{ext}}[\rho^{\text{e}}, \rho^{\text{p}}]$ is the interaction of the two densities with the external potential created by the classical nuclei; $E_{\text{ref}}[\rho^{\text{e}}, \rho^{\text{p}}]$ includes the noninteracting kinetic energies of the electrons and quantum protons, as well as the electron−electron, electron−proton, and proton−proton classical Coulomb

https://dx.doi.org/10.1021/acs.chemrev.9b00798
Chem. Rev. XXXX, XXX, XXX−XXX

energies; and the last three terms correspond to the electron−electron exchange-correlation functional, the proton−proton exchange-correlation functional, and the electron−proton correlation functional.

Application of the variational principle leads to two sets of Kohn−Sham equations for the electrons and quantum protons[12]

$$\left(-\frac{1}{2}\nabla^2 + v^{\mathrm{e}}_{\mathrm{eff}}(\mathbf{r}^{\mathrm{e}}_1)\right)\psi^{\mathrm{e}}_i = \varepsilon^{\mathrm{e}}_i\psi^{\mathrm{e}}_i$$
$$\left(-\frac{1}{2m_{\mathrm{p}}}\nabla^2 + v^{\mathrm{p}}_{\mathrm{eff}}(\mathbf{r}^{\mathrm{p}}_1)\right)\psi^{\mathrm{p}}_I = \varepsilon^{\mathrm{p}}_I\psi^{\mathrm{p}}_I \tag{9}$$

where the effective potentials contain terms based on the functional derivatives of terms in eq 8 with respect to either the electron or the proton density. Here $\psi^{\mathrm{e}}_i(\mathbf{r}^{\mathrm{e}}_1)$ and $\psi^{\mathrm{p}}_I(\mathbf{r}^{\mathrm{p}}_1)$ are the electron and proton Kohn−Sham spatial orbitals, respectively, associated with the single-particle densities $\rho^{\mathrm{e}}(\mathbf{r}^{\mathrm{e}}_1) = 2\sum_{i=1}^{N_{\mathrm{e}}/2}|\psi^{\mathrm{e}}_i(\mathbf{r}^{\mathrm{e}}_1)|^2$ and $\rho^{\mathrm{p}}(\mathbf{r}^{\mathrm{p}}_1) = \sum_{I=1}^{N_{\mathrm{p}}}|\psi^{\mathrm{p}}_I(\mathbf{r}^{\mathrm{p}}_1)|^2$. Analogous to the NEO-HF method discussed above, the electronic and nuclear spatial orbitals are expressed as linear combinations of electronic and nuclear basis functions, respectively, and the two sets of Kohn−Sham equations are solved iteratively to self-consistency.[12] These Kohn−Sham equations are written for a restricted closed-shell electron system with each spatial electronic orbital doubly occupied and a high-spin proton system with each spatial protonic orbital singly occupied. These equations are easily extended to open-shell electron systems.

The implementation of NEO-DFT requires an electron−electron exchange-correlation functional, a proton−proton exchange-correlation functional, and an electron−proton correlation functional. Within the NEO framework, the electron−electron exchange-correlation functional is defined identically to the conventional electronic functionals.[13] Thus, any electronic functional can be used within the NEO framework.[15,18] As discussed in Section 2.1, the proton−proton exchange and correlation energies are negligible in molecular systems because of the spatial localization of the protons. As a result, the proton−proton exchange-correlation functional is simply equated to the diagonal Hartree−Fock exchange terms to eliminate self-interaction error, although in practice all proton−proton exchange terms may be included. The major challenge within this field has been the development of electron−proton correlation functionals. Previous attempts that treated this term as a correction to the energy after the SCF procedure[32,39] were not able to produce even qualitatively accurate proton densities and therefore were unreliable. Electron−proton correlation functionals based on the explicitly correlated nuclear-electronic wave function[12,14,15] given in eq 7 were included during the SCF procedure and led to improved proton densities for the hydrogen stretching modes. However, these functionals did not provide sufficiently accurate proton densities for the hydrogen bending modes[120,143] and were computationally expensive.

Recently, a series of electron−proton correlation functionals based on a multicomponent extension[16−18,20] of the Colle−Salvetti formalism[144] were developed and shown to produce accurate proton densities, energies, and optimized geometries in a computationally efficient manner. These functionals have been denoted epc17,[16,17] epc18,[18] and epc19[20] based on the year in which each one was developed. Previously, this formalism produced the well-known Lee−Yang−Parr (LYP) electron−electron correlation functional,[145] but several essential differences were required for its application to electron−proton correlation. The multicomponent Colle−Salvetti formulation started with the following multicomponent electron−proton wave function ansatz[16]

$$\Psi(\mathbf{x}^{\mathrm{e}}, \mathbf{x}^{\mathrm{p}}) = \Psi^{\mathrm{e}}_{\mathrm{FCI}}(\mathbf{x}^{\mathrm{e}})\Psi^{\mathrm{p}}_{\mathrm{FCI}}(\mathbf{x}^{\mathrm{p}})\prod_{i\in N_{\mathrm{e}}, I\in N_{\mathrm{p}}}[1 - \varphi(\mathbf{r}^{\mathrm{e}}_i, \mathbf{r}^{\mathrm{p}}_I)] \tag{10}$$

where the correlation factor is

$$\varphi(\mathbf{r}^{\mathrm{e}}_i, \mathbf{r}^{\mathrm{p}}_I) = \exp[-\beta^2(\mathbf{R})r^2][1 - \xi(\mathbf{R})(1 - r)] \tag{11}$$

Here $\mathbf{R} = \mathbf{r}^{\mathrm{p}}_I$, $r = |\mathbf{r}^{\mathrm{e}}_i - \mathbf{r}^{\mathrm{p}}_I|$, and $\beta(\mathbf{R})$ is the inverse correlation length associated with electron−proton correlation. The subscript FCI for the wave functions given on the right-hand side of eq 10 denotes full configuration interaction for a given type of particle, including all exchange and correlation effects between particles of this type but only including a mean-field Coulomb interaction with the other type of particle.

An important aspect of these electron−proton correlation functionals is that the inverse correlation length depends on both the electron and proton densities. The analogous LYP electronic correlation functionals[145] assumed that the inverse correlation length was the inverse Wigner−Seitz radius for the electron: $\beta(\mathbf{R}) \propto [\rho^{\mathrm{e}}(\mathbf{R})]^{1/3}$. For the epc17[16,17] and epc19[20] functionals, the inverse correlation length was defined as the geometric mean of the inverse Wigner−Seitz radii for the electron and the proton: $\beta(\mathbf{R}) \propto [\rho^{\mathrm{e}}(\mathbf{R})]^{1/6}[\rho^{\mathrm{p}}(\mathbf{R})]^{1/6}$. Following this assumption, $\xi(\mathbf{R})$ was expressed in terms of $\beta(\mathbf{R})$, followed by a Taylor series expansion of the correlation energy, truncation of this expansion, and several other approximations described elsewhere.[16]

The epc17 functionals retained only terms depending on the electron−proton pair density and therefore are considered to be a local density approximation (LDA) type of functional. These functionals have the following form:[16]

$$E_{\mathrm{epc}}[\rho^{\mathrm{e}}, \rho^{\mathrm{p}}] = -\int \mathrm{d}\mathbf{r}\frac{\rho^{\mathrm{e}}(\mathbf{r})\rho^{\mathrm{p}}(\mathbf{r})}{a - b[\rho^{\mathrm{e}}(\mathbf{r})]^{1/2}[\rho^{\mathrm{p}}(\mathbf{r})]^{1/2} + c\rho^{\mathrm{e}}(\mathbf{r})\rho^{\mathrm{p}}(\mathbf{r})} \tag{12}$$

The three parameters a, b, and c were determined by fitting to the proton densities and energies of HCN and FHF^-. The epc17-1 functional[16] focused on reproducing accurate proton densities but does not provide accurate energies. The epc17-2 functional[17] was parametrized to reproduce reasonably accurate proton densities and energies, although the proton densities are not as accurate as those obtained with the epc17-1 functional.

Previous multicomponent functionals based on the Colle−Salvetti formulation assumed that $\beta(\mathbf{R}) \propto [\rho^{\mathrm{e}}(\mathbf{R})]^{1/3}$, identical to the form used to develop the analogous LYP electronic functionals.[32,33,39,43] This assumption is not physically reasonable for multicomponent functionals because the correlation length between two different types of particles should depend on both densities. Moreover, typically these previous functionals were not included in the SCF procedure but rather were added as corrections to the energies.[32,39] In this case, the proton densities are the same as the NEO-HF proton densities and are much too localized. If the proton

https://dx.doi.org/10.1021/acs.chemrev.9b00798
Chem. Rev. XXXX, XXX, XXX−XXX

densities are nonphysical, other properties such as vibrationally optimized geometries, molecular vibrational frequencies, and vibronic couplings are not reliable.

In contrast, the epc17 functional is included in the SCF procedure and leads to dramatic improvement in the proton densities.[16] This improvement is illustrated by NEO calculations for FHF^-, where the proton and all electrons are treated quantum mechanically with fixed heavy nuclei (Figure 2 and Figure 3). The grid-based reference proton density

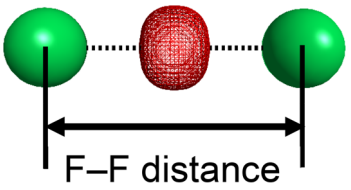

Figure 2. Protonic orbital (red mesh) in the FHF^- molecule calculated with the grid-based method. The fluorine atoms are shown in green, and the F–F distance is indicated.

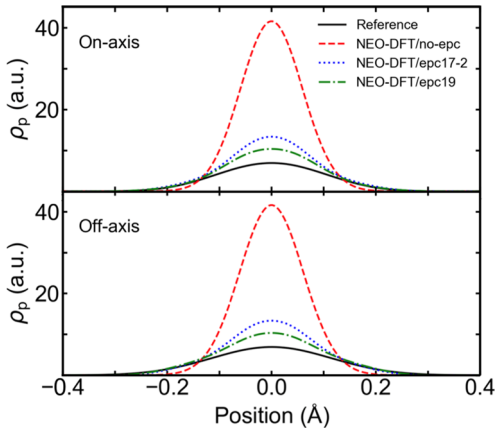

Figure 3. On-axis (top) and off-axis (bottom) proton density for the FHF^- molecule calculated with the grid-based reference (solid black curve), NEO-DFT/no-epc (dashed red curve), NEO-DFT/epc17-2 (dotted blue curve), and NEO-DFT/epc19 (dashed-dotted green curve) methods. The quantum proton basis functions are positioned at the origin, and the fluorine atoms are positioned at ±1.1507 Å. On-axis refers to the slice of the proton density along the axis connecting the heavy nuclei, while off-axis refers to the slice perpendicular to this axis, crossing through the midpoint between the two heavy nuclei. The B3LYP electronic functional, def2-QZVP electronic basis set, and 8s8p8d nuclear basis set were used to compute these densities. Data obtained from ref 20.

(black solid curve in Figure 3) was obtained by the FGH method described above using DFT to compute the energies on the three-dimensional grid.[133] The NEO-DFT/no-epc method (red dashed curve) includes electronic exchange-correlation with the B3LYP functional[145−147] but does not include any electron−proton correlation, and the NEO-DFT/epc17-2 method (blue dotted curve) includes electron−proton correlation as well as electronic exchange−correlation. The NEO-HF proton densities are nearly identical to the NEO-DFT/no-epc proton densities and therefore are not included in Figure 3. All of these proton densities are normalized in three-dimensional space. This figure illustrates that the proton density computed without electron−proton correlation is highly overlocalized and that the inclusion of electron−proton correlation significantly delocalizes the proton density, leading to much better agreement with the grid-based reference. Similar behavior was observed for the HCN molecule. These differences are quantified by the root-mean-square deviation (RMSD) of the proton density provided by each NEO method relative to the proton density obtained with the grid-based reference method. The average of the RMSDs for the proton densities associated with the HCN and FHF^- molecules is provided in Table 2.

Table 2. Mean Unsigned Error (MUE) of Calculated Proton Affinities with Respect to Experimentally Determined Values, RMSD of Proton Density Calculated with NEO Method versus FGH Reference, and Equilibrium F−F Distance for FHF^-[a]

method	proton affinity MUE[b]	proton density RMSD[c]	equilibrium F−F distance[d]
NEO-DFT/no-epc	0.78	0.775	2.3308
NEO-DFT/epc17-2	0.06	0.261	2.3206
NEO-DFT/epc19	0.06	0.170	2.3302
FGH[e]	N.A.	N.A.	2.3185
DFT	0.05	N.A.	2.2978

[a]The calculations reported in this table used the B3LYP electronic functional, the def2-QZVP electronic basis set, and the 10s10p10d nuclear basis set, with the exception of the proton density RMSD calculations, which used the 8s8p8d nuclear basis set. [b]The MUEs for the proton affinities are in units of eV. The 23 molecules studied are NH_3, CH_3NH_2, $CH_3CH_2NH_2$, $CH_3CH_2CH_2NH_2$, $(CH_3)_2NH$, $(CH_3)_3N$, CN^-, HS^-, NOO^-, $HCOO^-$, CH_3COO^-, $CH_3CH_2COO^-$, $CH_3CH_2CH_2COO^-$, $CH_3CH_2CH_2CH_2COO^-$, CH_3COCOO^-, CH_2FCOO^-, CHF_2COO^-, CF_3COO^-, CH_2ClCOO^-, $CH_2ClCH_2COO^-$, $C_6H_5O^-$, $C_6H_5COO^-$, and $C_6H_5NH_2$. Data from ref 17. [c]The RMSD was computed as the square root of the average of the squares of the differences between the NEO-DFT and FGH proton density at each grid point of the three-dimensional grid. For FHF^-, the F atoms are located at ±1.1507 Å, and the cubic grid ranges from −0.5610 Å to 0.5984 Å along and perpendicular to the F−F axis. For HCN, the carbon and nitrogen atoms are positioned at 0.0 Å and −1.1463 Å, respectively, and the cubic grid ranges from 0.3245 to 1.8652 Å along the C−N axis and from −0.7455 to 0.7952 Å perpendicular to this axis. The reported RMSD value is the average RMSD obtained for the HCN and FHF^- systems given in atomic units. Data from ref 20. [d]The equilibrium F−F distances are in units of Å. Data from ref 20. [e]The FGH grid method serves as a benchmark reference for the calculated equilibrium F−F distances.

In addition to the proton densities, the NEO-DFT method in conjunction with the epc17 functional provides accurate proton affinities.[17] The proton affinities were computed for a set of 23 diverse molecules, including amines, aromatics, inorganics, and carboxylates. The proton affinity of a molecule A was determined from the difference between E_A, which is the energy of A computed with conventional DFT, and E_{AH^+}, which is the energy of AH^+ computed with NEO-DFT treating only the additional proton quantum mechanically (Figure 4). The constant 5/2 RT, where T = 298 K, is added to this energy difference to account for the conversion from energy to enthalpy and the change in translational energy upon protonation of A. Thus, the proton affinity is calculated from the following expression:[17]

$$\mathrm{PA(A)} = E_A - E_{AH^+} + \frac{5}{2}RT \tag{13}$$

The geometries of both A and AH^+ were optimized variationally for these calculations, and the differences in the

https://dx.doi.org/10.1021/acs.chemrev.9b00798
Chem. Rev. XXXX, XXX, XXX−XXX

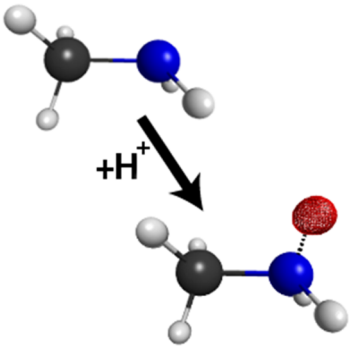

Figure 4. Schematic representation of the calculation of the proton affinity for methylamine within the NEO framework, where the protonic orbital is depicted as red mesh, and the carbon, nitrogen, and hydrogen atoms are depicted as gray, blue, and white spheres, respectively. Reprinted with permission from ref 17. Copyright 2017 American Chemical Society.

vibrational energies associated with the nuclei other than the quantum proton for these two molecules were assumed to be negligible. This assumption was tested and shown to be reasonable within the desired level of accuracy.[23] The mean unsigned error (MUE) compared to experiment was 0.78 eV for NEO-DFT/no-epc and 0.06 eV for NEO-DFT/epc17-2, indicating a significant improvement upon inclusion of electron−proton correlation. Note that the epc17-2 functional was parametrized to reproduce qualitatively reasonable proton densities and energies for HCN and FHF^-.[17] Without further parametrization, this functional produced accurate proton affinities for the other 22 molecules in this set. Although conventional electronic DFT with harmonic zero-point energy corrections produces a similar MUE of 0.05 eV,[17] this conventional approach does not include anharmonic effects, which are important in other contexts discussed below. In related work, the APMO method was combined with second-order propagator theory to compute accurate proton affinities,[35,148−152] but this approach does not provide accurate proton densities and therefore is not easily used to compute other molecular properties.

Another advantage of the NEO approach over conventional electronic DFT is that proton delocalization, anharmonicity, and zero-point energy are included in geometry optimizations. To illustrate this effect, the equilibrium F−F distance in FHF^- was determined by minimizing the NEO-DFT energy. The inclusion of nuclear quantum effects of the proton increases the equilibrium F−F distance by ∼0.02 Å compared to the equilibrium distance obtained with conventional electronic DFT.[17] The NEO-DFT/no-epc method overestimates this distance, and the NEO-DFT/epc17-2 method produces a distance within 0.01 Å of the grid-based reference value.

As discussed above, the derivation of the epc17 functional was based on the assumption that the inverse correlation length is proportional to the geometric mean of the inverse Wigner−Seitz radii of the electron and the proton. To test the sensitivity of this approach to the form of the inverse correlation length, the epc18 functionals[18] were developed with the assumption that the inverse correlation length was the arithmetic mean of the inverse Wigner−Seitz radii of the electron and the proton: $\beta(\mathbf{R}) \propto [\rho^e(\mathbf{R})]^{1/3} + [\rho^p(\mathbf{R})]^{1/3}$.[18] After suitable parametrization, the epc18-1 and epc18-2 functionals are of similar accuracy as the analogous epc17-1 and epc17-2 functionals for the proton densities and proton affinities.[18] Thus, the specific form of the inverse correlation length is not critical, as long as it depends on both the electron and proton densities. Because the epc17 functionals are more straightforward to implement, the epc17-2 functional has been used most extensively. Both the epc17 and epc18 functionals are based on the local density approximation (LDA) in the sense that they depend on only the local electron and proton densities.

The more recently developed epc19 functional depends on the electron and proton density gradients, as well as the densities, and is a type of generalized gradient approximation (GGA) functional.[20] This functional was obtained by following the formalism described above for the epc17 functional and retaining two additional terms that depend on the electron and proton density gradients. The epc19 functional has the following form:

$$E_{epc}[\rho^e, \rho^p, \nabla\rho^e, \nabla\rho^p] = -\int d\mathbf{r} \frac{\rho^e(\mathbf{r})\rho^p(\mathbf{r})}{a - b[\rho^e(\mathbf{r})]^{1/2}[\rho^p(\mathbf{r})]^{1/2} + c\rho^e(\mathbf{r})\rho^p(\mathbf{r})} \times \left\{1 - d\left(\frac{[\rho^e(\mathbf{r})\rho^p(\mathbf{r})]^{-1/3}}{(1+m_p)^2}\left[m_p^2\frac{\nabla^2\rho^e(\mathbf{r})}{\rho^e(\mathbf{r})} - 2m_p\frac{\nabla\rho^e(\mathbf{r})\cdot\nabla\rho^p(\mathbf{r})}{\rho^e(\mathbf{r})\rho^p(\mathbf{r})} + \frac{\nabla^2\rho^p(\mathbf{r})}{\rho^p(\mathbf{r})}\right]\right)\exp\left[\frac{-k}{[\rho^e(\mathbf{r})\rho^p(\mathbf{r})]^{1/6}}\right]\right\} \quad (14)$$

This functional includes two additional parameters, d and k, compared to the epc17 functional, leading to a total of five parameters, and it depends on the mass of the quantum nucleus m_p. The epc19 functional was shown to provide more accurate proton densities and similarly accurate energies compared to the epc17-2 functional.[20] The improved proton density for FHF^- is depicted in Figure 3 (green dashed-dotted curve). The MUE for the proton affinities of the set of 23 molecules discussed above is identical for the epc17-2 and epc19 functionals (Table 2).[20] The equilibrium F−F distance for FHF^- obtained with the epc19 functional deviates slightly more from the grid-based reference value compared to the distance obtained with the epc17-2 functional, but the differences between these distances are very small.[20]

Furthermore, although the epc19 functional was parametrized for hydrogen, it was also shown to provide accurate densities and energies for deuterium without further parametrization. The NEO-DFT method in conjunction with either the epc17-2 or epc19 functional can be used to compute geometric isotope effects. For example, the decrease in the equilibrium F−F distance upon deuteration of FHF^- was determined to be 0.0055 Å, 0.0021 Å, and 0.0008 Å when computed with the grid-based reference method, the NEO-DFT/epc17-2 method, and the NEO-DFT/epc19 method, respectively.[20] Given that the proton densities computed with NEO-DFT/epc19 are significantly more accurate than those computed with NEO-DFT/epc17-2 (Figure 3 and Table 2), the slightly more accurate geometric isotope effect obtained with NEO-DFT/epc17-2 appears to be fortuitous. Moreover, the differences in these equilibrium F−F distances are quite small and arise from a subtle balance between the stretch and bend modes for hydrogen and deuterium. More extensive parametrization of the epc19 functional for hydrogen and/or deuterium could lead to further improvements.

A number of fundamental mathematical properties of the exact universal multicomponent functional have been

https://dx.doi.org/10.1021/acs.chemrev.9b00798
Chem. Rev. XXXX, XXX, XXX−XXX

derived.[13] Although the epc17, epc18, and epc19 functionals were formulated from a wave function ansatz that satisfies some of the limiting conditions of the exact functional, the approximate parametrized form was designed to describe physical properties of molecular systems. The analysis of the properties of these functionals and the development of functional forms that satisfy the conditions for the exact universal functional are potential future directions.

Electron−electron correlation and electron−proton correlation have been found to be predominantly uncoupled within the NEO framework,[15] allowing the independent development of electronic exchange-correlation functionals and electron−proton correlation functionals. The epc17, epc18, and epc19 functionals[16−18,20] were parametrized and tested in conjunction with the B3LYP electronic exchange-correlation functional.[145−147] To test the transferability of these electron−proton correlation functionals, the proton affinities were computed with a series of seven other electronic exchange-correlation functionals in conjunction with the epc17-2 and epc18-2 functionals (Figure 5).[18] For both of

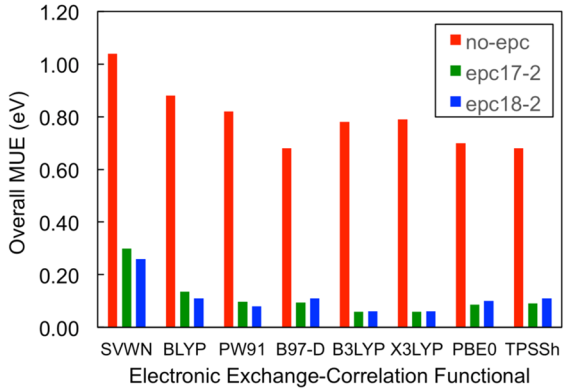

Figure 5. MUEs for the calculated proton affinities for the set of 23 molecules given in Table 2 relative to the experimental values. The proton affinities were calculated with the NEO-DFT/no-epc (red), NEO-DFT/epc17-2 (green), and NEO-DFT/epc18-2 (blue) methods using eight different electronic exchange-correlation functionals. Reprinted with permission from ref 18. Copyright 2018 American Institute of Physics.

these electron−proton correlation functionals, the MUE for the computed proton affinities for the set of 23 diverse molecules relative to the experimental values is similar for all electronic functionals studied.[18] An exception is the SVWN electronic functional,[153,154] which resulted in a larger MUE because of inherent limitations in the accuracy of this functional. Thus, these electron−proton correlation functionals are transferable and can be used in conjunction with any reasonable electronic exchange-correlation functional.

3.2. NEO-TDDFT for Excited States

The NEO-TDDFT method builds upon the conventional electronic formulation of TDDFT.[155−164] The formalism for multicomponent TDDFT with all particles treated quantum mechanically was developed by van Leeuwen and Gross.[84,85] Subsequently, the NEO-TDDFT method[19,21] was developed to compute excited electronic and proton vibrational states within the NEO framework, where only specified nuclei are treated quantum mechanically. In this approach, the linear response of the NEO Kohn−Sham system to perturbative external nuclear and electronic fields is computed. The working equation for NEO-TDDFT is[19,21]

$$\begin{pmatrix} \mathbf{A}^{e} & \mathbf{B}^{e} & \mathbf{C} & \mathbf{C} \\ \mathbf{B}^{e} & \mathbf{A}^{e} & \mathbf{C} & \mathbf{C} \\ \mathbf{C}^{T} & \mathbf{C}^{T} & \mathbf{A}^{p} & \mathbf{B}^{p} \\ \mathbf{C}^{T} & \mathbf{C}^{T} & \mathbf{B}^{p} & \mathbf{A}^{p} \end{pmatrix} \begin{pmatrix} \mathbf{X}^{e} \\ \mathbf{Y}^{e} \\ \mathbf{X}^{p} \\ \mathbf{Y}^{p} \end{pmatrix} = \omega \begin{pmatrix} \mathbf{I} & 0 & 0 & 0 \\ 0 & -\mathbf{I} & 0 & 0 \\ 0 & 0 & \mathbf{I} & 0 \\ 0 & 0 & 0 & -\mathbf{I} \end{pmatrix} \begin{pmatrix} \mathbf{X}^{e} \\ \mathbf{Y}^{e} \\ \mathbf{X}^{p} \\ \mathbf{Y}^{p} \end{pmatrix} \tag{15}$$

where

$$A^{e}_{ia,jb} = (\varepsilon_a - \varepsilon_i)\delta_{ab}\delta_{ij} + \langle aj|ib\rangle + \frac{\delta^2 E_{exc}}{\delta P^{e}_{jb}\delta P^{e}_{ai}} + \frac{\delta^2 E_{epc}}{\delta P^{e}_{jb}\delta P^{e}_{ai}}$$

$$B^{e}_{ia,jb} = \langle ab|ij\rangle + \frac{\delta^2 E_{exc}}{\delta P^{e}_{jb}\delta P^{e}_{ia}} + \frac{\delta^2 E_{epc}}{\delta P^{e}_{jb}\delta P^{e}_{ia}}$$

$$A^{p}_{IA,JB} = (\varepsilon_A - \varepsilon_I)\delta_{AB}\delta_{IJ} + \langle AJ|IB\rangle + \frac{\delta^2 E_{pxc}}{\delta P^{p}_{JB}\delta P^{p}_{AI}} + \frac{\delta^2 E_{epc}}{\delta P^{p}_{JB}\delta P^{p}_{AI}}$$

$$B^{p}_{IA,JB} = \langle AB|IJ\rangle + \frac{\delta^2 E_{pxc}}{\delta P^{p}_{JB}\delta P^{p}_{IA}} + \frac{\delta^2 E_{epc}}{\delta P^{p}_{JB}\delta P^{p}_{IA}}$$

$$C_{ia,JB} = -\langle aB|iJ\rangle + \frac{\delta^2 E_{epc}}{\delta P^{p}_{JB}\delta P^{e}_{ai}} \tag{16}$$

Here, the lower case indices i and j denote occupied electronic orbitals, while the indices a and b denote virtual electronic orbitals. The upper case indices are defined analogously for protonic orbitals. The density matrix is denoted by P, and the orbital energies are denoted by ε. Because the derivation of eq 15 is based on the adiabatic approximation, in which the kernel is assumed to be frequency-independent, this formulation can only capture single excitations. In principle, the character of these excitations may be pure electron, pure proton, or mixed electron−proton, as long as the excitation can be described as a linear combination of products of electron and proton determinants with only one singly excited determinant in each term.

The solution of eq 15 provides the electronic and proton vibrational excitation energies ω in a single calculation at a similar cost to electronic TDDFT. Moreover, $\mathbf{X}^{e}$ and $\mathbf{Y}^{e}$ are composed of the transition amplitudes for electronic excitations and de-excitations, respectively, and the protonic counterparts are defined analogously. The eigenvectors of eq 15 are subject to the orthonormalization condition

$$\langle \mathbf{X}^{e}_{m}|\mathbf{X}^{e}_{n}\rangle - \langle \mathbf{Y}^{e}_{m}|\mathbf{Y}^{e}_{n}\rangle + \langle \mathbf{X}^{p}_{m}|\mathbf{X}^{p}_{n}\rangle - \langle \mathbf{Y}^{p}_{m}|\mathbf{Y}^{p}_{n}\rangle = \pm\delta_{mn} \tag{17}$$

For predominantly adiabatic systems, the electronic and proton vibrational excitations are distinct, and each excitation is dominated by either $\mathbf{X}^{e}$ and $\mathbf{Y}^{e}$ or $\mathbf{X}^{p}$ and $\mathbf{Y}^{p}$ (Figure 6).[19,21] In this case, the electronic excitation energies are very similar to those computed with conventional electronic TDDFT with the same electronic functional, exhibiting variations of only ∼0.01 eV for the lower excited electronic states of the systems studied.[19] However, significantly larger variations are observed for some of the higher excited electronic states in these systems, illustrating nonadiabatic vibronic mixing between the

https://dx.doi.org/10.1021/acs.chemrev.9b00798
Chem. Rev. XXXX, XXX, XXX−XXX

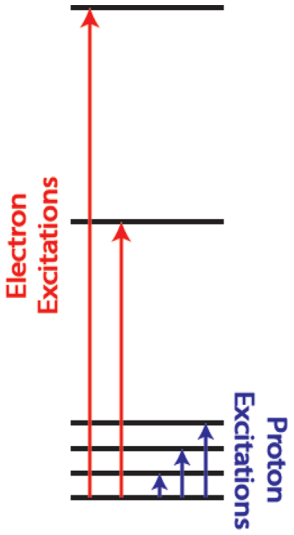

Figure 6. Schematic depiction of the electron and proton excitations that can be obtained from a single NEO-TDDFT calculation. The separation between the electronic and proton vibrational excitations depicted in this figure is typical of predominantly adiabatic systems. For systems with significant nonadiabatic effects between the electrons and proton(s), the single excitations would represent electron−proton vibronic excitations that are not separable. Reprinted with permission from ref 19. Copyright 2018 American Chemical Society.

electronic and protonic excitations. Moreover, this vibronic mixing is expected to become more significant for predominantly nonadiabatic systems and processes.

The proton vibrational excitation energies computed with NEO-TDDFT have been compared to those computed with the grid-based reference method (i.e., the FGH method) described above. The NEO-TDDFT proton vibrational excitation energies have been found to be mostly within 20 cm^{-1} of the grid-based reference values for the systems studied, with occasional differences of ∼100 cm^{-1} (Table 3).[21] Note that this level of quantitative accuracy requires large nuclear and electronic basis sets for the quantum proton. Furthermore, the NEO-TDDFT proton vibrational excitation energies are not as accurate for the vibrational states higher than those corresponding to the fundamental modes, most likely due to limitations of the electron−proton correlation functional or the linear response treatment within the NEO framework.

Table 3. Proton Vibrational Excitation Energies (in cm^{-1}) Calculated with the FGH Reference Method and the NEO-TDDFT Method[a]

			NEO-TDDFT	
	vibrational mode	grid	epc17-2	no-epc
HCN	CH bend	642	670	662
	CH stretch	3122	3110	3098
FHF^-	FH bend	1245	1272	1249
	FH stretch	1659	1754	1823
HNF_2^+	NH asymmetric bend	466	610	621
	NH symmetric bend	1275	1262	1260
	NH stretch	2962	2986	2923

[a]The heavy nuclei were fixed for these calculations. The 8s8p8d8f nuclear basis set and the cc-pV6Z electronic basis set were used for the hydrogen nucleus. The cc-pVTZ electronic basis set was used for the heavy nuclei with the exception that the cc-pVDZ electronic basis set was used for the two fluorine atoms in HNF_2^+. The electronic and nuclear basis functions for the quantum proton were centered at the XH bond distance obtained from a conventional electronic DFT geometry optimization, where X = C, F, or N. The B3LYP electronic functional was used. Data from ref 21.

Despite violating the sum rules, the Tamm−Dancoff approximation has been shown to produce excitation energies similar to those obtained from the corresponding full linear response treatment in conventional electronic structure theory.[19] The Tamm−Dancoff approximation within the NEO framework, denoted the NEO-TDDFT-TDA method, is represented by[19]

$$\begin{pmatrix} \mathbf{A}^e & \mathbf{C} \\ \mathbf{C}^T & \mathbf{A}^p \end{pmatrix} \begin{pmatrix} \mathbf{X}^e \\ \mathbf{X}^p \end{pmatrix} = \omega \begin{pmatrix} \mathbf{X}^e \\ \mathbf{X}^p \end{pmatrix} \tag{18}$$

where the definitions of the $\mathbf{A}^e$, $\mathbf{A}^p$, and $\mathbf{C}$ blocks are given in eq 16. In contrast to the electronic excitation energies, the proton vibrational excitation energies obtained with the NEO-TDDFT-TDA method were found to exhibit errors of thousands of wavenumbers, indicating the importance of the $\mathbf{B}^e$ and $\mathbf{B}^p$ blocks, as well as the $\mathbf{C}$ block, in NEO-TDDFT.[19] Interestingly, these NEO-TDDFT proton vibrational excitation energies are not very sensitive to the electron−proton correlation functional (i.e., the results are similar for NEO-DFT/no-epc and NEO-DFT/epc17-2, as shown in Table 3), suggesting that the NEO-TDDFT formulation is able to incorporate electron−proton correlation in an alternative manner through the de-excitations. This observation also highlights the importance of the $\mathbf{B}^e$ and $\mathbf{C}$ blocks for the accuracy of NEO-TDDFT because the $\mathbf{B}^p$ blocks are zero in the case of NEO-DFT/no-epc for a single proton.

In addition to excitation energies, the formalism for computing transition densities and transition dipole moments within the NEO framework has been developed.[19,21] For a given protonically dominated excitation, the transition densities for NEO-TDDFT are calculated according to

$$\rho^p_{trans}(\mathbf{r}) = \sum_{IA} [\psi_I(\mathbf{r})\psi^*_A(\mathbf{r})X^p_{IA} + \psi^*_I(\mathbf{r})\psi_A(\mathbf{r})Y^p_{IA}] \tag{19}$$

where the indices I and A denote protonic occupied and virtual orbitals, respectively. The terms X^p_{IA} and Y^p_{IA} are elements of the NEO-TDDFT eigenvectors calculated according to eq 15. Protonic transition densities can be used to characterize and visualize NEO-TDDFT excitations, as illustrated in Figure 7 for FHF^-. Another quantity that is useful for the characterization of NEO-TDDFT excitations is the transition dipole moment vector, which indicates the polarization of the

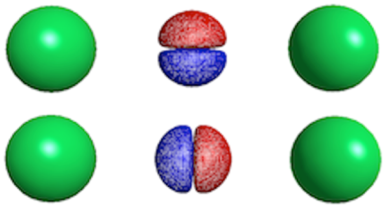

Figure 7. Transition densities for degenerate bend mode (top) and stretch mode (bottom) for FHF^-, as computed with NEO-TDDFT in conjunction with the B3LYP electronic functional and the epc17-2 electron−proton correlation functional. Reprinted with permission from ref 21. Copyright 2019 American Institute of Physics.

https://dx.doi.org/10.1021/acs.chemrev.9b00798
Chem. Rev. XXXX, XXX, XXX−XXX

transition. For a given NEO excited state $|\Psi_k\rangle$, the transition dipole moment vector is defined according to

$$\langle\Psi_0|\hat{r}_\gamma|\Psi_k\rangle = \sum_{IA}[X^{\mathrm{p}}_{IA}\langle I|r_\gamma|A\rangle + Y^{\mathrm{p}}_{IA}\langle A|r_\gamma|I\rangle] + \sum_{ia}[X^{\mathrm{e}}_{ia}\langle i|r_\gamma|a\rangle + Y^{\mathrm{e}}_{ia}\langle a|r_\gamma|i\rangle] \quad (20)$$

where $\hat{r}_\gamma = \hat{x}$, $\hat{y}$, or $\hat{z}$ for $\gamma = 1$, 2, or 3, respectively, and the $\mathbf{X}$ and $\mathbf{Y}$ vector elements are obtained from solving eq 15. The transition dipole moment vectors are of particular importance when calculating full molecular vibrational frequencies with the NEO-DFT(V) approach, as will be discussed in Section 4.1.

The NEO-TDDFT method has also been used to compute proton vibrational excitation energies for molecules with multiple quantum protons.[122] In this case, the collective protonic excitations correspond to linear combinations of single excitations associated with different protons (Figure 8).

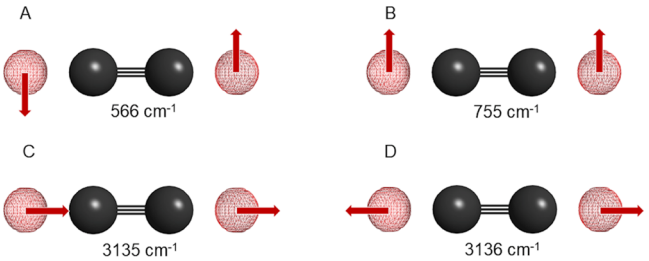

Figure 8. Proton vibrational modes and excitation energies calculated with NEO-TDDFT in conjunction with the B3LYP electronic functional and the epc17-2 electron−proton correlation functional for HCCH with the carbon nuclei fixed at a separation of 1.207 Å. The red mesh depicts the ground-state quantum proton density, and the red arrows indicate the direction of the transition dipole moment vector associated with each quantum proton. Mode (A) is a doubly degenerate CH symmetric bend; mode (B) is a doubly degenerate asymmetric CH bend; mode (C) is an asymmetric CH stretch; and mode (D) is a symmetric CH stretch. Reprinted with permission from ref 122. Copyright 2019 American Chemical Society.

These collective protonic excitation energies are in good agreement with those obtained from normal mode calculations with fixed heavy nuclei, but they have the distinct advantage of incorporating the anharmonic effects associated with the quantum nuclei. As discussed in Section 4.1, the accuracy of these computed protonic excitations has been validated by calculations of full molecular vibrational frequencies.

3.3. Stability Analysis

The goal of a NEO-DFT calculation is to use the SCF procedure to find a solution that is the global minimum associated with the molecular orbital coefficients.[165] A converged SCF solution identifies a stationary point, which may not correspond to the global minimum with respect to the molecular orbital coefficients. To determine whether the solution is a minimum or a saddle point, a stability analysis is required. While the gradient is always zero for an SCF solution, the orbital Hessian must be positive semidefinite for the solution to be a minimum rather than a saddle point. The stability matrix (i.e., the orbital Hessian) for NEO-DFT is identical to the working matrix in NEO-TDDFT given in eq 15 but has a different metric.[19,165] When the orbital Hessian has a negative eigenvalue, the underlying SCF solution corresponds to a saddle point, which is considered an instability. Electron−proton systems could potentially exhibit electronic, protonic, and electron−proton vibronic instabilities. Analysis of the internal and external stabilities with different constraints on the spin and spatial orbitals enables the characterization of SCF solutions.[165] This type of stability analysis is also useful when searching for lower-energy solutions.

4. MOLECULAR PROPERTIES WITHIN THE NEO FRAMEWORK

4.1. Computing Molecular Vibrational Frequencies

The calculation of molecular vibrational frequencies for comparison to experimental spectra is a challenge within the NEO framework because the Born−Oppenheimer separation is invoked between the subsystem containing the electrons and quantum protons and the subsystem containing the classical nuclei. In this case, the quantum protons are assumed to respond instantaneously to the motion of the classical nuclei, and the NEO potential energy surface depends on only the classical nuclei. For each classical nuclear configuration (i.e., for each point on the NEO potential energy surface), typically the quantum nuclear basis function centers are optimized variationally for a finite basis set. The NEO Hessian matrix, $\mathbf{H}_{\mathrm{NEO}}$, is composed of the second derivatives of the NEO energy with respect to the classical nuclear coordinates.[166] In practice, this Hessian can be computed via a matrix folding procedure that rigorously accounts for the effect of the variational optimization of the basis function centers associated with the quantum nuclei.[121] Diagonalization of the mass-weighted NEO Hessian produces vibrational modes with contributions from only the classical nuclei. However, clearly the quantum and classical nuclear motions are coupled in the molecular vibrational frequencies measured experimentally. Thus, the challenge is to compute vibrational frequencies corresponding to modes composed of both quantum and classical nuclei.

The NEO-DFT(V) procedure[121,122] addresses this challenge by coupling the NEO-DFT Hessian for the classical nuclei with the vibrational excitations produced by NEO-TDDFT for the quantum nuclei. This procedure requires the generation of an extended Hessian that depends on the classical nuclear coordinates, represented by the collective coordinate $\mathbf{r}^{\mathrm{c}}$, and the expectation values of the quantum protons, represented by the collective coordinate $\mathbf{r}^{\mathrm{q}}$. Here $\mathbf{r}^{\mathrm{q}}$ is a concatenation of the expectation value $\mathbf{r}^{\mathrm{q}}_i = \int \mathbf{r}\rho^{\mathrm{q}}_i(\mathbf{r})\mathrm{d}\mathbf{r}$ for each quantum nucleus, where $\rho^{\mathrm{q}}_i(\mathbf{r})$ is the density of the i^{th} quantum nucleus. This approach is based on the assumption that each quantum nucleus occupies a distinct nuclear orbital that is spatially localized, and $\rho^{\mathrm{q}}_i(\mathbf{r})$ is the square of this nuclear orbital. Such an assumption of effective distinguishability among the quantum nuclei is valid for most molecular systems of interest. The potential energy surface associated with the extended coordinate space, which depends on the coordinates of the classical nuclei and the expectation values of the quantum nuclei, can be generated by introducing Lagrange multipliers to impose constraints on the expectation values.[167] The stationary points in this extended coordinate space are identical to those in the original NEO coordinate space. The NEO-DFT(V) procedure does not use this extended potential energy surface but rather uses information from NEO-TDDFT to incorporate anharmonic effects associated with the quantum protons.

The extended NEO Hessian matrix is written as

https://dx.doi.org/10.1021/acs.chemrev.9b00798
Chem. Rev. XXXX, XXX, XXX−XXX

$$\mathbf{H}_{\mathrm{NEO}}^{\mathrm{ext}} = \begin{pmatrix} \mathbf{H}_0 & \mathbf{H}_1^{\mathrm{T}} \\ \mathbf{H}_1 & \mathbf{H}_2 \end{pmatrix} \tag{21}$$

where $\mathbf{H}_0 = \left(\frac{\partial^2 E}{\partial \mathbf{r}^{c\,2}}\right)_{\mathbf{r}^q}$, $\mathbf{H}_1 = \frac{\partial^2 E}{\partial \mathbf{r}^q \partial \mathbf{r}^c}$, and $\mathbf{H}_2 = \left(\frac{\partial^2 E}{\partial \mathbf{r}^{q\,2}}\right)_{\mathbf{r}^c}$. The $\mathbf{H}_0$ submatrix is composed of second derivatives of the NEO energy with respect to the classical nuclei with the expectation values of the quantum nuclei fixed. After mathematical manipulations of various partial derivatives, this submatrix can be rigorously expressed as

$$\mathbf{H}_0 = \mathbf{H}_{\mathrm{NEO}} + \mathbf{H}_1^{\mathrm{T}}\mathbf{H}_2^{-1}\mathbf{H}_1 = \mathbf{H}_{\mathrm{NEO}} + \mathbf{R}^{\mathrm{T}}\mathbf{H}_2\mathbf{R} \tag{22}$$

The NEO Hessian matrix $\mathbf{H}_{\mathrm{NEO}}$ can be obtained analytically or numerically, assuming the Born−Oppenheimer separation between the classical and quantum nuclei. The $\mathbf{R}$ matrix is defined as

$$\mathbf{R} = \frac{\mathrm{d}\mathbf{r}^q}{\mathrm{d}\mathbf{r}^c} \tag{23}$$

where the derivative for each quantum nucleus is given as

$$\frac{\mathrm{d}\mathbf{r}_i^q}{\mathrm{d}\mathbf{r}^c} = \frac{\mathrm{d}}{\mathrm{d}\mathbf{r}^c}\int \mathbf{r}\rho_i^q(\mathbf{r})\mathrm{d}\mathbf{r} = \int \mathbf{r}\frac{\mathrm{d}\rho_i^q(\mathbf{r})}{\mathrm{d}\mathbf{r}^c}\mathrm{d}\mathbf{r} \tag{24}$$

and can be calculated numerically or analytically from the gradient of the expectation value of each quantum nucleus with respect to each classical nucleus. The $\mathbf{H}_1$ submatrix can also be expressed in a mathematically rigorous manner as

$$\mathbf{H}_1 = -\mathbf{H}_2\mathbf{R} \tag{25}$$

Eqs 21−25 indicate that if the $\mathbf{H}_2$ submatrix is known then the target $\mathbf{H}_{\mathrm{NEO}}^{\mathrm{ext}}$ can be constructed. The direct calculation of $\mathbf{H}_2$ is challenging, however, because its elements are second derivatives of the NEO energy with respect to specific components of the expectation values of the quantum nuclei with other components fixed.

To address this challenge, the vibrational excitation energies contained in the submatrix $\mathbf{H}_2$ are approximated by those obtained from a NEO-TDDFT calculation according to

$$\mathbf{H}_2 = \left(\frac{\partial^2 E}{\partial \mathbf{r}^{q\,2}}\right)_{\mathbf{r}^c} = \mathbf{M}\mathbf{U}\boldsymbol{\Omega}\mathbf{U}^{-1} \tag{26}$$

Here $\mathbf{M}$ is the diagonal mass matrix corresponding to the quantum nuclei; $\boldsymbol{\Omega}$ is the diagonal matrix with elements ω^2 corresponding to the NEO-TDDFT proton vibrational frequencies for fixed classical nuclei; and $\mathbf{U}$ is a matrix that transforms the diagonal frequency matrix to the coordinate system of the classical nuclei. Note that this approach incorporates anharmonic effects inherent to NEO-TDDFT calculations of vibrational excitations. The expressions for the matrix elements of $\mathbf{H}_0$ and $\mathbf{H}_1$ are mathematically rigorous, and the main approximation in the construction of the extended NEO Hessian lies in the generation of $\mathbf{H}_2$ from quantities computed with NEO-TDDFT.

To provide more details, the $\mathbf{U}$ matrix is constructed from the transition dipole moment vectors obtained from a NEO-TDDFT calculation according to

$$\mathbf{U} = \begin{pmatrix} u_x^{11} & u_x^{21} & u_x^{31} & & u_x^{(k-2)1} & u_x^{(k-1)1} & u_x^{k1} \\ u_y^{11} & u_y^{21} & u_y^{31} & \cdots & u_y^{(k-2)1} & u_y^{(k-1)1} & u_y^{k1} \\ u_z^{11} & u_z^{21} & u_z^{31} & & u_z^{(k-2)1} & u_z^{(k-1)1} & u_z^{k1} \\ \vdots & & & \ddots & & \vdots & \\ u_x^{1N_p} & u_x^{2N_p} & u_x^{3N_p} & & u_x^{(k-2)N_p} & u_x^{(k-1)N_p} & u_x^{kN_p} \\ u_y^{1N_p} & u_y^{2N_p} & u_y^{3N_p} & \cdots & u_y^{(k-2)N_p} & u_y^{(k-1)N_p} & u_y^{kN_p} \\ u_z^{1N_p} & u_z^{2N_p} & u_z^{3N_p} & & u_z^{(k-2)N_p} & u_z^{(k-1)N_p} & u_z^{kN_p} \end{pmatrix} \tag{27}$$

where

$$u_\gamma^{kQ} = \frac{\langle\Psi_0|\hat{r}_\gamma^Q|\Psi_k\rangle}{\sqrt{\sum_Q^{N_p} m_Q \sum_{\gamma=1}^{3} |\langle\Psi_0|\hat{r}_\gamma^Q|\Psi_k\rangle|^2}} \tag{28}$$

In eqs 27 and 28, N_p is the number of quantum protons; $|\Psi_k\rangle$ is a NEO excited state corresponding to the kth proton vibrational excited state; Q denotes a quantum proton with mass m_Q; and $u_\gamma^{kQ} = u_x^{kQ}$, u_y^{kQ}, and u_z^{kQ} for γ = 1, 2, and 3, respectively. The operator $\hat{r}_\gamma^Q$ in eq 28 acts on only the Qth quantum proton occupying the Qth nuclear orbital in the ground state and is associated with the matrix element

$$\langle\Psi_0|\hat{r}_\gamma^Q|\Psi_k\rangle = \sum_A [X_{QA}^p\langle Q|r_\gamma|A\rangle + Y_{QA}^p\langle A|r_\gamma|Q\rangle] \tag{29}$$

Here $\hat{r}_\gamma = \hat{x}$, $\hat{y}$, or $\hat{z}$ for γ = 1, 2, or 3; A denotes virtual protonic orbitals; and X_{QA}^p and Y_{QA}^p are protonic excitation and de-excitation amplitudes, respectively. For a single type of quantum nucleus (as in the purely protonic case presented here), the mass m_Q in the denominator of the expression for u_γ^{kQ} can be factored out. However, eq 28 is a general expression for u_γ^{kQ} and is valid for systems with quantum nuclei of different masses.

The diagonalization of the mass-weighted extended NEO Hessian provides coupled vibrational frequencies that depend on both the classical and quantum nuclear coordinates.[121,122] An example for HCN is depicted in Figure 9. For HCN, the NEO Hessian provides only a single vibrational mode corresponding to the CN stretch, where the electrons and proton respond instantaneously to this motion. NEO-TDDFT provides the three fundamental vibrational excitations associated with the quantum proton, namely, two degenerate bend modes and one stretch mode. The CN mode from the NEO Hessian and the three proton vibrational modes from NEO-TDDFT are combined to produce four molecular vibrational frequencies that couple the CN mode with the proton vibrational modes. The resulting molecular vibrational frequencies are in excellent agreement with experimental values and with values obtained from conventional DFT calculations that include anharmonic effects perturbatively[168] (Table 4).

Focusing on molecules with a single quantum proton, the XH stretch frequencies computed with NEO-DFT(V) for HCN, HNC, HCFO, HCF_3, and FHF^- are in good agreement with conventional DFT calculations that include anharmonic effects perturbatively.[121] Comparison to conventional DFT calculations based on the harmonic approximation illustrates that the inclusion of anharmonic effects lowers the frequencies for the terminal hydrogen vibrational stretch modes. The

https://dx.doi.org/10.1021/acs.chemrev.9b00798
Chem. Rev. XXXX, XXX, XXX−XXX

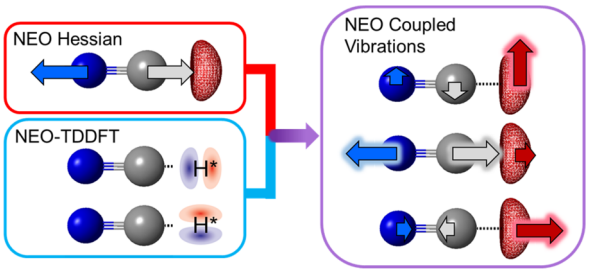

Figure 9. Diagrammatic representation of the NEO-DFT(V) procedure for HCN. The quantum proton is represented by red mesh, and the classical nitrogen and carbon nuclei are represented by blue and gray spheres, respectively. The top left panel shows the single vibrational mode obtained from the NEO Hessian. The bottom left panel shows the protonic NEO-TDDFT excitations for the doubly degenerate bend and the stretch with the classical nuclei fixed. The right panel shows the coupling of the mode obtained from the NEO Hessian with the NEO-TDDFT proton vibrational excitations to obtain the full molecular vibrational frequencies corresponding to a doubly degenerate bend and two stretch modes. Reprinted with permission from ref 121. Copyright 2019 American Chemical Society.

Table 4. Hydrogen Stretch Frequencies (cm^{-1}) Computed with NEO-DFT(V) and Conventional Electronic Anharmonic and Harmonic DFT[a]

	experiment	NEO-DFT(V)	conv. anharmonic	conv. harmonic
HCN	3311	3317	3321	3439
HNC	3653	3645	3644	3814
HCFO	2976	2947	2942	3081
HCF_3	3035	2988	2999	3119
FHF^-	1331	1695	1615	1451
C_2H_2 sym	3374	3378	3390	3503
C_2H_2 asym	3289	3263	3294	3388
H_2O_2 sym	3609−3618	3599	3528	3792
H_2O_2 asym	3610−3619	3596	3522	3789
H_2CO sym	2783	2724	2706	2882
H_2CO asym	2843	2772	2651	2935
H_2NF sym	3234	3241	3192	3420
H_2NF asym	3346	3336	3266	3506

[a]Calculated data from ref 121 for the single-proton systems and ref 122 for the multiple proton systems. These calculations were performed with the B3LYP electronic functional and the epc17-2 electron−proton correlation functional. The electronic and nuclear basis sets used in these calculations are given in refs 121 and 122. Experimental data from refs 170−175. The conventional harmonic DFT frequencies were obtained from the Hessian, and the conventional anharmonic DFT frequencies included anharmonic effects perturbatively.

frequencies obtained from both the NEO-DFT(V) and conventional electronic anharmonic DFT calculations are in excellent agreement with the experimental frequencies for the terminal hydrogen vibrational stretch modes.[121] In contrast to the observations for the terminal hydrogen stretch modes, the inclusion of anharmonic effects increases the stretch frequency for the internal hydrogen in FHF^-. In this case, the frequencies obtained from the NEO-DFT(V) and conventional electronic anharmonic DFT calculations are similar to each other but do not agree well with the experimental frequency. Coupled cluster singles and doubles with perturbative triples (CCSD(T)) calculations for FHF^- indicate a similar magnitude of increase in the hydrogen stretch frequency ($148\ cm^{-1}$) due to anharmonic effects.[169] However, the CCSD(T) calculations that include anharmonic effects are in much better agreement with the experimental frequency, suggesting that the discrepancy for NEO-DFT(V) arises mainly from limitations of DFT.

The NEO-DFT(V) approach has also been applied to molecules with multiple quantum protons.[122] In this case, the modes associated with the quantum protons are transformed to the classical nuclear coordinate system using the transition dipole moments computed with NEO-TDDFT. Table 4 provides the symmetric and asymmetric hydrogen stretch modes for the C_2H_2, H_2O_2, H_2CO, and H_2NF molecules. For the NEO calculations, all electrons and all protons were treated quantum mechanically. For each of these molecules, the NEO Hessian produces a single vibrational mode associated with the two heavy atoms, and NEO-TDDFT produces six collective modes composed of both quantum protons (Figure 8). The NEO-DFT(V) approach couples the classical and quantum nuclear modes to produce seven molecular vibrational modes for linear molecules and six molecular vibrational modes for nonlinear molecules. The resulting vibrational frequencies are in excellent agreement with frequencies obtained experimentally and with conventional DFT including anharmonic effects perturbatively (Table 4).[122]

The NEO-DFT(V) approach relies on three underlying assumptions: (1) the harmonic approximation underlying the Hessian formalism; (2) the representation of the quantum nuclei by their expectation values; and (3) the construction of the quantum nuclear submatrix from the proton vibrational excitation energies and transition dipole moment vectors computed with NEO-TDDFT. This approach incorporates the anharmonic effects associated with the quantum nuclei through the NEO-DFT geometry optimizations and the NEO-TDDFT vibrational excitation energies. In principle, the anharmonic effects associated with the classical nuclei could be included perturbatively. Note that this molecular vibrational analysis approach is also applicable to wave function-based NEO methods, which will be discussed in Section 5.

4.2. Diagonal Born−Oppenheimer Corrections

As discussed above, the Born−Oppenheimer separation is invoked between the subsystem containing the electrons and the quantum protons and the subsystem containing the classical nuclei in the NEO framework. Thus, the quantum protons, as well as the electrons, are assumed to respond instantaneously to the classical nuclei. Analogous to conventional electronic structure calculations,[176−179] the multicomponent diagonal Born−Oppenheimer corrections (DBOCs) can be added to the NEO potential energy surface to incorporate some of the non-Born−Oppenheimer effects between the classical and quantum nuclei.[27] For a NEO wave function of the form $\Psi_{NEO} = \Phi^e\Phi^p$, the adiabatic NEO potential energy surface including the DBOCs can be expressed as

$$E_{adiab}(\mathbf{r}^c) = E_{NEO}(\mathbf{r}^c) - \sum_I^{N_c} \frac{1}{2M_I}[\langle\Phi^e|\nabla_I^2\Phi^e\rangle + \langle\Phi^p|\nabla_I^2\Phi^p\rangle] \quad (30)$$

The electronic and protonic DBOCs can be expressed as follows:

https://dx.doi.org/10.1021/acs.chemrev.9b00798
Chem. Rev. XXXX, XXX, XXX−XXX

$$E^{e}_{DBOC} = -\sum_{I}^{N_c} \frac{1}{2M_I}\langle \Phi^{e}|\nabla_I^2\Phi^{e}\rangle = \sum_{I}^{N_c} \frac{1}{2M_I}\langle \nabla_I\Phi^{e}|\nabla_I\Phi^{e}\rangle$$
$$E^{p}_{DBOC} = -\sum_{I}^{N_c} \frac{1}{2M_I}\langle \Phi^{p}|\nabla_I^2\Phi^{p}\rangle = \sum_{I}^{N_c} \frac{1}{2M_I}\langle \nabla_I\Phi^{p}|\nabla_I\Phi^{p}\rangle \quad (31)$$

Interestingly, the magnitudes of the electronic and protonic DBOCs are similar for the molecules that have been studied,[27] namely HCN, HNC, HCC^-, HCCH, H_2CCH_2, H_3CCH_3, FHF^-, and $H_5O_2^+$, in part because the molecules contain substantially more electrons than quantum protons. In addition, the investigation of model systems indicates that the DBOC is proportional to an intrinsic energy scale as well as the ratio of the masses of the two types of particles, and this intrinsic energy scale is smaller for the quantum protons than for the electrons.[27]

Most importantly, inclusion of the DBOC has negligible impact on the equilibrium geometries and vibrational frequencies for the molecules that have been studied.[27] For these molecules, the DBOC impacts the bond lengths of the optimized geometries by less than 10^{-3} Å. Moreover, the DBOC impacts the vibrational frequencies by 1−2 cm^{-1} per quantum proton bonded to the heavy nuclei involved in the vibrational mode. Thus, the Born−Oppenheimer separation between hydrogen and the other nuclei does not impact the molecular properties at equilibrium. However, the DBOCs may become more important for regions of the potential energy surface far from equilibrium or for floppier molecules or clusters. In such cases, the minimum energy paths and dynamics could be propagated on the full adiabatic NEO potential energy surface, including the DBOCs, as given by eq 30. Furthermore, the DBOCs can also be computed for correlated wave function NEO methods, such as NEO-CCSD and configuration interaction methods, by extending analogous formulations developed for conventional electronic structure theory.[179−183]

5. MULTICOMPONENT WAVE FUNCTION METHODS

5.1. Theoretical Formalism for Configuration Interaction (NEO-CI) and Coupled Cluster (NEO-CC) Approaches

Multicomponent wave function methods, in which more than one type of particle is treated quantum mechanically, offer another route for inclusion of correlation effects between quantum particles.[10] The advantages of wave function methods[184−186] are that they are parameter-free and systematically improvable, ultimately leading to the exact solution for a given multicomponent system. For simplicity, the theoretical formalism in this section will be presented in the context of electrons and quantum protons, but it can be applied to any multicomponent system, including those with electrons and positrons.

The NEO Hamiltonian defined in eq 1 is expressed in second quantization notation as

$$\hat{H}_{NEO} = h_q^p a_p^q + \frac{1}{4}\overline{g}_{rs}^{pq} a_{pq}^{rs} + h_Q^P a_P^Q + \frac{1}{4}\overline{g}_{RS}^{PQ} a_{PQ}^{RS} - g_{qQ}^{pP} a_{pP}^{qQ} \quad (32)$$

The occupied electronic spin orbitals in the NEO-HF reference wave function are denoted by i, j, k, l, ...; the unoccupied (virtual) electronic spin orbitals are denoted by a, b, c, d, ...; and the general electronic spin orbitals are denoted by p, q, r, s, ... The protonic spin orbitals are defined analogously using upper-case indices. In this equation, $a_{p_1^p q_2^p \cdots q_n^p}^{q_1^p q_2^p \cdots q_n^p} = a_{q_1^p}^{\dagger} a_{q_2^p}^{\dagger} \cdots a_{q_n^p}^{\dagger} a_{p_n^p} \cdots a_{p_2^p} a_{p_1^p}$ are second-quantized excitation operators written as a string of electronic creation ($a_p^{\dagger}$) and annihilation (a_p) operators. The protonic and mixed electronic−protonic excitation operators are defined analogously. Moreover, $h_q^p \equiv \langle q|\hat{h}^e|p\rangle$ is a matrix element of the electronic one-particle core Hamiltonian, and $\overline{g}_{rs}^{pq} \equiv \langle rs||pq\rangle = \langle rs|pq\rangle - \langle rs|qp\rangle$ is the antisymmetrized two-electron Coulomb repulsion tensor element. The corresponding protonic one-particle core Hamiltonian and the antisymmetrized two-proton Coulomb repulsion tensor element are defined analogously. Finally, $g_{qQ}^{pP} = \langle qQ|pP\rangle$ is the electron−proton attraction tensor element. The standard Kutzelnigg and Mukherjee tensor notation along with the Einstein summation convention over repeated indices are used herein.[187]

The NEO Hamiltonian in eq 32 is rewritten using the Wick's theorem contraction rules[187,188] as

$$\hat{H}_{NEO} = (h_q^p + \overline{g}_{qi}^{pi} - g_{qI}^{pI})\tilde{a}_p^q + \frac{1}{4}\overline{g}_{rs}^{pq}\tilde{a}_{pq}^{rs}$$
$$+ (h_Q^P + \overline{g}_{QI}^{PI} - g_{Qi}^{Pi})\tilde{a}_P^Q + \frac{1}{4}\overline{g}_{RS}^{PQ}\tilde{a}_{PQ}^{RS} - g_{qQ}^{pP}\tilde{a}_{pP}^{qQ}$$
$$+ h_i^i + \frac{1}{2}\overline{g}_{ij}^{ij} + h_I^I + \frac{1}{2}\overline{g}_{IJ}^{IJ} - g_{iI}^{iI} \quad (33)$$

or simply

$$\hat{H}_{NEO} = \hat{F}_N^e + \hat{W}_N^e + \hat{F}_N^p + \hat{W}_N^p + \hat{W}_N^{ep} + E_{NEO\text{-}HF}$$
$$= \hat{H}_N + E_{NEO\text{-}HF} \quad (34)$$

Here, $\hat{H}_N$ is the normal-ordered (with respect to the NEO-HF reference wave function) NEO Hamiltonian, where $\hat{F}_N^e = F_q^p\tilde{a}_p^q$ ($\hat{F}_N^p = F_Q^p\tilde{a}_P^Q$) and $\hat{W}_N^e = \frac{1}{4}\overline{g}_{rs}^{pq}\tilde{a}_{pq}^{rs}$ ($\hat{W}_N^p = \frac{1}{4}\overline{g}_{RS}^{PQ}\tilde{a}_{PQ}^{RS}$) are normal-ordered electronic (protonic) NEO Fock and fluctuation operators, respectively. Furthermore, the electronic NEO Fock matrix element is defined as $F_q^p = h_q^p + \overline{g}_{qi}^{pi} - g_{qI}^{pI}$, and the protonic NEO Fock matrix element is defined analogously. In addition, $\hat{W}_N^{ep} = -g_{qQ}^{pP}\tilde{a}_{pP}^{qQ}$ is the normal-ordered electronic−protonic fluctuation operator. Finally, the NEO-HF energy is

$$E_{NEO\text{-}HF} = \langle 0^e0^p|\hat{H}_{NEO}|0^e0^p\rangle$$
$$= h_i^i + \frac{1}{2}\overline{g}_{ij}^{ij} + h_I^I + \frac{1}{2}\overline{g}_{IJ}^{IJ} - g_{iI}^{iI} \quad (35)$$

where $|0^e0^p\rangle$ is the NEO-HF reference wave function. Note that $\hat{H}_N$ is also known as the correlation Hamiltonian because its action on a wave function produces the correlation energy contribution. For the exact wave function, it will give the exact correlation energy contribution to the total energy.

Two common approaches for constructing the exact wave function lead to the same exact solution of the Schrödinger equation: full configuration interaction (FCI) and full coupled cluster expansion (FCC). The FCI approach assumes the linear wave function ansatz $|\Psi_{NEO\text{-}FCI}\rangle = (1 + \hat{T})|0^e0^p\rangle$, whereas the FCC approach assumes the exponential wave function ansatz $|\Psi_{NEO\text{-}FCC}\rangle = e^{\hat{T}}|0^e0^p\rangle$.[23,64] The operator $\hat{T} = \sum_\mu t_\mu\tilde{a}_\mu$ is the cluster excitation operator that generates single, double, triple, and further excited determinants by acting on the reference state. These excited determinants are weighted by the unknown amplitudes (i.e., coefficients) t_μ, and they have

https://dx.doi.org/10.1021/acs.chemrev.9b00798
Chem. Rev. XXXX, XXX, XXX−XXX

different values for the two approaches. Here, μ represents the excitation manifold (i.e., single, double, and so forth) produced from excitations of the same particles (i.e., electrons or protons) or mixed particles (i.e., electrons and protons).

In the limit where all excited configurations are included in the wave function expansion, these two approaches will produce the exact solution in the complete basis set limit. However, due to the factorial scaling of these methods, this limit is attainable for only small molecules with modest basis sets. For practical purposes, the cluster operator is often truncated to include up to double excitations. This truncation leads to configuration interaction with singles and doubles (NEO-CISD) and coupled cluster with singles and doubles (NEO-CCSD).[23] In this case, the cluster operator has the form

$$\begin{aligned}\hat{T} &= \hat{T}_1^{\mathrm{e}} + \hat{T}_2^{\mathrm{e}} + \hat{T}_1^{\mathrm{p}} + \hat{T}_2^{\mathrm{p}} + \hat{T}_2^{\mathrm{ep}} \\ &= t_a^i \tilde{a}_i^a + \frac{1}{4} t_{ab}^{ij} \tilde{a}_{ij}^{ab} + t_A^I \tilde{a}_I^A + \frac{1}{4} t_{AB}^{IJ} \tilde{a}_{IJ}^{AB} + t_{aA}^{iI} \tilde{a}_{iI}^{aA}\end{aligned} \tag{36}$$

where $\hat{T}_1^{\mathrm{e}} = t_a^i \tilde{a}_i^a$ ($\hat{T}_1^{\mathrm{p}} = t_A^I \tilde{a}_I^A$) and $\hat{T}_2^{\mathrm{e}} = \frac{1}{4} t_{ab}^{ij} \tilde{a}_{ij}^{ab}$ ($\hat{T}_2^{\mathrm{p}} = \frac{1}{4} t_{AB}^{IJ} \tilde{a}_{IJ}^{AB}$) are the electronic (protonic) single and double cluster excitation operators, and $\hat{T}_2^{\mathrm{ep}} = t_{aA}^{iI} \tilde{a}_{iI}^{aA}$ is the mixed electronic−protonic double cluster excitation operator that promotes both particles simultaneously.

The correlation energy and unknown cluster amplitudes are calculated for a multicomponent system in an analogous manner as with the conventional electronic structure counterparts. Thus, these quantities are computed for NEO-CISD from the equations

$$E_{\text{NEO-CISD}}^{\text{corr}} = \langle 0^{\mathrm{e}} 0^{\mathrm{p}} | \hat{H}_{\mathrm{N}} (1 + \hat{T}) | 0^{\mathrm{e}} 0^{\mathrm{p}} \rangle \tag{37}$$

$$t_\mu E_{\text{NEO-CISD}}^{\text{corr}} = \langle \mu | \hat{H}_{\mathrm{N}} (1 + \hat{T}) | 0^{\mathrm{e}} 0^{\mathrm{p}} \rangle \tag{38}$$

and for NEO-CCSD from the equations

$$E_{\text{NEO-CCSD}}^{\text{corr}} = \langle 0^{\mathrm{e}} 0^{\mathrm{p}} | e^{-\hat{T}} \hat{H}_{\mathrm{N}} e^{\hat{T}} | 0^{\mathrm{e}} 0^{\mathrm{p}} \rangle \tag{39}$$

$$0 = \langle \mu | e^{-\hat{T}} \hat{H}_{\mathrm{N}} e^{\hat{T}} | 0^{\mathrm{e}} 0^{\mathrm{p}} \rangle \tag{40}$$

where $\langle \mu | \equiv \{ \langle_i^a |, \langle_{ij}^{ab} |, \langle_I^A |, \langle_{IJ}^{AB} |, \langle_{iI}^{aA} | \}$ is a set of excited determinants.[23] These excited determinants are defined as $\langle_i^a | = \langle 0^{\mathrm{e}} 0^{\mathrm{p}} | \tilde{a}_a^i$, and other excited determinants are defined analogously.

Additional approximate methods have been developed by neglecting the single excitations within the NEO-CISD and NEO-CCSD methods. This neglect of the single excitations leads to the configuration interaction with doubles (NEO-CID) and coupled cluster with doubles (NEO-CCD) methods. Furthermore, the second-order Møller−Plesset perturbation theory (NEO-MP2)[22,31] method may be viewed as an approximation to the NEO-CCD method. This approximation is achieved by imposing the Møller−Plesset partitioning of the normal-ordered NEO Hamiltonian, in which the zeroth-order contribution is a sum of normal-ordered Fock operators and the first-order correction is a sum of normal-ordered fluctuation operators. The NEO-MP2 energy and excitation amplitude equations are defined as

$$E_{\text{NEO-MP2}}^{\text{corr}} = \langle 0^{\mathrm{e}} 0^{\mathrm{p}} | (\hat{W}_{\mathrm{N}}^{\mathrm{e}} + \hat{W}_{\mathrm{N}}^{\mathrm{p}} + \hat{W}_{\mathrm{N}}^{\mathrm{ep}}) \hat{T}_2^{(1)} | 0^{\mathrm{e}} 0^{\mathrm{p}} \rangle \tag{41}$$

$$0 = \langle 0^{\mathrm{e}} 0^{\mathrm{p}} | (\hat{F}_{\mathrm{N}}^{\mathrm{e}} + \hat{F}_{\mathrm{N}}^{\mathrm{p}}) \hat{T}_2^{(1)} + (\hat{W}_{\mathrm{N}}^{\mathrm{e}} + \hat{W}_{\mathrm{N}}^{\mathrm{p}} + \hat{W}_{\mathrm{N}}^{\mathrm{ep}}) | 0^{\mathrm{e}} 0^{\mathrm{p}} \rangle \tag{42}$$

where

$$\begin{aligned}\hat{T}_2^{(1)} &= \hat{T}_2^{\mathrm{e}(1)} + \hat{T}_2^{\mathrm{p}(1)} + \hat{T}_2^{\mathrm{ep}(1)} \\ &= \frac{1}{4} t_{ab}^{ij(1)} \tilde{a}_{ij}^{ab} + \frac{1}{4} t_{AB}^{IJ(1)} \tilde{a}_{IJ}^{AB} + t_{aA}^{iI(1)} \tilde{a}_{iI}^{aA}\end{aligned}$$

is the first-order excitation cluster operator and $t^{(1)}$ are the first-order amplitudes. The programmable expressions for eqs 37−42 have been obtained[23,26] by applying the generalized Wick's theorem.[187,188]

In the context of calculating properties with wave function-based methods, it is convenient to express the correlation energy contributions defined in eqs 37, 39, and 41 in terms of the one- and two-particle reduced density matrices. For these NEO methods, the correlation contribution to the energy is given as

$$E^{\text{corr}} = F_q^p \tilde{\gamma}_p^q + \frac{1}{4} \bar{g}_{rs}^{pq} \tilde{\Gamma}_{pq}^{rs} + F_Q^P \tilde{\gamma}_P^Q + \frac{1}{4} \bar{g}_{RS}^{PQ} \tilde{\Gamma}_{PQ}^{RS} - g_{qQ}^{pP} \tilde{\Gamma}_{pP}^{qQ} \tag{43}$$

where $\tilde{\gamma}$ and $\tilde{\Gamma}$ are correlation one- and two-particle reduced density matrices.[25] These matrices are defined as

$$\tilde{\gamma}_p^q = \langle \Psi_{\text{NEO}} | \tilde{a}_p^q | \Psi_{\text{NEO}} \rangle \tag{44}$$

$$\tilde{\Gamma}_{pq}^{rs} = \langle \Psi_{\text{NEO}} | \tilde{a}_{pq}^{rs} | \Psi_{\text{NEO}} \rangle \tag{45}$$

$$\tilde{\gamma}_P^Q = \langle \Psi_{\text{NEO}} | \tilde{a}_P^Q | \Psi_{\text{NEO}} \rangle \tag{46}$$

$$\tilde{\Gamma}_{PQ}^{RS} = \langle \Psi_{\text{NEO}} | \tilde{a}_{PQ}^{RS} | \Psi_{\text{NEO}} \rangle \tag{47}$$

$$\tilde{\Gamma}_{pP}^{qQ} = \langle \Psi_{\text{NEO}} | \tilde{a}_{pP}^{qQ} | \Psi_{\text{NEO}} \rangle \tag{48}$$

where $|\Psi_{\text{NEO}}\rangle$ is a normalized NEO wave function. For variational methods such as NEO-CISD, the calculation of these matrices is straightforward because $\langle \Psi_{\text{NEO}} | \equiv |\Psi_{\text{NEO}}\rangle^\dagger$. In NEO-CCSD, where the amplitudes are obtained nonvariationally, this property does not hold, and the bra is defined as $\langle \Psi_{\text{NEO}} | = \langle 0^{\mathrm{e}} 0^{\mathrm{p}} | (1 + \hat{\Lambda}) e^{-\hat{T}}$, whereas the ket is defined as $|\Psi_{\text{NEO}}\rangle = e^{\hat{T}} | 0^{\mathrm{e}} 0^{\mathrm{p}} \rangle$. Here

$$\begin{aligned}\hat{\Lambda} &= \lambda_i^a \tilde{a}_a^i + \frac{1}{4} \lambda_{ij}^{ab} \tilde{a}_{ab}^{ij} + \lambda_I^A \tilde{a}_A^I + \frac{1}{4} \lambda_{IJ}^{AB} \tilde{a}_{AB}^{IJ} + \lambda_{iI}^{aA} \tilde{a}_{aA}^{iI} \\ &\equiv \sum_\mu \lambda_\mu \tilde{a}_\mu^\dagger\end{aligned}$$

is a de-excitation operator, and λ_μ is a set of unknown de-excitation amplitudes also known as Lagrange multipliers.[189,190] These de-excitation amplitudes are determined by solving a set of Λ-equations defined as[25]

$$0 = \langle 0^{\mathrm{e}} 0^{\mathrm{p}} | (1 + \hat{\Lambda}) [e^{-\hat{T}} \hat{H}_{\mathrm{N}} e^{\hat{T}}, \tilde{a}_\mu] | 0^{\mathrm{e}} 0^{\mathrm{p}} \rangle \tag{49}$$

Equation 49 was obtained by making the NEO-CCSD correlation energy functional, $E_{\text{NEO-CCSD}}^{\text{corr}}(t_\mu, \lambda_\mu) = \langle 0^{\mathrm{e}} 0^{\mathrm{p}} | (1 + \hat{\Lambda}) e^{-\hat{T}} \hat{H}_{\mathrm{N}} e^{\hat{T}} | 0^{\mathrm{e}} 0^{\mathrm{p}} \rangle$, stationary with respect to the excitation cluster amplitudes t_μ.[190−192] The calculation of the NEO-MP2 density matrices is analogous to the coupled cluster procedure, except $\hat{\Lambda}$ is replaced by the first-order de-excitation operator $\hat{\Lambda}_2^{(1)}$ defined as $\hat{\Lambda}_2^{(1)} = \hat{T}_2^{(1)\dagger}$. The programmable expressions for the NEO-CCSD Λ-equations as well as the reduced density matrices for different NEO wave function methods have been obtained[25] by applying the generalized Wick's theorem.[187,188]

https://dx.doi.org/10.1021/acs.chemrev.9b00798
Chem. Rev. XXXX, XXX, XXX−XXX

5.2. Orbital-Optimized Coupled Cluster with Doubles (NEO-OOCCD) and Second-Order Perturbation Theory (NEO-OOMP2) Methods

In addition to the methods that rely on the NEO-HF orbitals discussed in the previous subsection, other types of orbitals have also been explored. For example, the Brueckner orbitals are defined to be the optimal orbitals in the presence of correlation effects.[193] In the basis of the Brueckner orbitals, singly excited determinants do not contribute to the FCI expansion of the wave function.[193] One way of obtaining the Brueckner orbitals is by a projective technique,[194−198] in which the single excitation amplitudes in the NEO-CCSD method are removed by repeated unitary rotations of the orbitals. This approach is known as Brueckner coupled cluster with doubles and is denoted NEO-BCCD within the NEO framework.[25] Note that early implementations of multicomponent CCD and BCCD included only electron−proton correlation, neglecting electron−electron correlation, with applications limited to diatomic systems.[31]

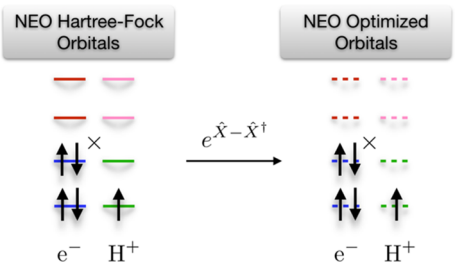

Figure 10. Schematic depiction of the NEO-HF orbitals and NEO-optimized orbitals. Reprinted with permission from ref 26. Copyright 2020 American Chemical Society.

Related to the Brueckner orbitals are the optimized orbitals[199−202] (Figure 10) that are obtained by minimizing the energy expression

$$E_{\text{NEO-OOCCD}} = \langle 0^e 0^p | (1 + \hat{\Lambda}_2) e^{-\hat{T}_2} e^{\hat{X}^\dagger - \hat{X}} \hat{H}_{\text{NEO}} e^{\hat{X} - \hat{X}^\dagger} e^{\hat{T}_2} | 0^e 0^p \rangle \tag{50}$$

with respect to the orbital rotation parameters x_{μ_1} in addition to the t_μ and λ_μ wave function parameters. This procedure corresponds to the orbital-optimized coupled cluster with doubles (NEO-OOCCD) method.[26] In this equation, $\hat{T}_2$ and $\hat{\Lambda}_2$ consist of double excitation and de-excitation operators, respectively, and $\hat{X} = \hat{X}^e + \hat{X}^p = x_a^i a_i^a + x_A^I a_I^A \equiv \sum_{\mu_1} x_{\mu_1} a^{\mu_1}$, where $a^{\mu_1} = a_{\mu_1}{}^\dagger = \{a_i^a, a_I^A\}$ are the second-quantized electron and proton single excitation operators. The unknown orbital rotation parameters, $\mathbf{x} = \{x_a^i, x_A^I\}$, are obtained iteratively by solving the Newton−Raphson equation, $\mathbf{x} = \mathbf{A}^{-1}\mathbf{w}$, where $\mathbf{w}$ and $\mathbf{A}$ are the orbital gradient and the orbital Hessian, respectively. These quantities are defined as

$$(\mathbf{w})_{\mu_1} = \left.\frac{\partial E_{\text{NEO-OOCCD}}}{\partial x^{\mu_1}}\right|_{\mathbf{x}=0} \tag{51}$$

$$(\mathbf{A})_{\mu_1}^{\nu_1} = \left.\frac{\partial^2 E_{\text{NEO-OOCCD}}}{\partial x^{\mu_1} \partial x_{\nu_1}}\right|_{\mathbf{x}=0} \tag{52}$$

and their programmable expressions are given in ref 26.

As discussed in the previous subsection, the NEO-MP2 method can be viewed as an approximation to the NEO-CCD method. Minimization of the NEO-MP2 energy given in eq 6 with respect to the orbital rotation parameters, $\mathbf{x} = \{x_a^i, x_A^I\}$, using the procedure described above produces the orbital-optimized second-order perturbation theory (NEO-OOMP2) method.[26] This method becomes significantly more accurate by applying scaling factors for the opposite-spin (c_{os}) and same-spin (c_{ss}) components in the second-order correction to the electronic correlation energy $E^{ee(2)}$.[203−206] In the analogous conventional electronic scaled-opposite-spin (SOS) method, these two parameters were set to $c_{os} = 1.2$ and $c_{ss} = 0.0$. These same parameter values were used for the multicomponent NEO-SOS-OOMP2 method.[26] The accuracy of this method can be further improved by scaling the second-order correction to the electron−proton correlation energy, $E^{ep(2)}$, by an additional parameter, $c_{ep} = 1.2$, producing the NEO-SOS′-OOMP2 method.[26] An advantage of these scaled-opposite-spin methods is that they can be implemented with N^4 scaling with a combination of density fitting[207] and Laplace transformation of the energy denominators.[208]

5.3. Benchmarking and Applications of NEO-CI, NEO-CC, and NEO-OOMP2 Methods

The NEO-CISD, NEO-CID, NEO-CCSD, NEO-CCD, NEO-BCCD, NEO-MP2, NEO-OOCCD, NEO-OOMP2, NEO-SOS-OOMP2, and NEO-SOS′-OOMP2 methods have been implemented and applied to molecular systems for benchmarking purposes.[23,25,26] As discussed above, the proton density is a particularly important quantity within the NEO framework. For the methods discussed in this section, the proton density is computed as

$$\rho^p(\mathbf{r}^p) = \sum_{PQ} \gamma_P^Q \psi_P(\mathbf{r}^p) \psi_Q(\mathbf{r}^p) \tag{53}$$

where $\{\psi_P\}$ are the real protonic orbitals and $\gamma_P^Q = \overline{\gamma}_P^Q + \tilde{\gamma}_P^Q$ is a matrix element of the total proton density with $\overline{\gamma}$ defined as the NEO-HF one-particle proton density matrix and $\tilde{\gamma}_P^Q$ defined in eq 46. The proton densities were calculated with various NEO wave function methods for the FHF^- and HCN molecules. These proton densities were compared to the grid-based reference method with the potential energy for the proton on the three-dimensional grid computed at the CCSD/aug-cc-pVTZ level of theory. As discussed above, the FGH method provides numerically accurate proton densities for predominantly electronically adiabatic systems. Figure 11 depicts one-dimensional slices of the proton densities for FHF^-, where the hydrogen nucleus and all electrons are treated quantum mechanically (Figure 2). Table 5 provides the RMSD between each NEO method and the grid-based reference averaged over the HCN and FHF^- systems.

The proton densities calculated with the NEO-HF method are highly overlocalized compared to the grid-based reference proton densities. The NEO-CCSD method produces significantly improved proton densities, whereas its approximate analogues NEO-CCD and NEO-MP2, as well as NEO-CISD and NEO-CID, provide negligible improvement compared to the NEO-HF method.[23,25] The superior performance of the NEO-CCSD method can be explained in terms of the exponential form of the single excitations in the coupled cluster ansatz. According to the Thouless theorem,[209] the single excitations in the NEO-CCSD method account for

https://dx.doi.org/10.1021/acs.chemrev.9b00798
Chem. Rev. XXXX, XXX, XXX−XXX

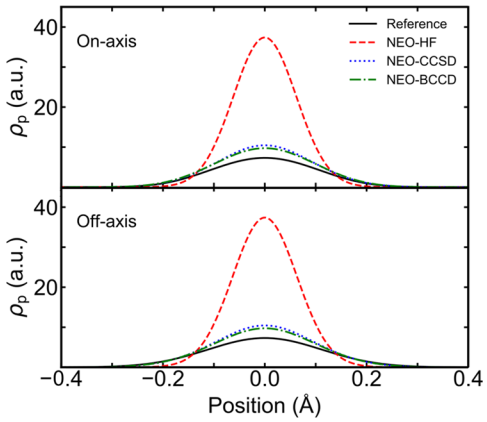

Figure 11. On-axis (top) and off-axis (bottom) proton density for the FHF^- molecule calculated with the grid-based reference (solid black curve), NEO-HF (dashed red curve), NEO-CCSD (dotted blue curve), and NEO-BCCD (dashed-dotted green curve) methods. The quantum proton basis functions are positioned at the origin, and the fluorine atoms are positioned at ±1.1335 Å. On-axis refers to the slice of the proton density along the axis connecting the heavy nuclei, while off-axis refers to the slice perpendicular to this axis, crossing through the midpoint between the two heavy nuclei. These densities were computed with the aug-cc-pVTZ electronic basis set for the classical nuclei, the aug-cc-pVQZ electronic basis set for the quantum hydrogen, and the 8s8p8d8f nuclear basis set. Data obtained from ref 25.

partial orbital relaxation by mixing the unoccupied orbital character into the new reference wave function.[23,25] This orbital relaxation is particularly important within the NEO framework because NEO-HF is a poor starting point as a reference wave function. In the FCI ansatz, the orbital relaxation effects are included not only through linear single excitations but also through the higher excitation ranks of the cluster operator. The NEO-CISD method neglects the excitation ranks higher than double excitations, and the linear form of the single excitations does not account for a sufficient amount of orbital relaxation. In contrast, the exponential form of the single excitations in NEO-CCSD includes more orbital relaxation even with the neglect of higher-order excitations. In the NEO-BCCD method,[25] the reference orbitals are fully optimized, showing slight improvement over the NEO-CCSD method in the prediction of proton densities (Figure 11 and Table 5).

Furthermore, variational optimization of the orbitals, as in the NEO-OOCCD and NEO-OOMP2 methods, significantly improves the proton densities[26] compared to the corresponding NEO-CCD and NEO-MP2 methods that use the NEO-HF orbitals (Table 5). Similar conclusions about the importance of orbital relaxation were reached in the context of the recently developed NEO-CISDTQ method.[210] The NEO-CCSD, NEO-BCCD, and NEO-OOCCD methods produce similar proton densities as those obtained by NEO-DFT with the epc17-1,[16] epc18-1,[18] and epc19[20] functionals but avoid any parametrization and are systematically improvable. The NEO-SOS′-OOMP2 method also produces similarly accurate proton densities as NEO-DFT and, given the same formal scaling, can be used as an alternative to the NEO-DFT method to avoid some of the problems inherent to DFT.[211,212] Moreover, the tails of the proton densities appear to be more accurate with the NEO-CCSD, NEO-BCCD, NEO-OOCCD, and NEO-SOS′-OOMP2 methods compared to the NEO-DFT methods.

Table 5. Mean Unsigned Error (MUE) of Calculated Proton Affinities with Respect to Experimentally Determined Values, RMSD of Proton Density Calculated with NEO Method versus FGH Reference, and Equilibrium F−F Distance for FHF^-[a]

method	proton affinity MUE[b]	proton density RMSD[c]	equilibrium F−F distance[d]
NEO-HF	0.62	0.750	2.278
NEO-MP2	0.32	0.748	2.307
NEO-CID	0.21	0.748	2.278
NEO-CISD	0.20	0.723	2.280
NEO-CCD	0.16	0.741	2.290
NEO-CCSD	0.04	0.165	2.293
NEO-BCCD	0.04	0.148	2.290
NEO-OOCCD	0.04	0.231	2.289
NEO-OOMP2	0.25	0.358	2.312
NEO-SOS-OOMP2	0.11	0.362	2.307
NEO-SOS′-OOMP2	0.05	0.234	2.305
FGH[e]	N.A.	N.A.	2.289
CCSD[f]	0.08	N.A.	2.267

[a]The calculations reported in this table used the aug-cc-pVTZ electronic basis set for the classical nuclei and the aug-cc-pVQZ basis set for the quantum hydrogen, along with the even-tempered 8s8p8d8f nuclear basis set. [b]The MUEs for the proton affinities are in units of eV. The 12 molecules studied are CN^-, NO_2^-, $HCOO^-$, NH_3, HO^-, HS^-, H_2O, H_2S, CO, N_2, CO_2, and CH_2O. Data from refs 23, 25, and 26. [c]The RMSD was computed as the square root of the average of the squares of the differences between the NEO wave function method and FGH proton density at each grid point of the three-dimensional grid. For FHF^-, the F atoms are located at ±1.1335 Å, and the cubic grid ranges from −0.5610 to 0.5984 Å along and perpendicular to the F−F axis. For HCN, the carbon and nitrogen atoms are positioned at −1.058 and −2.206 Å, respectively, and the cubic grid ranges from −0.7258 to 0.7742 Å along and perpendicular to the C−N axis. The reported RMSD value is the average RMSD obtained for the HCN and FHF^- systems given in atomic units. Data from refs 25 and 26. [d]The equilibrium F−F distances are in units of Å. Data from refs 25 and 26. [e]The FGH grid method serves as a benchmark reference for the calculated equilibrium F−F distances. [f]The conventional electronic CCSD method includes harmonic zero-point energies for the proton affinities.

The NEO wave function methods have also been employed to compute the proton affinities of 12 small molecules.[23,25,26] Table 5 provides the MUEs of the computed proton affinities relative to the experimentally determined proton affinities. The NEO-CCSD, NEO-BCCD, NEO-OOCCD, and NEO-SOS′-OOMP2 methods produce accurate proton affinities with a MUE of 0.04−0.05 eV. This MUE is within both chemical accuracy (∼0.05 eV) and experimental accuracy (∼0.09 eV) for proton affinity measurements. The other correlated methods produce a lower MUE than that obtained with the NEO-HF method, but their errors are still above chemical accuracy. The accuracy of the NEO-CCSD, NEO-BCCD, and NEO-OOCCD methods for predicting proton affinities is similar to the accuracy of the NEO-DFT method with the epc17-2, epc18-2, and epc19 functionals. Again, the main advantage of the NEO-CCSD, NEO-BCCD, and NEO-OOCCD methods is that they are parameter-free, although they are more computationally expensive than the NEO-DFT methods. The parametrized NEO-SOS′-OOMP2 method, which has the same formal computational scaling as the NEO-DFT method, also exhibits similar accuracy while

https://dx.doi.org/10.1021/acs.chemrev.9b00798
Chem. Rev. XXXX, XXX, XXX−XXX

Table 6. Ground-State Correlation Energies and Excitation Energies for PsH Computed with Various NEO Methods[a]

state	NEO-FCI	NEO-FCC	NEO-EOM-CCSD[b]	NEO-CISD
ground state	−0.090593	−0.090593	−0.085978	−0.085733
1st excited state	0.156700	0.156700	0.155107	0.179252
2nd excited state	0.165857	0.165857	0.166041	0.187039
3rd excited state	0.242055	0.242055	0.239553	0.254243

[a]The aug-cc-pVTZ basis set was used for both electrons and positrons. The excitation energy ω for each excited state is defined relative to the ground-state energy. The energies are given in units of Hartree. Data from ref 24. [b]For the NEO-EOM-CCSD calculations, the ground-state energy was determined with the NEO-CCSD method.

retaining many of the advantages of wave function-based methods.

Another important characteristic of the NEO method is the incorporation of nuclear quantum effects during geometry optimizations, thus enabling the straightforward calculation of vibrationally averaged geometries. Table 5 provides the calculated equilibrium F−F distances for the FHF^- molecule. The inclusion of nuclear quantum effects for the hydrogen nucleus using the grid-based reference method increases the equilibrium F−F distance by 0.022 Å. The NEO-CCSD, NEO-BCCD, and NEO-OOCCD methods predict equilibrium F−F distances that are in excellent agreement with the grid-based reference value.

The NEO-CCSD method can also be used to calculate geometric isotope effects in systems containing hydrogen or deuterium. The equilibrium F−F distance for FHF^- decreases upon deuteration by 0.006 Å using the FGH method with the grid generated at the conventional electronic CCSD level. The NEO-CCSD method predicts this decrease upon deuteration to be 0.007 Å. This agreement illustrates that the NEO-CCSD method is able to accurately describe changes in equilibrium geometries resulting from deuterium substitution.

5.4. Equation-of-Motion Coupled Cluster with Singles and Doubles (NEO-EOM-CCSD) for Excited States

The equation-of-motion coupled cluster with singles and doubles (NEO-EOM-CCSD) method allows the calculation of the excited-state energies and properties of a multicomponent system.[24] This approach uses the ground-state NEO-CCSD wave function, $|\Psi_{\text{NEO-CCSD}}\rangle = e^{\hat{T}}|0^e0^p\rangle$, as a reference. Then the target left and right excited-state wave functions are

$$|\Psi^R_{\text{NEO-ex}}\rangle = \hat{R}e^{\hat{T}}|0^e0^p\rangle \tag{54}$$

$$\langle\Psi^L_{\text{NEO-ex}}| = \langle 0^e0^p|e^{-\hat{T}}\hat{L} \tag{55}$$

where $\hat{R}$ and $\hat{L}$ ($\hat{R}^\dagger \neq \hat{L}$) are linear excitation and de-excitation operators,[213−215] respectively, defined as

$$\hat{R} = \hat{R}_1 + \hat{R}_2 = r^i_a\tilde{a}^a_i + r^I_A\tilde{a}^A_I + \frac{1}{4}r^{ij}_{ab}\tilde{a}^{ab}_{ij} + \frac{1}{4}r^{IJ}_{AB}\tilde{a}^{AB}_{IJ} + r^{iI}_{aA}\tilde{a}^{aA}_{iI} \tag{56}$$

$$\hat{L} = \hat{L}_1 + \hat{L}_2 = l^a_i\tilde{a}^i_a + l^A_I\tilde{a}^I_A + \frac{1}{4}l^{ab}_{ij}\tilde{a}^{ij}_{ab} + \frac{1}{4}l^{AB}_{IJ}\tilde{a}^{IJ}_{AB} + l^{aA}_{iI}\tilde{a}^{iI}_{aA} \tag{57}$$

using the same notation as introduced in Section 5.1.

The excitation energies ω and the r and l amplitudes that parametrize the right and left excited-state wave functions are determined by solving the right and left eigenproblems, respectively, given as[24]

$$\begin{bmatrix}\bar{H}_{SS} & \bar{H}_{SD}\\ \bar{H}_{DS} & \bar{H}_{DD}\end{bmatrix}\begin{bmatrix}R_1\\ R_2\end{bmatrix} = \omega\begin{bmatrix}R_1\\ R_2\end{bmatrix} \tag{58}$$

$$\begin{bmatrix}L_1 & L_2\end{bmatrix}\begin{bmatrix}\bar{H}_{SS} & \bar{H}_{SD}\\ \bar{H}_{DS} & \bar{H}_{DD}\end{bmatrix} = \omega\begin{bmatrix}L_1 & L_2\end{bmatrix} \tag{59}$$

where the building blocks of the non-Hermitian Hamiltonian are $\bar{H}_{SS} = \langle S|\bar{H}_N|S\rangle$, $\bar{H}_{SD} = \langle S|\bar{H}_N|D\rangle$, $\bar{H}_{DS} = \langle D|\bar{H}_N|S\rangle$, and $\bar{H}_{DD} = \langle D|\bar{H}_N|D\rangle$.[213,215] Here $\bar{H}_N$ is the normal-ordered similarity-transformed NEO Hamiltonian defined to be $\bar{H}_N = e^{-\hat{T}}\hat{H}_N e^{\hat{T}}$.[24] These equations are similar to the conventional electronic EOM-CCSD equations but differ in the dimensionality of the non-Hermitian Hamiltonian because $|S\rangle \equiv \{|^a_i\rangle, |^A_I\rangle\}$ and $|D\rangle \equiv \{|^{ab}_{ij}\rangle, |^{AB}_{IJ}\rangle, |^{aA}_{iI}\rangle\}$. The programmable expressions have been obtained[24] utilizing the generalized Wick's theorem.[187,188] An additional advantage of the NEO-EOM-CCSD method for the calculation of excitation energies is that the excitation energies are size-intensive,[216,217] signifying that the excitation energies are unaffected by the presence of noninteracting fragments.[24]

The NEO-EOM-CCSD method has been applied to positronium hydride (PsH) and has been compared to the NEO-FCI and NEO-FCC methods for benchmarking purposes.[24] In this system, both electrons and the positron are treated quantum mechanically, and the hydrogen nucleus is treated classically. The NEO-FCC method for PsH is attained by extending the NEO-CCSD cluster excitation operator with $\hat{T}_3 = \frac{1}{4}t^{ijI}_{abA}\tilde{a}^{abA}_{ijI}$ to account for mixed triple excitations, in which both electrons and the single positron are promoted. The operators $\hat{R}$ and $\hat{L}$ are extended with an analogous term. Then the normal-ordered similarity-transformed NEO Hamiltonian is diagonalized in the basis of the excited determinants $\{|^a_i\rangle, |^A_I\rangle, |^{ab}_{ij}\rangle, |^{AB}_{IJ}\rangle, |^{aA}_{iI}\rangle, |^{abA}_{ijI}\rangle\}$.[24] Alternatively, the same result is obtained with the NEO-FCI method by diagonalization of the normal-ordered NEO Hamiltonian in the basis of the ground-state reference wave function and excited determinants $\{|0^e0^p\rangle, |^a_i\rangle, |^A_I\rangle, |^{ab}_{ij}\rangle, |^{AB}_{IJ}\rangle, |^{aA}_{iI}\rangle, |^{abA}_{ijI}\rangle\}$.[24,52] The two approaches produce the same results for all excited states, as shown in Table 6 for the PsH system.

Table 6 provides the ground-state correlation energy and the first three excitation energies calculated with the NEO-FCI, NEO-FCC, NEO-EOM-CCSD, and NEO-CISD methods for the PsH system.[24] Based on the leading NEO-EOM-CCSD amplitudes, the ground and the first three excited states have been characterized to have dominant contributions from the $1s^2_e1s^1_p$, $1s^2_e2p^1_p$, $1s^2_e2s^1_p$, and $1s^1_e2s^1_e1s^1_p$ configurations, respectively, where the subscripts e and p correspond to electronic and positronic orbitals. The first two excitations are

https://dx.doi.org/10.1021/acs.chemrev.9b00798
Chem. Rev. XXXX, XXX, XXX−XXX

predominantly positronic, and the third excitation is predominantly electronic. A schematic representation of PsH along with its ground and excited states with assigned configurations is depicted in Figure 12. The NEO-EOM-

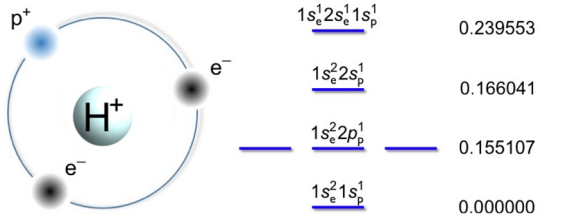

Figure 12. Schematic representation of the PsH system (left) and the ground and excited states (right). The energy levels are depicted with equal spacing, but the excitation energies are given relative to the ground state (Table 6). Reprinted with permission from ref 24. Copyright 2019 American Institute of Physics.

CCSD and NEO-FCI excitation energies are in excellent agreement, deviating by ∼1 mHartree, whereas the NEO-CISD excitation energies deviate by ∼20 mHartree. This observation is consistent with conventional electronic CISD, which does not provide accurate excitation energies due to an unbalanced treatment of correlation effects in the ground and excited states.[218]

The NEO-EOM-CCSD method can be applied to other types of multicomponent systems, such as those where all electrons and specified protons are treated quantum mechanically. Similar to the NEO-TDDFT method described in Section 3.2, the NEO-EOM-CCSD method allows the simultaneous calculation of the excited electronic and proton vibrational states, as well as excited mixed electron−proton vibronic states. Due to the systematically improvable nature of the NEO-EOM-CCSD method, there is a clear path forward for accurately calculating excited states that correspond to double excitations.[219,220] Furthermore, the NEO-DFT(V) method discussed in Section 4.1 could be extended such that the NEO-EOM-CCSD method is used to compute the fundamental proton vibrational frequencies, thereby producing the molecular vibrational frequencies at the CCSD level. The DBOC terms discussed in Section 4.2 could also be computed at the NEO-CCSD level to augment the potential energy surface during calculations of reaction paths and dynamics at this level.

6. DELTA SELF-CONSISTENT FIELD (NEO-ΔSCF) AND MULTICOMPONENT MULTIREFERENCE METHODS

6.1. NEO-ΔSCF

Another method for computing excited states is NEO-ΔSCF,[165] which is a natural extension of ΔSCF in conventional electronic structure theory.[221−225] The goal of this approach is to identify higher-energy stationary solutions corresponding to local minima in orbital space. NEO-ΔSCF has been used to compute the relative energies of HCN and HNC using different initial guesses corresponding to the proton localized near the carbon or the nitrogen, producing an SCF solution on each side.[165] The energy splitting between these two SCF solutions is within 0.3 kcal/mol of the energy difference computed with the grid-based reference method. A more interesting example is the calculation of the excited proton vibrational state for 2-cyanomalonaldehyde, where the proton moves in an asymmetric potential, as depicted in Figure 13. For two different initial guesses localizing the proton near

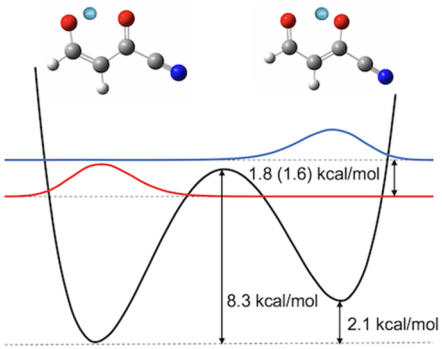

Figure 13. One-dimensional slice of the proton potential energy surface and the lowest two proton vibrational states calculated with the other nuclei fixed to an average reactant/product geometry for 2-cyanomalonaldehyde. The potential and proton vibrational wave function slices are generated along the line connecting the optimized positions of the transferring hydrogen (depicted in cyan mesh) on each oxygen (depicted as red spheres). The energy splitting between the lowest two proton vibrational states was calculated with the reference FGH method and with the combined NEO-DFT and NEO-ΔSCF methods, as given in parentheses, indicating excellent agreement within 0.2 kcal/mol. The NEO-DFT calculations were performed with the B3LYP electronic functional and the epc17-2 electron−proton correlation functional. The electronic and nuclear basis sets used in these calculations are given in ref 165. Reprinted with permission from ref 165. Copyright 2018 American Institute of Physics.

one oxygen or the other, two different SCF solutions were obtained.[165] The splitting between these two solutions is within 0.2 kcal/mol of the splitting computed with the grid-based reference method. For both of these examples, the higher-energy SCF solutions were shown to be minima in orbital space using the stability analysis discussed in Section 3.3. These cases were relatively straightforward because of very small overlap between the two SCF solutions.

More challenging applications may require different techniques. To compute the excited proton vibrational states for molecules such as HCN or FHF^-, the initial guess can be chosen to correspond to the proton in the virtual orbital with the appropriate symmetry (i.e., a single node, analogous to the transition density depicted in Figure 7) instead of using the aufbau principle. In some cases, the standard iterative procedure starting from this initial guess will produce an SCF solution of the proper character due to the different symmetries of the excited and ground states. Other cases may require implementation of the maximum overlap method,[222] which maximizes the overlap between the occupied orbitals of the current and preceding SCF iterations, or the initial maximum overlap method,[224] which maximizes the overlap between the occupied orbitals and the initial orbitals, to prevent variational collapse to the ground state. Another possibility is to extend the excited constrained DFT approach that has been used to compute low-lying excited electronic states[226] to the NEO framework. Although the excited proton vibrational states obtained with these types of methods may be of the proper character, their energies relative to the ground state tend to be significantly overestimated.

To address this issue and to enable the description of certain types of double excitations, the NEO-ΔSCF and NEO-

https://dx.doi.org/10.1021/acs.chemrev.9b00798
Chem. Rev. XXXX, XXX, XXX−XXX

TDDFT methods can be combined. The general strategy is that NEO-ΔSCF solutions can be used as reference states in NEO-TDDFT calculations. The underlying principles of this strategy are related to spin-flip approaches used in conventional electronic TDDFT.[227] For 2-cyanomalonaldehyde, NEO-ΔSCF accurately describes the lowest proton vibrational state in the higher-energy well and produces a quantitatively accurate energy splitting between this state and the ground proton vibrational state localized in the lower-energy well (Figure 13 and solid red arrow in lower potential of Figure 14).[165] Using either the ground proton vibrational state or the excited proton vibrational state obtained from NEO-ΔSCF as a reference state, NEO-TDDFT produces accurate fundamental proton vibrational excitations within each of these wells (Table 7 and blue arrows in lower potential of Figure 14).

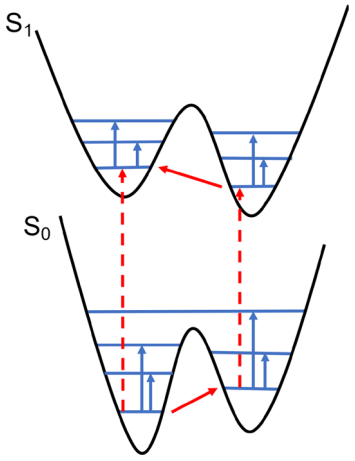

Figure 14. Schematic depiction of different excitations that could potentially be described by combining NEO-TDDFT and NEO-ΔSCF. The lower and upper potentials correspond to the ground and excited electronic states, respectively. The solid and dashed red arrows depict excitations that could be obtained with NEO-ΔSCF, and the blue arrows depict proton vibrational excitations that could be described with NEO-TDDFT using the reference at the start of the arrow.

Table 7. NEO-TDDFT Excitation Energies (in cm^{-1}) for 2-Cyanomalonaldehyde[a]

excitation energy	NEO[a]	grid
$E_0' - E_0$[b]	587	623
$E_1 - E_0$	1050	974
$E_2 - E_0$	1357	1245
$E_1' - E_0$	1652	1612

[a]The energies with primes correspond to NEO-TDDFT states localized in the higher-energy well (right well in Figure 13), and the energies without primes correspond to NEO-TDDFT states localized in the lower-energy well (left well in Figure 13). All calculations were performed with the B3LYP electronic functional and the epc17-2 electron−proton correlation functional. The cc-pVDZ electronic basis set was used for all atoms except the quantum hydrogen. For computational tractability, the cc-pV5Z electronic basis set and the 8s8p8d8f nuclear basis set used for the quantum hydrogen were located at the minimum of only the left or the right well for each calculation. [b]This energy splitting was obtained from a NEO-ΔSCF calculation to compute the lowest proton vibrational state in the higher-energy well. This proton vibrational state, which has energy E_0', was used as the reference to compute E_1'.

A similar strategy can be employed to describe double excitations involving both an electronic and a proton vibrational excitation. This strategy entails the following steps: (1) perform a NEO-TDDFT calculation and identify the electronic excitation of interest; (2) use the dominant determinant associated with this electronic excitation as the target for a maximum overlap method NEO-ΔSCF calculation to compute the NEO vibronic state of interest (dashed red arrows in Figure 14); and (3) use this vibronic state as the reference state in a NEO-TDDFT calculation to compute the proton vibrational excitations relative to this state (blue arrows in upper potential of Figure 14). This approach is feasible for an open-shell radical system if the electronic excitation of interest is dominated by the HOMO to LUMO (i.e., HOMO +1) transition. However, complications are expected to arise for certain types of electronic excitations, such as excited singlet states, because of issues including unstable SCF solutions, spin contamination, and triplet instabilities.[228,229]

As a proof of concept, a calculation of this type has been performed on HNF_2^+. The geometry for HNF_2^+ was optimized at the B3LYP/def2-QZVP level of theory. The subsequent calculations on this system used the B3LYP electronic functional, the cc-pVDZ electronic basis set, the epc17-2 electron−proton correlation functional, and the DZSPDN nuclear basis set.[10] Following the scheme outlined above, first a NEO-TDDFT calculation was performed on this system, and an electronic excitation dominated by a HOMO to LUMO excitation in the alpha set of orbitals was identified and found to have an excitation energy of 7.541 eV. Subsequently, the NEO-ΔSCF approach with the maximum overlap method was used to compute the excitation energy associated with this state, leading to an electronic excitation energy of 7.371 eV (dashed red arrow in Figure 14). Using the NEO-ΔSCF state as a reference, a NEO-TDDFT calculation was performed to compute the proton vibrational excitation energies in the excited electronic state (i.e., blue arrows in the S_1 state in Figure 14). All of the resulting excitation energies, which correspond predominantly to proton vibrational excitations in the excited electronic state, were real. These results are not quantitative, given the relatively small basis sets used, and this method has not been extensively studied. The results presented here are intended only to demonstrate the feasibility of performing such calculations. Thus, further developments are required, and caution in using these types of methods is warranted.

6.2. Nonorthogonal Configuration Interaction (NEO-NOCI) for Tunneling Splittings

Multireference approaches are required for describing proton vibrational wave functions delocalized over two wells.[123,230] One such approach is the NEO−nonorthogonal configuration interaction (NEO-NOCI) method.[123] For a system such as malonaldehyde (Figure 15), a set of electronic and nuclear basis functions can be positioned near the minimum of each well. For single-reference methods, such as NEO-HF and NEO-DFT, the NEO vibronic wave functions naturally localize onto one of these basis function centers[230] and can be computed with different initial guesses, as in NEO-ΔSCF. The resulting two vibronic wave functions, each of which is localized in one well, are nonorthogonal and can be used as the determinants in a two-state NEO-NOCI calculation to produce the adiabatic proton vibrational states delocalized over both wells. At the NEO-HF level, the proton vibrational

https://dx.doi.org/10.1021/acs.chemrev.9b00798
Chem. Rev. XXXX, XXX, XXX−XXX

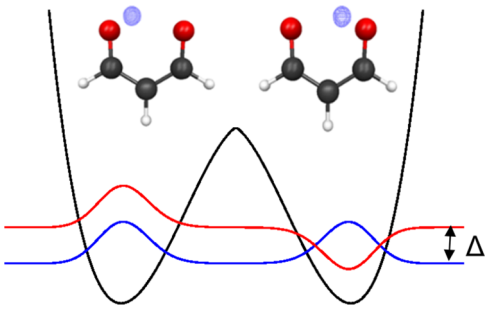

Figure 15. Schematic depiction of a proton moving in a symmetric double-well potential and NEO-DFT states localized in each well (blue mesh in chemical structures) for malonaldehyde. NEO-NOCI mixes the NEO-DFT localized states to generate the adiabatic states delocalized over both wells (blue/red curves). The tunneling splitting Δ is the energy difference between the NEO-NOCI delocalized states.

wave functions in each well are much too localized and cannot produce even qualitatively reasonable hydrogen tunneling splittings and vibronic couplings. To address this problem, the localized protonic orbitals were fit to grid-based wave functions for an application of NEO-NOCI to malonaldehyde,[124] but such an approach is not self-contained.

Alternatively, the accurate proton densities provided by NEO-DFT with the epc17-2[17] or epc19[20] electron−proton correlation functionals within each well can be used in conjunction with the NEO-NOCI method in a multistate NEO-DFT approach. The NEO-DFT method includes dynamical electron−proton correlation to obtain accurate proton densities in each well, and the NEO-NOCI method includes static correlation to combine these two states in a manner that leads to proton vibrational wave functions delocalized over both wells (Figure 15). In contrast to constrained DFT,[231,232] which applies spatial or spin constraints to localize the electronic wave function, no constraints need to be applied in the NEO framework because the vibronic wave functions naturally localize in one well with the single-reference methods studied to date. Thus, the localized states can be obtained with NEO-ΔSCF using different initial guesses. Although this type of combined approach is not theoretically rigorous, it provides a qualitatively reasonable starting point for the development of more rigorous methods.

A challenge of this approach is the definition of the off-diagonal Hamiltonian matrix elements in the basis of the localized Kohn−Sham determinants, denoted Ψ_A and Ψ_B. Analogous to the multistate DFT approach of Gao and co-workers,[233,234] this off-diagonal matrix element could be approximated as

$$H_{AB} = \langle \Psi_A | H_{NEO} | \Psi_B \rangle + \frac{1}{2} S_{AB} (E_A^{corr} + E_B^{corr}) \quad (60)$$

where $\langle \Psi_A | H_{NEO} | \Psi_B \rangle$ is the energy computed with the NEO-HF Hamiltonian and the Kohn−Sham determinants; $S_{AB} = \langle \Psi_A | \Psi_B \rangle$ is the overlap between the Kohn−Sham determinants; and $E_A^{corr} = E_A^{DFT} - E_A^{HF}$ is the difference between the NEO-DFT and NEO-HF energies for Ψ_A. This form of the off-diagonal matrix elements ensures that the vibronic coupling obtained after symmetric orthogonalization is the same as the NEO-NOCI coupling using the Kohn−Sham determinants. Other forms of the off-diagonal Hamiltonian matrix element could also be utilized. These types of multistate NEO-DFT approaches represent an exciting future direction.

The calculation of accurate tunneling splittings in a molecule such as malonaldehyde also requires coupling of the transferring hydrogen nucleus to the vibrations of the other nuclei. For this purpose, the NEO method for the quantum mechanical treatment of the transferring hydrogen nucleus has been combined with vibronic coupling theory for the quantum mechanical treatment of the other nuclei.[124] Note that there are many highly accurate approaches, such as the MCTDH[235,236] and diffusion Monte Carlo[237−239] methods, for computing hydrogen tunneling splittings. The NEO approach is not expected to be as accurate as such methods but has the advantage of computational efficiency, which will be important for larger molecular systems.

6.3. Complete Active Space Self-Consistent Field (NEO-CASSCF) and Orbital-Optimized Configuration Interaction with Singles (NEO-OOCIS) Methods

Due to the strong correlation effects between electrons and protons, the NEO wave function may have significant multireference character. One method for estimating the degree of multireference character in electronic systems is to analyze the t_1 amplitudes obtained from the CCSD method, which is known as the T_1 diagnostic.[240] This diagnostic is defined as the Euclidian norm of the t_1 amplitudes normalized by the number of correlated electrons.[240] Systems with $T_1 < 0.02$ are usually well described by single-reference methods. For the HCN molecule with the basis sets given in Section 5.3, the conventional electronic CCSD method produces $T_1 = 0.012$, and the NEO-CCSD method produces $T_1^e = 0.012$ and $T_1^p = 0.534$ for the electronic and protonic T_1 diagnostics, respectively, indicating significant multireference character of the NEO wave function. Note that the diagnostic threshold designed for electrons may not be transferable to different types of particles, such as protons. Analysis of the NEO-CISDTQ wave function led to a similar conclusion about the multireference character of the NEO wave function.[210] Clearly multireference methods are essential for describing systems with substantial multireference character.

A general multireference approach is the NEO complete active space SCF (NEO-CASSCF) method,[10] which is analogous to its conventional electronic structure counterpart.[241] In this multicomponent multireference approach, an active space composed of electronic and nuclear orbitals is chosen, and all possible configurations generated by excitations within this active space are included in a CI expansion. The total energy is minimized with respect to the electronic and nuclear molecular orbitals as well as the CI coefficients. In principle, dynamical correlation could be included by applying second-order perturbation theory to the NEO-CASSCF reference function, analogous to the conventional electronic structure CASPT2 method.[242,243] To date, NEO-CASSCF has not been found to include sufficient electron−proton correlation to produce accurate proton densities,[10] but larger active spaces and basis sets may improve the accuracy.

Another option is the NEO orbital-optimized configuration interaction with single excitations (NEO-OOCIS) method, which also minimizes the energy with respect to the CI coefficients and molecular orbitals. This method is the NEO extension of the conventional electronic OOCIS method proposed by Subotnik and co-workers.[244] In this method, the NEO-CIS energy for a given excited state is stationary with

https://dx.doi.org/10.1021/acs.chemrev.9b00798
Chem. Rev. XXXX, XXX, XXX−XXX

respect to the electronic and protonic singles amplitudes (i.e., $\mathbf{X}^{e}$ and $\mathbf{X}^{p}$ in eq 18 within the Hartree−Fock framework) and orbital expansion coefficients. The orbitals are optimized in an analogous manner as that described in the context of the NEO-OOCCD method in section 5.2. The proton vibrational excitation energies for the HCN molecule are summarized in Table 8.

Table 8. Proton Vibrational Excitation Energies (in cm^{-1}) for HCN Calculated with the NEO-CIS and NEO-OOCIS Methods[a]

method	CH bend	CH stretch
NEO-CIS	3714	4911
NEO-OOCIS	638	3607
grid	642	3122

[a]The heavy nuclei were fixed with a C−N distance of 1.148 Å, as obtained from a conventional electronic CCSD/aug-cc-pVTZ geometry optimization. The nuclear and electronic basis function centers for the quantum proton were positioned at a distance of 1.058 Å from the carbon atom, corresponding to the hydrogen position for this optimized geometry. The NEO calculation employed the 8s8p8d8f nuclear basis set and the cc-pV6Z electronic basis set for the hydrogen nucleus. The cc-pVDZ electronic basis set was used for the heavy nuclei. The grid reference was obtained from Table 3.

As also indicated in Section 3.2 in the context of the TDA approximation, the NEO-CIS method produces inaccurate proton vibrational excitation energies relative to the reference grid results (Table 8). In contrast, the NEO-OOCIS method predicts proton vibrational excitation energies that are in reasonable agreement with the reference values. These calculations indicate that orbital optimization is crucial for obtaining even qualitatively accurate proton vibrational excitation energies. Moreover, these results suggest that the NEO-CASSCF method is a promising, more general approach for computing proton vibrational excitation energies. An advantage of these wave function approaches is the clear path forward for improving the excitation energies.

7. OTHER APPROACHES FOR DESCRIBING NUCLEAR QUANTUM EFFECTS AND NON-BORN−OPPENHEIMER EFFECTS

As discussed in the Introduction, several other multicomponent orbital methods have been developed.[29−34,36,41,43,44,46,47,49,50,52,81,84,85,148] Although the multicomponent Hartree−Fock and second-order perturbation theory methods suffer from overlocalized proton densities, the coupled cluster methods[23,25,31,64,65] are promising, albeit more expensive. The explicitly correlated wave function methods developed by Adamowicz and co-workers[66−76] to treat all electrons and all nuclei quantum mechanically on the same level are highly accurate but computationally expensive. As also discussed in the Introduction, the formalism for multicomponent DFT and TDDFT has been well-established.[13,47,79−81,84,85] Two earlier types of electron−proton correlation functionals based on the Colle−Salvetti formalism made the nonphysical assumption that the inverse correlation length depends on only the electron density, rather than both the electron and proton densities.[32,33,39,43] These functionals have not been shown to be broadly applicable for computing molecular properties. The NEO-DFT method with the epc17 functional[16,17] has been shown to produce accurate proton densities, optimized geometries, energies, and frequencies. The NEO-DFT/epc17 method is available in quantum chemistry packages such as GAMESS[245] and Q-Chem[246] and has also been incorporated into the deMon2k code[247] in conjunction with density fitting methods to enhance the efficiency.[248]

Other types of approaches for incorporating non-Born−Oppenheimer effects have also been developed. Abedi, Maitra, Gross, and co-workers have developed the exact factorization method,[249−252] which rigorously reformulates the time-dependent Schrödinger equation to describe the quantum dynamics of an interacting electronic and nuclear system in terms of two coupled equations, providing the basis for nonadiabatic dynamics calculations. Path integral and quantum Monte Carlo methods can also be used to remove the Born−Oppenheimer approximation.[96,97,99,100,102,104,113−117] The rigorous methods[113−117] are also computationally expensive and limited in terms of the size of the system that can be studied.

Many more methods have been developed to include nuclear quantum effects within the Born−Oppenheimer approximation, where the nuclei move quantum mechanically on the adiabatic potential energy surface. The multiconfigurational time-dependent Hartree (MCTDH) method[110−112] has been highly successful but often relies on an analytical potential energy surface, although recently it has been used without precomputed potential energy surfaces.[253,254] A variety of quantum nuclear wavepacket methods[107−109] have been developed in conjunction with generating the potential energy surface on-the-fly, although the computational expense and scaling properties impose limitations on the system size. Path integral methods have also been widely used for propagating nuclei on an adiabatic potential energy surface. The ring polymer molecular dynamics (RPMD)[93,95] and centroid molecular dynamics (CMD)[88−92] methods have been highly successful in treating all nuclei quantum mechanically in a computationally tractable manner. Real-time path integral methods are also promising, although more expensive.[98,101]

Nonadiabatic dynamics methods allow the study of processes that involve multiple potential energy surfaces. The most widely used nonadiabatic dynamics methods treat the nuclear motion classically. In the Ehrenfest method, the nuclei move classically on an effective potential energy surface corresponding to a weighted average of the electronic states.[255] Alternative approaches based on the initial value representation have also been developed.[256−258] In the fewest switches surface hopping method,[259] individual trajectories move classically on a single potential energy surface, and nonadiabatic transitions are incorporated between the surfaces according to the electronic time-dependent Schrödinger equation. The more elaborate multiple spawning method treats the nuclei as quantum mechanical wavepackets that move on individual surfaces but multiply and propagate to different surfaces as needed.[260−264] The MCTDH method has been extended to nonadiabatic processes,[111] and nonadiabatic extensions of the ring polymer molecular dynamics method have also been proposed.[94,96,97,99,100,102,104] This discussion of other methods for including nuclear quantum effects and non-Born−Oppenheimer or nonadiabatic effects does not cover all of the possibilities but illustrates the wide range of options.

8. EFFICIENCY AND ACCESSIBILITY OF NEO APPROACHES

The NEO methods are not designed to replace the more rigorous and powerful wavepacket and path integral methods

https://dx.doi.org/10.1021/acs.chemrev.9b00798
Chem. Rev. XXXX, XXX, XXX−XXX

for treating all nuclei quantum mechanically. Instead, the NEO methods are designed for situations in which only specified nuclei, typically the hydrogen nuclei, are treated quantum mechanically to capture the most essential nuclear quantum effects. Advantages of the NEO approaches over some of these other methods for certain applications are the computational efficiency and scaling, as well as the inclusion of non-Born−Oppenheimer effects between the electrons and quantum nuclei. The computational cost of a NEO calculation is typically similar to the cost of the analogous electronic structure calculation because of the much smaller number of protons compared to electrons and the relative localization of the protons in molecular systems.

Although HF and NEO-HF, as well as the DFT counterparts, have the same formal computational scaling, the NEO methods have a larger prefactor because of the need to converge both the electronic and protonic densities. Specifically, NEO SCF methods typically require more iterative cycles than their conventional electronic structure counterparts. However, the number of cycles can be greatly reduced by using suitable SCF protocols. For the initial guess, it is advantageous to first converge a pure electronic SCF calculation and use this electronic density as a guess when constructing the protonic Fock matrix. Moreover, several options are possible for the iterative procedure. One option is to perform one electronic (protonic) orbital update followed by full convergence of the proton (electron) density in an alternating fashion. A second option is to fully converge the electronic and protonic SCF equations in an alternating fashion. A third option is to perform one electronic orbital update and one protonic orbital update in an alternating fashion. The second option, in conjunction with dynamically decreasing convergence criteria, has been found to be particularly effective. However, the convergence behavior depends on the specific system. These techniques, combined with direct inversion in the iterative subspace (DIIS) or Newton−Raphson methods, typically result in the convergence of a NEO calculation with a reasonable number of cycles.

In terms of post-HF wave function methods, the increase in computational expense is typically even less pronounced. For methods such as NEO-CCSD or NEO-CISD, the computational expense and memory requirement are dominated by the optimization of the electronic t amplitudes defined in section 5.1 because typically the number of electronic basis functions is much greater than the number of protonic basis functions. The total number of double excitation t amplitudes is $o_e^2v_e^2 + o_p^2v_p^2 + o_ev_eo_pv_p$, where o_e, o_p, v_e, and v_p denote the occupied electronic and protonic and virtual (unoccupied) electronic and protonic orbitals, respectively. As an example, consider the HCN molecule with 7 occupied and 100 unoccupied electronic orbitals, as obtained with a modest electronic basis set. For the 8s8p8d nuclear basis set, this molecule would have 1 occupied and 71 unoccupied protonic orbitals. This system would have 490,000 versus 544,741 double excitation amplitudes for conventional electronic CCSD versus NEO-CCSD. For wave function methods that are used for excited-state calculations, such as NEO-CISD and NEO-EOM-CCSD, the dimension of the singles−singles block in eq 58 is $o_ev_e + o_pv_p$. For the HCN example above, the dimension of the singles−singles block matrix for the conventional electronic versus NEO method is 700 versus 771. Thus, the computational cost of post-SCF methods is dominated by the size of the electronic space.

In additional to the computational efficiency, the NEO approaches are as straightforward to use as the analogous electronic structure methods, simply requiring the selection of the quantum nuclei, a nuclear basis set, and an electron−proton correlation functional in the case of NEO-DFT. Thus, the NEO approaches enable nonexperts to include nuclear quantum effects of specified protons into quantum chemistry calculations with similar ease and computational expense as conventional quantum chemistry calculations. The NEO approaches are available in several different quantum chemistry packages, including GAMESS[245] and Q-Chem 5.3.[246]

9. REMAINING CHALLENGES AND FUTURE DIRECTIONS

Multicomponent quantum chemistry is still a relatively young and emerging field. As a result, many challenges still need to be solved. The development of more effective and efficient nuclear basis sets will enable a broader set of applications. Within the field of NEO-DFT, the development of more accurate electron−proton correlation functionals is another important direction. Although the NEO-TDDFT method provides accurate fundamental vibrational excitations, the calculation of higher vibrational states will probably require the development of new electron−proton correlation functionals. Moreover, the development of methods for computing double excitations must go beyond the linear-response NEO-TDDFT method. Within the wave function methods, the accuracy of the NEO-CCSD approach would be enhanced by the inclusion of triple excitations, even if only in a perturbative manner. The NEO-EOM-CCSD method is a promising but computationally expensive direction for computing electronic, vibrational, and vibronic excitations and could be extended to describe double excitations. Multireference NEO methods, such as NEO-NOCI or NEO-CASSCF with a large, carefully selected active space, will be required to compute accurate hydrogen tunneling splittings and vibronic couplings.

To enable the study of even larger systems, such as proteins, the NEO approach can be combined with the vast array of hybrid approaches that have been developed for conventional electronic structure theory. The NEO fragment molecular orbital (FMO) method has already been implemented and tested.[265] Variants of embedding theory have also been formulated within the NEO framework.[143] In addition, mixed quantum mechanical/molecular mechanical (QM/MM) methods or QM/QM methods in which the NEO approach is used for one of the QM levels can easily be implemented. The NEO methods can also be used in conjunction with a dielectric continuum solvent,[266] thereby enabling the calculation of more accurate pK_as and solvation free energies of molecular systems.

The NEO approach will also be useful for studying reaction paths for chemical systems. The generation of minimum energy paths along the intrinsic reaction coordinate (IRC) will require analytic gradients, which are already available for the NEO-DFT methods, and analytic Hessians, which are under development. Within the NEO framework, the IRC will be composed of contributions from only the classical nuclear coordinates. In conventional electronic structure calculations, typically the IRC near the transition state is dominated by the transferring hydrogen nuclear coordinate for hydrogen transfer reactions. In the NEO approach, the transferring hydrogen nucleus is treated quantum mechanically on the same level as the electrons, and therefore it cannot contribute to the IRC in this manner. Thus, hydrogen transfer becomes analogous to

https://dx.doi.org/10.1021/acs.chemrev.9b00798
Chem. Rev. XXXX, XXX, XXX−XXX

electron transfer within the NEO framework, and the IRC is dominated by the motions of heavy nuclei that alter the environment of the transferring hydrogen. If the hydrogen samples an environment corresponding to a symmetric double-well potential, where the proton vibrational wave function is bilobal, then multireference methods will be necessary. For proton-coupled electron transfer reactions,[7−9] analysis of the electron and proton densities along the minimum energy path will provide insights into the fundamental mechanisms of electron and proton transfer, distinguishing between sequential and concerted, or asynchronous and synchronous, mechanisms. Thus, these types of calculations will provide new insights into chemical reactions.

Another promising direction for the NEO approach is the investigation of the dynamics of chemical processes. At the simplest level, the classical nuclei can be propagated classically on the ground-state NEO electron−proton vibronic potential energy surface. In this case, the vibronic potential energy surface implicitly includes the zero-point energies of the quantum nuclei and depends explicitly on only the classical nuclear coordinates. This approach relies on the Born−Oppenheimer separation between the quantum and classical nuclei. In order to account for non-Born−Oppenheimer effects between the quantum and classical nuclei, the classical nuclei can be propagated on potential energy surfaces that include the diagonal Born−Oppenheimer corrections. However, initial studies suggest that these diagonal Born−Oppenheimer corrections may not impact the NEO potential energy surfaces significantly for many types of systems.

A major advantage of the NEO approach is the inclusion of non-Born−Oppenheimer effects between the electrons and the quantum nuclei, as well as the ability to combine this approach with methods designed to include nonadiabatic effects between quantum and classical subsystems. To simulate nonadiabatic processes, surface hopping[259] or multiple spawning[260−262] methods can be used to incorporate nonadiabatic transitions between the electron−proton vibronic surfaces generated with NEO-TDDFT. Similar to conventional electronic TDDFT, the simulations could encounter difficulties if conical intersections between the ground and excited states play an important role.[267] Multicomponent analogues of spin-flip TDDFT and related methods may enable a proper description of conical intersections involving the ground state.[227]

Another exciting direction is the development of real-time NEO-TDDFT, an extension of the conventional electronic real-time TDDFT.[268,269] In the multicomponent extension, the time-dependent Schrödinger equation for electrons and quantum nuclei is integrated numerically. Recently, a real-time NEO-TDDFT approach was developed and implemented, highlighting the interplay between the electronic and nuclear quantum dynamics beyond the Born-Oppenheimer approximation.[270] This approach not only provides information about the dynamics of the electrons and quantum protons, but also can describe the nonadiabatic dynamics of the classical nuclei through Ehrenfest dynamics.[271] The combination of real-time NEO-TDDFT to describe the non-Born−Oppenheimer quantum dynamical effects between the electrons and quantum protons with Ehrenfest dynamics or other approaches to describe the nonadiabatic effects between the quantum and classical nuclei will be very powerful.

Given all of these exciting directions to explore, the future of multicomponent quantum chemistry is wide open for innovation and technical advances. Many of the multi-component methods are extensions of their conventional electronic counterparts. However, the additional complexity arising from treating both electrons and nuclei quantum mechanically on the same level often leads to technical challenges. Moreover, in some cases, methods that are effective for electron−electron correlation are not adequate for electron−proton correlation, requiring the development of new types of approaches. The efficient and accurate simulation of mixed nuclear-electronic quantum dynamics also requires creative solutions. Thus, multicomponent quantum chemistry provides many opportunities for the development of novel approaches to overcome the wide array of remaining challenges.

AUTHOR INFORMATION

Corresponding Author

Sharon Hammes-Schiffer − *Department of Chemistry, Yale University, New Haven, Connecticut 06520, United States;* orcid.org/0000-0002-3782-6995; Email: sharon.hammes-schiffer@yale.edu

Authors

Fabijan Pavošević − *Department of Chemistry, Yale University, New Haven, Connecticut 06520, United States*

Tanner Culpitt − *Department of Chemistry, Yale University, New Haven, Connecticut 06520, United States*

Complete contact information is available at: https://pubs.acs.org/10.1021/acs.chemrev.9b00798

Notes

The authors declare no competing financial interest.

Biographies

Fabijan Pavošević received his M.Sc. in Chemical Engineering from the University of Zagreb in 2009 and Ph.D. in Chemistry from Virginia Tech in 2017. His Ph.D. work under the supervision of Prof. Edward F. Valeev included development of explicitly correlated methods for large molecular systems. In 2018 he joined the laboratory of Prof. Hammes-Schiffer at Yale University where he is developing accurate multicomponent wave function based methods within the NEO framework.

Tanner Culpitt received his B.S. in Chemistry, with second and third majors in Physics and Applied Mathematics, respectively, from University of Wisconsin—La Crosse in 2014 and Ph.D. in Chemistry from University of Illinois at Urbana—Champaign in 2019 where he worked under the supervision of Prof. Hammes-Schiffer. His Ph.D. work included development of multicomponent DFT and TDDFT methods within the NEO framework. He is currently a postdoctoral associate at Yale University in the Hammes-Schiffer laboratory.

Sharon Hammes-Schiffer received her B.A. in Chemistry from Princeton University in 1988 and her Ph.D. in Chemistry from Stanford University in 1993, followed by two years at AT&T Bell Laboratories. She was the Clare Boothe Luce Assistant Professor at the University of Notre Dame from 1995 to 2000 and then became the Eberly Professor of Biotechnology at Pennsylvania State University until 2012, when she became the Swanlund Professor of Chemistry at the University of Illinois at Urbana—Champaign. Since 2018, she has been the John Gamble Kirkwood Professor of Chemistry at Yale University. Her research centers on the investigation of electron, proton, and proton-coupled electron transfer reactions in chemical, biological, and interfacial processes, with

https://dx.doi.org/10.1021/acs.chemrev.9b00798
Chem. Rev. XXXX, XXX, XXX−XXX

particular interests in quantum dynamical and non-Born−Oppenheimer effects. Her work encompasses the development of analytical theories and computational methods, as well as applications to a wide range of experimentally relevant systems.

ACKNOWLEDGMENTS

We are grateful for the important contributions to the NEO project from the following group members: Simon Webb, Tzvetelin Iordanov, Chet Swalina, Michael Pak, Andrès Reyes, Ari Chakraborty, Ben Auer, Anirban Hazra, Chaeyuk Ko, Andrew Sirjoosingh, Kurt Brorsen, Yang Yang, Patrick Schneider, Coraline (Zhen) Tao, Ben Rousseau, and Qi Yu. This work was supported by the National Science Foundation Grant No. CHE-1762018 and the U.S. Department of Energy, Office of Science, Offices of Basic Energy Sciences and Advanced Scientific Computing Research, Scientific Discovery through Advanced Computing (SciDAC).

ABBREVIATIONS

BCCD	Brueckner Coupled Cluster with Doubles
CASPT2	Complete Active Space Second-Order Perturbation Theory
CASSCF	Complete Active Space Self-Consistent Field
CCD	Coupled Cluster with Doubles
CCSD	Coupled Cluster with Singles and Doubles
CCSD(T)	Coupled Cluster with Singles, Doubles, and Perturbative Triples
CI	Configuration Interaction
CID	Configuration Interaction with Doubles
CIS	Configuration Interaction with Singles
CISD	Configuration Interaction with Singles and Doubles
DBOC	Diagonal Born−Oppenheimer Correction
DFT	Density Functional Theory
EOM-CCSD	Equation-of-Motion Coupled Cluster Singles and Doubles
epcX	Electron−Proton Correlation Functional Developed Year X
FCC	Full Coupled Cluster
FCI	Full Configuration Interaction
FGH	Fourier Grid Hamiltonian
FMO	Fragment Molecular Orbital
HF	Hartree−Fock
IRC	Intrinsic Reaction Coordinate
LDA	Local Density Approximation
LYP	Lee−Yang−Parr
MCTDH	Multiconfigurational Time-Dependent Hartree
MP2	Second-Order Møller−Plesset Perturbation Theory
MUE	Mean Unsigned Error
NEO	Nuclear-Electronic Orbital
NEO-DFT(V)	NEO-DFT for Vibrational Frequencies
NOCI	Nonorthogonal Configuration Interaction
OOCIS	Orbital-Optimized Configuration Interaction with Singles
OOCCD	Orbital-Optimized Coupled Cluster with Doubles
OOMP2	Orbital-Optimized Second-Order Møller−Plesset Perturbation Theory
PA	Proton Affinity
QM/MM	Quantum Mechanical/Molecular Mechanical
RMSD	Root-Mean-Square Deviation
RXCHF	Reduced Explicitly Correlated Hartree−Fock
SCF	Self-Consistent Field
SOS	Scaled-Opposite-Spin
TDA	Tamm−Dancoff Approximation
TDDFT	Time-Dependent Density Functional Theory
XCHF	Explicitly Correlated Hartree−Fock
ΔSCF	Delta Self-Consistent Field

REFERENCES

(1) Cha, Y.; Murray, C. J.; Klinman, J. P. Hydrogen Tunneling in Enzyme Reactions. *Science* **1989**, *243*, 1325−1330.
(2) Borgis, D.; Hynes, J. T. Dynamical Theory of Proton Tunneling Transfer Rates in Solution: General Formulation. *Chem. Phys.* **1993**, *170*, 315−346.
(3) Tuckerman, M. E.; Marx, D.; Klein, M. L.; Parrinello, M. On the Quantum Nature of the Shared Proton in Hydrogen Bonds. *Science* **1997**, *275*, 817−820.
(4) Raugei, S.; Klein, M. L. Nuclear Quantum Effects and Hydrogen Bonding in Liquids. *J. Am. Chem. Soc.* **2003**, *125*, 8992−8993.
(5) Skone, J. H.; Soudackov, A. V.; Hammes-Schiffer, S. Calculation of Vibronic Couplings for Phenoxyl/Phenol and Benzyl/Toluene Self-Exchange Reactions: Implications for Proton-Coupled Electron Transfer Mechanisms. *J. Am. Chem. Soc.* **2006**, *128*, 16655−16663.
(6) Sirjoosingh, A.; Hammes-Schiffer, S. Proton-Coupled Electron Transfer Versus Hydrogen Atom Transfer: Generation of Charge-Localized Diabatic States. *J. Phys. Chem. A* **2011**, *115*, 2367−2377.
(7) Hammes-Schiffer, S.; Stuchebrukhov, A. A. Theory of Coupled Electron and Proton Transfer Reactions. *Chem. Rev.* **2010**, *110*, 6939−6960.
(8) Warren, J. J.; Tronic, T. A.; Mayer, J. M. Thermochemistry of Proton-Coupled Electron Transfer Reagents and Its Implications. *Chem. Rev.* **2010**, *110*, 6961−7001.
(9) Weinberg, D. R.; Gagliardi, C. J.; Hull, J. F.; Murphy, C. F.; Kent, C. A.; Westlake, B. C.; Paul, A.; Ess, D. H.; McCafferty, D. G.; Meyer, T. J. Proton-Coupled Electron Transfer. *Chem. Rev.* **2012**, *112*, 4016−4093.
(10) Webb, S. P.; Iordanov, T.; Hammes-Schiffer, S. Multiconfigurational Nuclear-Electronic Orbital Approach: Incorporation of Nuclear Quantum Effects in Electronic Structure Calculations. *J. Chem. Phys.* **2002**, *117*, 4106−4118.
(11) Pak, M. V.; Chakraborty, A.; Hammes-Schiffer, S. Density Functional Theory Treatment of Electron Correlation in the Nuclear−Electronic Orbital Approach. *J. Phys. Chem. A* **2007**, *111*, 4522−4526.
(12) Chakraborty, A.; Pak, M. V.; Hammes-Schiffer, S. Development of Electron-Proton Density Functionals for Multicomponent Density Functional Theory. *Phys. Rev. Lett.* **2008**, *101*, 153001.
(13) Chakraborty, A.; Pak, M. V.; Hammes-Schiffer, S. Properties of the Exact Universal Functional in Multicomponent Density Functional Theory. *J. Chem. Phys.* **2009**, *131*, 124115.
(14) Sirjoosingh, A.; Pak, M. V.; Hammes-Schiffer, S. Derivation of an Electron−Proton Correlation Functional for Multicomponent Density Functional Theory within the Nuclear−Electronic Orbital Approach. *J. Chem. Theory Comput.* **2011**, *7*, 2689−2693.
(15) Sirjoosingh, A.; Pak, M. V.; Hammes-Schiffer, S. Multicomponent Density Functional Theory Study of the Interplay between Electron-Electron and Electron-Proton Correlation. *J. Chem. Phys.* **2012**, *136*, 174114.
(16) Yang, Y.; Brorsen, K. R.; Culpitt, T.; Pak, M. V.; Hammes-Schiffer, S. Development of a Practical Multicomponent Density Functional for Electron-Proton Correlation to Produce Accurate Proton Densities. *J. Chem. Phys.* **2017**, *147*, 114113.
(17) Brorsen, K. R.; Yang, Y.; Hammes-Schiffer, S. Multicomponent Density Functional Theory: Impact of Nuclear Quantum Effects on Proton Affinities and Geometries. *J. Phys. Chem. Lett.* **2017**, *8*, 3488−3493.

https://dx.doi.org/10.1021/acs.chemrev.9b00798
Chem. Rev. XXXX, XXX, XXX−XXX

(18) Brorsen, K. R.; Schneider, P. E.; Hammes-Schiffer, S. Alternative Forms and Transferability of Electron-Proton Correlation Functionals in Nuclear-Electronic Orbital Density Functional Theory. *J. Chem. Phys.* **2018**, *149*, 044110.
(19) Yang, Y.; Culpitt, T.; Hammes-Schiffer, S. Multicomponent Time-Dependent Density Functional Theory: Proton and Electron Excitation Energies. *J. Phys. Chem. Lett.* **2018**, *9*, 1765−1770.
(20) Tao, Z.; Yang, Y.; Hammes-Schiffer, S. Multicomponent Density Functional Theory: Including the Density Gradient in the Electron-Proton Correlation Functional for Hydrogen and Deuterium. *J. Chem. Phys.* **2019**, *151*, 124102.
(21) Culpitt, T.; Yang, Y.; Pavošević, F.; Tao, Z.; Hammes-Schiffer, S. Enhancing the Applicability of Multicomponent Time-Dependent Density Functional Theory. *J. Chem. Phys.* **2019**, *150*, 201101.
(22) Swalina, C.; Pak, M. V.; Hammes-Schiffer, S. Alternative Formulation of Many-Body Perturbation Theory for Electron-Proton Correlation. *Chem. Phys. Lett.* **2005**, *404*, 394−399.
(23) Pavošević, F.; Culpitt, T.; Hammes-Schiffer, S. Multicomponent Coupled Cluster Singles and Doubles Theory within the Nuclear-Electronic Orbital Framework. *J. Chem. Theory Comput.* **2019**, *15*, 338−347.
(24) Pavošević, F.; Hammes-Schiffer, S. Multicomponent Equation-of-Motion Coupled Cluster Singles and Doubles: Theory and Calculation of Excitation Energies for Positronium Hydride. *J. Chem. Phys.* **2019**, *150*, 161102.
(25) Pavošević, F.; Hammes-Schiffer, S. Multicomponent Coupled Cluster Singles and Doubles and Brueckner Doubles Methods: Proton Densities and Energies. *J. Chem. Phys.* **2019**, *151*, 074104.
(26) Pavošević, F.; Rousseau, B. J. G.; Hammes-Schiffer, S. Multicomponent Orbital-Optimized Perturbation Theory Methods: Approaching Coupled Cluster Accuracy at Lower Cost. *J. Phys. Chem. Lett.* **2020**, *11*, 1578−1583.
(27) Schneider, P. E.; Pavošević, F.; Hammes-Schiffer, S. Diagonal Born-Oppenheimer Corrections within the Nuclear-Electronic Orbital Framework. *J. Phys. Chem. Lett.* **2019**, *10*, 4639−4643.
(28) Thomas, I. L. Protonic Structure of Molecules. I. Ammonia Molecules. *Phys. Rev.* **1969**, *185*, 90.
(29) Nakai, H.; Sodeyama, K.; Hoshino, M. Non-Born-Oppenheimer Theory for Simultaneous Determination of Vibrational and Electronic Excited States: Ab Initio NO+MO/CIS Theory. *Chem. Phys. Lett.* **2001**, *345*, 118−124.
(30) Nakai, H. Simultaneous Determination of Nuclear and Electronic Wave Functions without Born-Oppenheimer Approximation: Ab Initio NO+MO/HF Theory. *Int. J. Quantum Chem.* **2002**, *86*, 511−517.
(31) Nakai, H.; Sodeyama, K. Many-Body Effects in Nonadiabatic Molecular Theory for Simultaneous Determination of Nuclear and Electronic Wave Functions: Ab Initio NOM/MBPT and CC Methods. *J. Chem. Phys.* **2003**, *118*, 1119−1127.
(32) Imamura, Y.; Kiryu, H.; Nakai, H. Colle-Salvetti-Type Correction for Electron−Nucleus Correlation in the Nuclear Orbital Plus Molecular Orbital Theory. *J. Comput. Chem.* **2008**, *29*, 735−740.
(33) Imamura, Y.; Tsukamoto, Y.; Kiryu, H.; Nakai, H. Extension of Density Functional Theory to Nuclear Orbital Plus Molecular Orbital Theory: Self-Consistent Field Calculations with the Colle−Salvetti Electron−Nucleus Correlation Functional. *Bull. Chem. Soc. Jpn.* **2009**, *82*, 1133−1139.
(34) Hoshino, M.; Nishizawa, H.; Nakai, H. Rigorous Non-Born-Oppenheimer Theory: Combination of Explicitly Correlated Gaussian Method and Nuclear Orbital Plus Molecular Orbital Theory. *J. Chem. Phys.* **2011**, *135*, 024111.
(35) Tsukamoto, Y.; Ikabata, Y.; Romero, J.; Reyes, A.; Nakai, H. The Divide-and-Conquer Second-Order Proton Propagator Method Based on Nuclear Orbital Plus Molecular Orbital Theory for the Efficient Computation of Proton Binding Energies. *Phys. Chem. Chem. Phys.* **2016**, *18*, 27422−27431.
(36) Tachikawa, M.; Mori, K.; Nakai, H.; Iguchi, K. An Extension of Ab Initio Molecular Orbital Theory to Nuclear Motion. *Chem. Phys. Lett.* **1998**, *290*, 437−442.
(37) Tachikawa, M. Simultaneous Optimization of Gaussian Type Function Exponents for Electron and Positron with Full-CI Wavefunction – Application to Ground and Excited States of Positronic Compounds with Multi-Component Molecular Orbital Approach. *Chem. Phys. Lett.* **2001**, *350*, 269−276.
(38) Shibl, M. F.; Tachikawa, M.; Kuhn, O. The Geometric (H/D) Isotope Effect in Porphycene: Grid-Based Born-Oppenheimer Vibrational Wavefunctions vs. Multi-Component Molecular Orbital Theory. *Phys. Chem. Chem. Phys.* **2005**, *7*, 1368−1373.
(39) Udagawa, T.; Tachikawa, M. H/D Isotope Effect on Porphine and Porphycene Molecules with Multicomponent Hybrid Density Functional Theory. *J. Chem. Phys.* **2006**, *125*, 244105.
(40) Ishimoto, T.; Tachikawa, M.; Nagashima, U. Electron-Electron and Electron-Nucleus Correlation Effects on Exponent Values of Gaussian-Type Functions for Quantum Protons and Deuterons. *J. Chem. Phys.* **2006**, *125*, 144103.
(41) Ishimoto, T.; Tachikawa, M.; Nagashima, U. A Fragment Molecular-Orbital-Multicomponent Molecular-Orbital Method for Analyzing H/D Isotope Effects in Large Molecules. *J. Chem. Phys.* **2006**, *124*, 014112.
(42) Ishimoto, T.; Tachikawa, M.; Nagashima, U. Review of Multicomponent Molecular Orbital Method for Direct Treatment of Nuclear Quantum Effect. *Int. J. Quantum Chem.* **2009**, *109*, 2677−2694.
(43) Udagawa, T.; Tsuneda, T.; Tachikawa, M. Electron-Nucleus Correlation Functional for Multicomponent Density-Functional Theory. *Phys. Rev. A: At., Mol., Opt. Phys.* **2014**, *89*, 052519.
(44) Kanematsu, Y.; Tachikawa, M. Development of Multicomponent Hybrid Density Functional Theory with Polarizable Continuum Model for the Analysis of Nuclear Quantum Effect and Solvent Effect on NMR Chemical Shift. *J. Chem. Phys.* **2014**, *140*, 164111.
(45) Udagawa, T.; Tsuneda, T.; Tachikawa, M. Electron-Nucleus Correlation Functional for Multicomponent Density-Functional Theory. *Phys. Rev. A: At., Mol., Opt. Phys.* **2014**, *89*, 052519.
(46) Bochevarov, A. D.; Valeev, E. F.; Sherrill, C. D. The Electron and Nuclear Orbitals Model: Current Challenges and Future Prospects. *Mol. Phys.* **2004**, *102*, 111−123.
(47) Kreibich, T.; van Leeuwen, R.; Gross, E. Multicomponent Density-Functional Theory for Electrons and Nuclei. *Phys. Rev. A: At., Mol., Opt. Phys.* **2008**, *78*, 022501.
(48) Reyes, A.; Pak, M. V.; Hammes-Schiffer, S. Investigation of Isotope Effects with the Nuclear-Electronic Orbital Approach. *J. Chem. Phys.* **2005**, *123*, 064104.
(49) González, S. A.; Aguirre, N. F.; Reyes, A. Theoretical Investigation of Isotope Effects: The Any-Particle Molecular Orbital Code. *Int. J. Quantum Chem.* **2008**, *108*, 1742−1749.
(50) Flores-Moreno, R.; Posada, E.; Moncada, F.; Romero, J.; Charry, J.; Díaz-Tinoco, M.; González, S. A.; Aguirre, N. F.; Reyes, A. LOWDIN: The Any Particle Molecular Orbital Code. *Int. J. Quantum Chem.* **2014**, *114*, 50−56.
(51) Goli, M.; Shahbazian, S. The Two-Component Quantum Theory of Atoms in Molecules (TC-QTAIM): Foundations. *Theor. Chem. Acc.* **2013**, *132*, 1362.
(52) Tachikawa, M. Simultaneous Optimization of Gaussian Type Function Exponents for Electron and Positron with Full-CI Wavefunction−Application to Ground and Excited States of Positronic Compounds with Multi-Component Molecular Orbital Approach. *Chem. Phys. Lett.* **2001**, *350*, 269−276.
(53) Adamson, P. E.; Duan, X. F.; Burggraf, L. W.; Pak, M. V.; Swalina, C.; Hammes-Schiffer, S. Modeling Positrons in Molecular Electronic Structure Calculations with the Nuclear-Electronic Orbital Method. *J. Phys. Chem. A* **2008**, *112*, 1346−1351.
(54) Pak, M. V.; Chakraborty, A.; Hammes-Schiffer, S. Calculation of the Positron Annihilation Rate in PsH with the Positronic Extension of the Explicitly Correlated Nuclear−Electronic Orbital Method. *J. Phys. Chem. A* **2009**, *113*, 4004−4008.

https://dx.doi.org/10.1021/acs.chemrev.9b00798
Chem. Rev. XXXX, XXX, XXX−XXX

(55) Sirjoosingh, A.; Pak, M. V.; Hammes-Schiffer, S. Analysis of Electron-Positron Wavefunctions in the Nuclear-Electronic Orbital Framework. *J. Chem. Phys.* **2012**, *136*, 174114.
(56) Moncada, F.; Cruz, D.; Reyes, A. Muonic Alchemy: Transmuting Elements with the Inclusion of Negative Muons. *Chem. Phys. Lett.* **2012**, *539*, 209−213.
(57) Sirjoosingh, A.; Pak, M. V.; Swalina, C.; Hammes-Schiffer, S. Reduced Explicitly Correlated Hartree-Fock Approach within the Nuclear-Electronic Orbital Framework: Applications to Positronic Molecular Systems. *J. Chem. Phys.* **2013**, *139*, 034103.
(58) Moncada, F.; Cruz, D.; Reyes, A. Electronic Properties of Atoms and Molecules Containing One and Two Negative Muons. *Chem. Phys. Lett.* **2013**, *570*, 16−21.
(59) Posada, E.; Moncada, F. l.; Reyes, A. s. Negative Muon Chemistry: The Quantum Muon Effect and the Finite Nuclear Mass Effect. *J. Phys. Chem. A* **2014**, *118*, 9491−9499.
(60) Brorsen, K. R.; Pak, M. V.; Hammes-Schiffer, S. Calculation of Positron Binding Energies and Electron−Positron Annihilation Rates for Atomic Systems with the Reduced Explicitly Correlated Hartree−Fock Method in the Nuclear−Electronic Orbital Framework. *J. Phys. Chem. A* **2017**, *121*, 515−522.
(61) Charry, J.; Varella, M. T. d. N.; Reyes, A. Binding Matter with Antimatter: The Covalent Positron Bond. *Angew. Chem., Int. Ed.* **2018**, *57*, 8859−8864.
(62) Sirjoosingh, A.; Pak, M. V.; Swalina, C.; Hammes-Schiffer, S. Reduced Explicitly Correlated Hartree-Fock Approach within the Nuclear-Electronic Orbital Framework: Theoretical Formulation. *J. Chem. Phys.* **2013**, *139*, 034102.
(63) Brorsen, K. R.; Sirjoosingh, A.; Pak, M. V.; Hammes-Schiffer, S. Nuclear-Electronic Orbital Reduced Explicitly Correlated Hartree-Fock Approach: Restricted Basis Sets and Open-Shell Systems. *J. Chem. Phys.* **2015**, *142*, 214108.
(64) Ellis, B. H.; Aggarwal, S.; Chakraborty, A. Development of the Multicomponent Coupled-Cluster Theory for Investigation of Multiexcitonic Interactions. *J. Chem. Theory Comput.* **2016**, *12*, 188−200.
(65) Ellis, B. H.; Chakraborty, A. Investigation of Many-Body Correlation in Biexcitonic Systems Using Electron−Hole Multicomponent Coupled-Cluster Theory. *J. Phys. Chem. C* **2017**, *121*, 1291−1298.
(66) Scheu, C. E.; Kinghorn, D. B.; Adamowicz, L. Non-Born-Oppenheimer Calculations on the LiH Molecule with Explicitly Correlated Gaussian Functions. *J. Chem. Phys.* **2001**, *114*, 3393−3397.
(67) Cafiero, M.; Bubin, S.; Adamowicz, L. Non-Born-Oppenheimer Calculations of Atoms and Molecules. *Phys. Chem. Chem. Phys.* **2003**, *5*, 1491−1501.
(68) Bubin, S.; Adamowicz, L. Non-Born-Oppenheimer Study of Positronic Molecular Systems: e^+LiH. *J. Chem. Phys.* **2004**, *120*, 6051−6055.
(69) Bubin, S.; Adamowicz, L. Nonrelativistic Molecular Quantum Mechanics without Approximations: Electron Affinities of LiH and LiD. *J. Chem. Phys.* **2004**, *121*, 6249−6253.
(70) Bubin, S.; Cafiero, M.; Adamowicz, L. Non-Born-Oppenheimer Variational Calculations of Atoms and Molecules with Explicitly Correlated Gaussian Basis Functions. *Adv. Chem. Phys.* **2005**, *131*, 377−475.
(71) Bubin, S.; Adamowicz, L. Nonrelativistic Variational Calculations of the Positronium Molecule and the Positronium Hydride. *Phys. Rev. A: At., Mol., Opt. Phys.* **2006**, *74*, 052502.
(72) Bubin, S.; Pavanello, M.; Tung, W.-C.; Sharkey, K. L.; Adamowicz, L. Born-Oppenheimer and Non-Born-Oppenheimer, Atomic and Molecular Calculations with Explicitly Correlated Gaussians. *Chem. Rev.* **2013**, *113*, 36−79.
(73) Mitroy, J.; Bubin, S.; Horiuchi, W.; Suzuki, Y.; Adamowicz, L.; Cencek, W.; Szalewicz, K.; Komasa, J.; Blume, D.; Varga, K. Theory and Application of Explicitly Correlated Gaussians. *Rev. Mod. Phys.* **2013**, *85*, 693.
(74) Bubin, S.; Formanek, M.; Adamowicz, L. Universal All-Particle Explicitly-Correlated Gaussians for Non-Born−Oppenheimer Calculations of Molecular Rotationless States. *Chem. Phys. Lett.* **2016**, *647*, 122−126.
(75) Bubin, S.; Stanke, M.; Adamowicz, L. Relativistic Corrections for Non-Born-Oppenheimer Molecular Wave Functions Expanded in Terms of Complex Explicitly Correlated Gaussian Functions. *Phys. Rev. A: At., Mol., Opt. Phys.* **2017**, *95*, 062509.
(76) Chavez, E. M.; Bubin, S.; Adamowicz, L. Implementation of Explicitly Correlated Complex Gaussian Functions in Calculations of Molecular Rovibrational J= 1 States without Born-Oppenheimer Approximation. *Chem. Phys. Lett.* **2019**, *717*, 147−151.
(77) Hohenberg, P.; Kohn, W. Inhomogeneous Electron Gas. *Phys. Rev.* **1964**, *136*, B864.
(78) Kohn, W.; Sham, L. J. Self-Consistent Equations Including Exchange and Correlation Effects. *Phys. Rev.* **1965**, *140*, A1133.
(79) Capitani, J. F.; Nalewajski, R. F.; Parr, R. G. Non-Born-Oppenheimer Density Functional Theory of Molecular Systems. *J. Chem. Phys.* **1982**, *76*, 568−573.
(80) Gidopoulos, N. Kohn-Sham Equations for Multicomponent Systems: The Exchange and Correlation Energy Functional. *Phys. Rev. B: Condens. Matter Mater. Phys.* **1998**, *57*, 2146.
(81) Kreibich, T.; Gross, E. Multicomponent Density-Functional Theory for Electrons and Nuclei. *Phys. Rev. Lett.* **2001**, *86*, 2984.
(82) Nieminen, R. M.; Boronski, E.; Lantto, L. J. Two-Component Density-Functional Theory: Application to Positron States. *Phys. Rev. B: Condens. Matter Mater. Phys.* **1985**, *32*, 1377.
(83) Boroński, E.; Nieminen, R. M. Electron-Positron Density-Functional Theory. *Phys. Rev. B: Condens. Matter Mater. Phys.* **1986**, *34*, 3820.
(84) van Leeuwen, R.; Gross, E., Multicomponent Density-Functional Theory. In *Time-Dependent Density Functional Theory*; Springer: 2006; pp 93−106.
(85) Butriy, O.; Ebadi, H.; de Boeij, P.; van Leeuwen, R.; Gross, E. Multicomponent Density-Functional Theory for Time-Dependent Systems. *Phys. Rev. A: At., Mol., Opt. Phys.* **2007**, *76*, 052514.
(86) Schweizer, K. S.; Stratt, R. M.; Chandler, D.; Wolynes, P. G. Convenient and Accurate Discretized Path Integral Methods for Equilibrium Quantum Mechanical Calculations. *J. Chem. Phys.* **1981**, *75*, 1347−1364.
(87) Marchi, M.; Chandler, D. Path-Integral Calculation of the Tunnel Splitting in Aqueous Ferrous-Ferric Electron Transfer. *J. Chem. Phys.* **1991**, *95*, 889−894.
(88) Cao, J. S.; Voth, G. A. The Formulation of Quantum Statistical Mechanics Based on the Feynman Path Centroid Density I: Equilibrium Properties. *J. Chem. Phys.* **1994**, *100*, 5093−5105.
(89) Cao, J. S.; Voth, G. A. The Formulation of Quantum Statistical Mechanics Based on the Feynman Path Centroid Density II: Dynamical Properties. *J. Chem. Phys.* **1994**, *100*, 5106−5117.
(90) Cao, J. S.; Voth, G. A. The Formulation of Quantum Statistical Mechanics Based on the Feynman Path Centroid Density III: Phase Space Formalism and Analysis of Centroid Molecular Dynamics. *J. Chem. Phys.* **1994**, *101*, 6157−6167.
(91) Cao, J. S.; Voth, G. A. The Formulation of Quantum Statistical Mechanics Based on the Feynman Path Centroid Density IV: Algorithms for Centroid Molecular Dynamics. *J. Chem. Phys.* **1994**, *101*, 6168−6183.
(92) Jang, S.; Voth, G. A. A Derivation of Centroid Molecular Dynamics and Other Approximate Time Evolution Methods for Path Integral Centroid Variables. *J. Chem. Phys.* **1999**, *111*, 2371−2384.
(93) Craig, I. R.; Manolopoulos, D. E. Chemical Reaction Rates from Ring Polymer Molecular Dynamics. *J. Chem. Phys.* **2005**, *122*, 084106.
(94) Shushkov, P.; Li, R.; Tully, J. C. Ring Polymer Molecular Dynamics with Surface Hopping. *J. Chem. Phys.* **2012**, *137*, 22A549.
(95) Habershon, S.; Manolopoulos, D. E.; Markland, T. E.; Miller, T. F., III Ring-Polymer Molecular Dynamics: Quantum Effects in Chemical Dynamics from Classical Trajectories in an Extended Phase Space. *Annu. Rev. Phys. Chem.* **2013**, *64*, 387−413.

https://dx.doi.org/10.1021/acs.chemrev.9b00798
Chem. Rev. XXXX, XXX, XXX−XXX

(96) Ananth, N. Mapping Variable Ring Polymer Molecular Dynamics: A Path-Integral Based Method for Nonadiabatic Processes. *J. Chem. Phys.* **2013**, *139*, 124102.
(97) Richardson, J. O.; Thoss, M. Communication: Nonadiabatic Ring-Polymer Molecular Dynamics. *J. Chem. Phys.* **2013**, *139*, 031102.
(98) Makri, N. Quantum-Classical Path Integral: A Rigorous Approach to Condensed Phase Dynamics. *Int. J. Quantum Chem.* **2015**, *115*, 1209−1214.
(99) Kretchmer, J. S.; Miller, T. F., III Kinetically-Constrained Ring-Polymer Molecular Dynamics for Non-Adiabatic Chemistries Involving Solvent and Donor-Acceptor Dynamical Effects. *Faraday Discuss.* **2016**, *195*, 191−214.
(100) Shakib, F. A.; Huo, P. Ring Polymer Surface Hopping: Incorporating Nuclear Quantum Effects into Nonadiabatic Molecular Dynamics Simulations. *J. Phys. Chem. Lett.* **2017**, *8*, 3073−3080.
(101) Makri, N. Modular Path Integral Methodology for Real-Time Quantum Dynamics. *J. Chem. Phys.* **2018**, *149*, 214108.
(102) Tao, X.; Shushkov, P.; Miller, T. F., III Path-Integral Isomorphic Hamiltonian for Including Nuclear Quantum Effects in Non-Adiabatic Dynamics. *J. Chem. Phys.* **2018**, *148*, 102327.
(103) Markland, T. E.; Ceriotti, M. Nuclear Quantum Effects Enter the Mainstream. *Nat. Rev. Chem.* **2018**, *2*, 0109.
(104) Chowdhury, S. N.; Huo, P. State Dependent Ring Polymer Molecular Dynamics for Investigating Excited Nonadiabatic Dynamics. *J. Chem. Phys.* **2019**, *150*, 244102.
(105) Deumens, E.; Diz, A.; Longo, R.; Ohrn, Y. Time-Dependent Theoretical Treatments of the Dynamics of Electrons and Nuclei in Molecular Systems. *Rev. Mod. Phys.* **1994**, *66*, 917−983.
(106) Deumens, E.; Ohrn, Y. Complete Electron Nuclear Dynamics. *J. Phys. Chem. A* **2001**, *105*, 2660−2667.
(107) Iyengar, S. S.; Jakowski, J. Quantum Wave Packet Ab Initio Molecular Dynamics: An Approach to Study Quantum Dynamics in Large Systems. *J. Chem. Phys.* **2005**, *122*, 114105.
(108) Iyengar, S. S. Ab Initio Dynamics with Wave Packets and Density Matrices. *Theor. Chem. Acc.* **2006**, *116*, 326−337.
(109) Li, J.; Li, X.; Iyengar, S. S. Vibrational Properties of Hydrogen-Bonded Systems Using the Multireference Generalization to the "on-the-Fly" Electronic Structure within Quantum Wavepacket Ab Initio Molecular Dynamics (QWAIMD). *J. Chem. Theory Comput.* **2014**, *10*, 2265−2280.
(110) Beck, M. H.; Jäckle, A.; Worth, G. A.; Meyer, H.-D. The Multiconfiguration Time-Dependent Hartree (MCTDH) Method: A Highly Efficient Algorithm for Propagating Wavepackets. *Phys. Rep.* **2000**, *324*, 1−105.
(111) Worth, G. A.; Meyer, H.-D.; Koppel, H.; Cederbaum, L. S.; Burghardt, I. Using the MCTDH Wavepacket Propagation Method to Describe Multimode Non-Adiabatic Dynamics. *Int. Rev. Phys. Chem.* **2008**, *27*, 569−606.
(112) Manthe, U. A Multilayer Multiconfigurational Time-Dependent Hartree Approach for Quantum Dynamics on General Potential Energy Surfaces. *J. Chem. Phys.* **2008**, *128*, 164116.
(113) Kylänpää, I.; Leino, M.; Rantala, T. T. Hydrogen Molecule Ion: Path-Integral Monte Carlo Approach. *Phys. Rev. A: At., Mol., Opt. Phys.* **2007**, *76*, 052508.
(114) Kylänpää, I.; Rantala, T. T. Finite Temperature Quantum Statistics of H_3^+ Molecular Ion. *J. Chem. Phys.* **2010**, *133*, 044312.
(115) Kylänpää, I.; Rantala, T. T. First-Principles Simulation of Molecular Dissociation−Recombination Equilibrium. *J. Chem. Phys.* **2011**, *135*, 104310.
(116) Tubman, N. M.; Kylänpää, I.; Hammes-Schiffer, S.; Ceperley, D. M. Beyond the Born-Oppenheimer Approximation with Quantum Monte Carlo Methods. *Phys. Rev. A: At., Mol., Opt. Phys.* **2014**, *90*, 042507.
(117) Yang, Y.; Kylänpää, I.; Tubman, N. M.; Krogel, J. T.; Hammes-Schiffer, S.; Ceperley, D. M. How Large Are Nonadiabatic Effects in Atomic and Diatomic Systems? *J. Chem. Phys.* **2015**, *143*, 124308.
(118) Swalina, C.; Pak, M. V.; Chakraborty, A.; Hammes-Schiffer, S. Explicit Dynamical Electron-Proton Correlation in the Nuclear-Electronic Orbital Framework. *J. Phys. Chem. A* **2006**, *110*, 9983−9987.
(119) Chakraborty, A.; Pak, M. V.; Hammes-Schiffer, S. Inclusion of Explicit Electron-Proton Correlation in the Nuclear-Electronic Orbital Approach Using Gaussian-Type Geminal Functions. *J. Chem. Phys.* **2008**, *129*, 014101.
(120) Sirjoosingh, A.; Pak, M. V.; Brorsen, K. R.; Hammes-Schiffer, S. Quantum Treatment of Protons with the Reduced Explicitly Correlated Hartree-Fock Approach. *J. Chem. Phys.* **2015**, *142*, 214107.
(121) Yang, Y.; Schneider, P. E.; Culpitt, T.; Pavošević, F.; Hammes-Schiffer, S. Molecular Vibrational Frequencies within the Nuclear−Electronic Orbital Framework. *J. Phys. Chem. Lett.* **2019**, *10*, 1167−1172.
(122) Culpitt, T.; Yang, Y.; Schneider, P. E.; Pavošević, F.; Hammes-Schiffer, S. Molecular Vibrational Frequencies with Multiple Quantum Protons within the Nuclear-Electronic Orbital Framework. *J. Chem. Theory Comput.* **2019**, *15*, 6840−6849.
(123) Skone, J. H.; Pak, M. V.; Hammes-Schiffer, S. Nuclear-Electronic Orbital Nonorthogonal Configuration Interaction Approach. *J. Chem. Phys.* **2005**, *123*, 134108.
(124) Hazra, A.; Skone, J. H.; Hammes-Schiffer, S. Combining the Nuclear-Electronic Orbital Approach with Vibronic Coupling Theory: Calculation of the Tunneling Splitting for Malonaldehyde. *J. Chem. Phys.* **2009**, *130*, 054108.
(125) Szabo, A.; Ostlund, N. S. *Modern Quantum Chemistry*; McGraw-Hill, Inc.: New York, 1989.
(126) Feller, D. F.; Ruedenberg, K. Systematic Approach to Extended Even-Tempered Orbital Bases for Atomic and Molecular Calculations. *Theor. Chim. Acta* **1979**, *52*, 231−251.
(127) Auer, B.; Hammes-Schiffer, S. Localized Hartree Product Treatment of Multiple Protons in the Nuclear-Electronic Orbital Framework. *J. Chem. Phys.* **2010**, *132*, 084110.
(128) Tachikawa, M.; Mori, K.; Osamura, Y. Isotope Effect of Hydrated Clusters of Hydrogen Chloride, $HCl(H_2O)_n$ and $DCl(H_2O)_n$ (n = 0−4): Application of Dynamic Extended Molecular Orbital Method. *Mol. Phys.* **1999**, *96*, 1207−1215.
(129) Tachikawa, M. Isotope Effect and Cluster Size Dependence for Water and Hydrated Hydrogen Halide Clusters: Multi-Component Molecular Orbital Approach. *Mol. Phys.* **2002**, *100*, 881−901.
(130) Udagawa, T.; Ishimoto, T.; Tokiwa, H.; Tachikawa, M.; Nagashima, U. The Geometrical Isotope Effect of C-H—O Type Hydrogen Bonds Revealed by Multi-Component Molecular Orbital Calculation. *Chem. Phys. Lett.* **2004**, *389*, 236−240.
(131) Reyes, A.; Moncada, F.; Charry, J. The Any Particle Molecular Orbital Approach: A Short Review of the Theory and Applications. *Int. J. Quantum Chem.* **2019**, *119*, No. e25705.
(132) Marston, C. C.; Balint-Kurti, G. G. The Fourier Grid Hamiltonian Method for Bound State Eigenvalues and Eigenfunctions. *J. Chem. Phys.* **1989**, *91*, 3571−3576.
(133) Webb, S. P.; Hammes-Schiffer, S. Fourier Grid Hamiltonian Multiconfigurational Self-Consistent-Field: A Method to Calculate Multidimensional Hydrogen Vibrational Wavefunctions. *J. Chem. Phys.* **2000**, *113*, 5214−5227.
(134) Rychlewski, J. *Explicitly Correlated Wave Functions in Chemistry and Physics: Theory and Applications*; Kluwer Academic Publishers: Dordrecht, 2003.
(135) Ryzhikh, G.; Mitroy, J.; Varga, K. The Structure of Exotic Atoms Containing Positrons and Positronium. *J. Phys. B: At., Mol. Opt. Phys.* **1998**, *31*, 3965.
(136) Mitroy, J.; Bromley, M. W. J.; Ryzhikh, G. G. Positron and Positronium Binding to Atoms. *J. Phys. B: At., Mol. Opt. Phys.* **2002**, *35*, R81−R116.
(137) Mitroy, J. Expectation Values of the e^+Li System. *Phys. Rev. A: At., Mol., Opt. Phys.* **2004**, *70*, 024502.
(138) Bromley, M. W.; Mitroy, J. Large-Dimension Configuration-Interaction Calculations of Positron Binding to the Group-II Atoms. *Phys. Rev. A: At., Mol., Opt. Phys.* **2006**, *73*, 032507.

https://dx.doi.org/10.1021/acs.chemrev.9b00798
Chem. Rev. XXXX, XXX, XXX−XXX

(139) Mitroy, J. Energy and Expectation Values of the PsH System. *Phys. Rev. A: At., Mol., Opt. Phys.* **2006**, *73*, 054502.
(140) Mitroy, J.; Bromley, M. W. J. Convergence of Configuration-Interaction Single-Center Calculations of Positron-Atom Interactions. *Phys. Rev. A: At., Mol., Opt. Phys.* **2006**, *73*, 052712.
(141) Mitroy, J. Structure of the LiPs and e^+Be Systems. *J. At. Mol. Sci.* **2018**, *1*, 275−279.
(142) Shigeta, Y.; Takahashi, H.; Yamanaka, S.; Mitani, M.; Nagao, H.; Yamaguchi, K. Density Functional Theory without the Born−Oppenheimer Approximation and Its Application. *Int. J. Quantum Chem.* **1998**, *70*, 659−669.
(143) Culpitt, T.; Brorsen, K. R.; Pak, M. V.; Hammes-Schiffer, S. Multicomponent Density Functional Theory Embedding Formulation. *J. Chem. Phys.* **2016**, *145*, 044106.
(144) Colle, R.; Salvetti, O. Approximate Calculation of the Correlation Energy for the Closed Shells. *Theor. Chem. Acc.* **1975**, *37*, 329−334.
(145) Lee, C.; Yang, W.; Parr, R. G. Development of the Colle-Salvetti Correlation-Energy Formula into a Functional of the Electron Density. *Phys. Rev. B: Condens. Matter Mater. Phys.* **1988**, *37*, 785.
(146) Becke, A. D. Density-Functional Exchange-Energy Approximation with Correct Asymptotic Behavior. *Phys. Rev. A: At., Mol., Opt. Phys.* **1988**, *38*, 3098.
(147) Becke, A. D. Density-Functional Thermochemistry. III. The Role of Exact Exchange. *J. Chem. Phys.* **1993**, *98*, 5648−5652.
(148) Romero, J.; Posada, E.; Flores-Moreno, R.; Reyes, A. A Generalized Any Particle Propagator Theory: Assessment of Nuclear Quantum Effects on Electron Propagator Calculations. *J. Chem. Phys.* **2012**, *137*, 074105.
(149) Díaz-Tinoco, M.; Romero, J.; Ortiz, J.; Reyes, A.; Flores-Moreno, R. A Generalized Any-Particle Propagator Theory: Prediction of Proton Affinities and Acidity Properties with the Proton Propagator. *J. Chem. Phys.* **2013**, *138*, 194108.
(150) Romero, J.; Charry, J. A.; Nakai, H.; Reyes, A. Improving Quasiparticle Second Order Electron Propagator Calculations with the Spin-Component-Scaled Technique. *Chem. Phys. Lett.* **2014**, *591*, 82−87.
(151) Romero, J.; Charry, J. A.; Flores-Moreno, R.; Varella, M. T. d. N.; Reyes, A. Calculation of Positron Binding Energies Using the Generalized Any Particle Propagator Theory. *J. Chem. Phys.* **2014**, *141*, 114103.
(152) Pedraza-González, L.; Romero, J.; Alí-Torres, J.; Reyes, A. Prediction of Proton Affinities of Organic Molecules Using the Any-Particle Molecular-Orbital Second-Order Proton Propagator Approach. *Phys. Chem. Chem. Phys.* **2016**, *18*, 27185−27189.
(153) Slater, J. C.; Phillips, J. C. Quantum Theory of Molecules and Solids Vol. 4: The Self-Consistent Field for Molecules and Solids. *Phys. Today* **1974**, *27*, 49.
(154) Vosko, S. H.; Wilk, L.; Nusair, M. Accurate Spin-Dependent Electron Liquid Correlation Energies for Local Spin Density Calculations: A Critical Analysis. *Can. J. Phys.* **1980**, *58*, 1200−1211.
(155) Runge, E.; Gross, E. K. Density-Functional Theory for Time-Dependent Systems. *Phys. Rev. Lett.* **1984**, *52*, 997.
(156) Gross, E.; Kohn, W. Time-Dependent Density-Functional Theory. *Adv. Quantum Chem.* **1990**, *21*, 255−291.
(157) Casida, M. E. Time-Dependent Density-Functional Response Theory for Molecules. In *Recent Advances in Density Functional Methods, Part I*; Chong, D. P., Ed.; World Scientific: Singapore, 1995; pp 155−192.
(158) Stratmann, R. E.; Scuseria, G. E.; Frisch, M. J. An Efficient Implementation of Time-Dependent Density-Functional Theory for the Calculation of Excitation Energies of Large Molecules. *J. Chem. Phys.* **1998**, *109*, 8218−8224.
(159) Furche, F.; Ahlrichs, R. Adiabatic Time-Dependent Density Functional Methods for Excited State Properties. *J. Chem. Phys.* **2002**, *117*, 7433−7447.
(160) Maitra, N. T.; Zhang, F.; Cave, R. J.; Burke, K. Double Excitations within Time-Dependent Density Functional Theory Linear Response. *J. Chem. Phys.* **2004**, *120*, 5932−5937.
(161) Dreuw, A.; Head-Gordon, M. Single-Reference Ab Initio Methods for the Calculation of Excited States of Large Molecules. *Chem. Rev.* **2005**, *105*, 4009−4037.
(162) Elliott, P.; Furche, F.; Burke, K. Excited States from Time-Dependent Density Functional Theory. In *Rev. Comp. Chem.*; Lipkowitz, K. B., Cundari, T. R., Eds.; Wiley: New York, 2008; Vol. *26*, p 91.
(163) Casida, M. E.; Huix-Rotllant, M. Progress in Time-Dependent Density-Functional Theory. *Annu. Rev. Phys. Chem.* **2012**, *63*, 287−323.
(164) Marques, M. A. L.; Maitra, N. T.; Nogueira, F. M. S.; Gross, E. K. U.; Rubio, A. *Fundamentals of Time-Dependent Density Functional Theory*; Springer: Heidelberg, 2012.
(165) Yang, Y.; Culpitt, T.; Tao, Z.; Hammes-Schiffer, S. Stability Conditions and Local Minima in Multicomponent Hartree-Fock and Density Functional Theory. *J. Chem. Phys.* **2018**, *149*, 084105.
(166) Iordanov, T.; Hammes-Schiffer, S. Vibrational Analysis for the Nuclear-Electronic Orbital (NEO) Method. *J. Chem. Phys.* **2003**, *118*, 9489−9496.
(167) Xu, X.; Yang, Y. Constrained Nuclear-Electronic Orbital Density Functional Theory: Energy Surfaces with Nuclear Quantum Effects. *J. Chem. Phys.* **2020**, *152*, 084107.
(168) Barone, V.; Bloino, J.; Guido, C. A.; Lipparini, F. A Fully Automated Implementation of VPT2 Infrared Intensities. *Chem. Phys. Lett.* **2010**, *496*, 157−161.
(169) Hirata, S.; Yagi, K.; Ajith Perera, S.; Yamazaki, S.; Hirao, K. Anharmonic Vibrational Frequencies and Vibrationally Averaged Structures and Nuclear Magnetic Resonance Parameters of FHF^-. *J. Chem. Phys.* **2008**, *128*, 214305.
(170) Bain, O.; Giguère, P. A. Hydrogen Peroxide and Its Analogues: VI. Infrared Spectra of H_2O_2, D_2O_2, and HDO_2. *Can. J. Chem.* **1955**, *33*, 527−545.
(171) Hunt, R. H.; Leacock, R. A.; Peters, C. W.; Hecht, K. T. Internal-Rotation in Hydrogen Peroxide: The Far-Infrared Spectrum and the Determination of the Hindering Potential. *J. Chem. Phys.* **1965**, *42*, 1931−1946.
(172) Giguere, P. A.; Srinivasan, T. K. K. A Raman Study of H_2O_2 and D_2O_2 Vapor. *J. Raman Spectrosc.* **1974**, *2*, 125−132.
(173) Shimanouchi, T.; Shimanouchi, T. *Tables of Molecular Vibrational Frequencies*; National Bureau of Standards: Washington, DC, 1980.
(174) Baumgaertel, H.; Jochims, H. W.; Ruehl, E.; Bock, H.; Dammel, R.; Minkwitz, J.; Nass, R. Photoelectron Spectra and Molecular Properties. 112. Photoelectron and Photoionization Mass Spectra of the Fluoroamines $NH_{3-n}F_n$. *Inorg. Chem.* **1989**, *28*, 943−949.
(175) Camy-Peyret, C.; Flaud, J. M.; Johns, J. W. C.; Noel, M. Torsion-Vibration Interaction in H_2O_2: First High-Resolution Observation of N3. *J. Mol. Spectrosc.* **1992**, *155*, 84−104.
(176) Sellers, H.; Pulay, P. The Adiabatic Correction to Molecular Potential Surfaces in the SCF Approximation. *Chem. Phys. Lett.* **1984**, *103*, 463−465.
(177) Handy, N. C.; Yamaguchi, Y.; Schaefer, H. F., III The Diagonal Correction to the Born-Oppenheimer Approximation: Its Effect on the Singlet-Triplet Splitting of CH_2 and Other Molecular Effects. *J. Chem. Phys.* **1986**, *84*, 4481−4484.
(178) Ioannou, A. G.; Amos, R. D.; Handy, N. C. The Diagonal Born-Oppenheimer Correction for He_2^+ and F^+H_2. *Chem. Phys. Lett.* **1996**, *251*, 52−58.
(179) Valeev, E. F.; Sherrill, C. D. The Diagonal Born-Oppenheimer Correction Beyond the Hartree-Fock Approximation. *J. Chem. Phys.* **2003**, *118*, 3921−3927.
(180) Schwenke, D. W. Beyond the Potential Energy Surface: Ab Initio Corrections to the Born−Oppenheimer Approximation for H2o. *J. Phys. Chem. A* **2001**, *105*, 2352−2360.
(181) Gauss, J.; Tajti, A.; Kállay, M.; Stanton, J. F.; Szalay, P. G. Analytic Calculation of the Diagonal Born-Oppenheimer Correction within Configuration-Interaction and Coupled-Cluster Theory. *J. Chem. Phys.* **2006**, *125*, 144111.

https://dx.doi.org/10.1021/acs.chemrev.9b00798
Chem. Rev. XXXX, XXX, XXX−XXX

(182) Tajti, A.; Szalay, P. G.; Gauss, J. Perturbative Treatment of the Electron-Correlation Contribution to the Diagonal Born-Oppenheimer Correction. *J. Chem. Phys.* **2007**, *127*, 014102.
(183) Liévin, J.; Demaison, J.; Herman, M.; Fayt, A.; Puzzarini, C. Comparison of the Experimental, Semi-Experimental and Ab Initio Equilibrium Structures of Acetylene: Influence of Relativisitic Effects and of the Diagonal Born−Oppenheimer Corrections. *J. Chem. Phys.* **2011**, *134*, 064119.
(184) Crawford, T. D.; Schaefer, H. F. An Introduction to Coupled Cluster Theory for Computational Chemists. *Rev. Comp. Chem.* **2007**, *14*, 33−136.
(185) Bartlett, R. J.; Musiał, M. Coupled-Cluster Theory in Quantum Chemistry. *Rev. Mod. Phys.* **2007**, *79*, 291.
(186) Shavitt, I.; Bartlett, R. J. *Many-Body Methods in Chemistry and Physics: MBPT and Coupled-Cluster Theory*; Cambridge University Press: 2009.
(187) Kutzelnigg, W.; Mukherjee, D. Normal Order and Extended Wick Theorem for a Multiconfiguration Reference Wave Function. *J. Chem. Phys.* **1997**, *107*, 432−449.
(188) Kong, L.; Nooijen, M.; Mukherjee, D. An Algebraic Proof of Generalized Wick Theorem. *J. Chem. Phys.* **2010**, *132*, 234107.
(189) Koch, H.; Jensen, H. J. A.; Jørgensen, P.; Helgaker, T.; Scuseria, G. E.; Schaefer, H. F., III Coupled Cluster Energy Derivatives. Analytic Hessian for the Closed-Shell Coupled Cluster Singles and Doubles Wave Function: Theory and Applications. *J. Chem. Phys.* **1990**, *92*, 4924−4940.
(190) Helgaker, T.; Jørgensen, P.; Olsen, J. *Molecular Electronic-Structure Theory*; John Wiley & Sons: 2014.
(191) Adamowicz, L.; Laidig, W. D.; Bartlett, R. J. Analytical Gradients for the Coupled-Cluster Method. *Int. J. Quantum Chem.* **1984**, *26*, 245−254.
(192) Salter, E. A.; Trucks, G. W.; Bartlett, R. J. Analytic Energy Derivatives in Many-Body Methods. I. First Derivatives. *J. Chem. Phys.* **1989**, *90*, 1752−1766.
(193) Nesbet, R. K. Brueckner's Theory and the Method of Superposition of Configurations. *Phys. Rev.* **1958**, *109*, 1632.
(194) Chiles, R. A.; Dykstra, C. E. An Electron Pair Operator Approach to Coupled Cluster Wave Functions. Application to He_2, Be_2, and Mg_2 and Comparison with CEPA Methods. *J. Chem. Phys.* **1981**, *74*, 4544−4556.
(195) Handy, N. C.; Pople, J. A.; Head-Gordon, M.; Raghavachari, K.; Trucks, G. W. Size-Consistent Brueckner Theory Limited to Double Substitutions. *Chem. Phys. Lett.* **1989**, *164*, 185−192.
(196) Stanton, J. F.; Gauss, J.; Bartlett, R. J. On the Choice of Orbitals for Symmetry Breaking Problems with Application to NO_3. *J. Chem. Phys.* **1992**, *97*, 5554−5559.
(197) Hampel, C.; Peterson, K. A.; Werner, H.-J. A Comparison of the Efficiency and Accuracy of the Quadratic Configuration Interaction (QCISD), Coupled Cluster (CCSD), and Brueckner Coupled Cluster (BCCD) Methods. *Chem. Phys. Lett.* **1992**, *190*, 1−12.
(198) Tew, D. P. Explicitly Correlated Coupled-Cluster Theory with Brueckner Orbitals. *J. Chem. Phys.* **2016**, *145*, 074103.
(199) Purvis, G. D., III; Bartlett, R. J. A Full Coupled-Cluster Singles and Doubles Model: The Inclusion of Disconnected Triples. *J. Chem. Phys.* **1982**, *76*, 1910−1918.
(200) Scuseria, G. E.; Schaefer, H. F., III The Optimization of Molecular Orbitals for Coupled Cluster Wavefunctions. *Chem. Phys. Lett.* **1987**, *142*, 354−358.
(201) Sherrill, C. D.; Krylov, A. I.; Byrd, E. F. C.; Head-Gordon, M. Energies and Analytic Gradients for a Coupled-Cluster Doubles Model Using Variational Brueckner Orbitals: Application to Symmetry Breaking in O_4^+. *J. Chem. Phys.* **1998**, *109*, 4171−4181.
(202) Bozkaya, U.; Turney, J. M.; Yamaguchi, Y.; Schaefer, H. F., III; Sherrill, C. D. Quadratically Convergent Algorithm for Orbital Optimization in the Orbital-Optimized Coupled-Cluster Doubles Method and in Orbital-Optimized Second-Order Møller-Plesset Perturbation Theory. *J. Chem. Phys.* **2011**, *135*, 104103.
(203) Grimme, S. Improved Second-Order Møller−Plesset Perturbation Theory by Separate Scaling of Parallel-and Antiparallel-Spin Pair Correlation Energies. *J. Chem. Phys.* **2003**, *118*, 9095−9102.
(204) Neese, F.; Schwabe, T.; Kossmann, S.; Schirmer, B.; Grimme, S. Assessment of Orbital-Optimized, Spin-Component Scaled Second-Order Many-Body Perturbation Theory for Thermochemistry and Kinetics. *J. Chem. Theory Comput.* **2009**, *5*, 3060−3073.
(205) Jung, Y.; Lochan, R. C.; Dutoi, A. D.; Head-Gordon, M. Scaled Opposite-Spin Second Order Møller−Plesset Correlation Energy: An Economical Electronic Structure Method. *J. Chem. Phys.* **2004**, *121*, 9793−9802.
(206) Lochan, R. C.; Head-Gordon, M. Orbital-Optimized Opposite-Spin Scaled Second-Order Correlation: An Economical Method to Improve the Description of Open-Shell Molecules. *J. Chem. Phys.* **2007**, *126*, 164101.
(207) Dunlap, B. I.; Connolly, J. W. D.; Sabin, J. R. On First-Row Diatomic Molecules and Local Density Models. *J. Chem. Phys.* **1979**, *71*, 4993−4999.
(208) Almlöf, J. Elimination of Energy Denominators in Møller—Plesset Perturbation Theory by a Laplace Transform Approach. *Chem. Phys. Lett.* **1991**, *181*, 319−320.
(209) Thouless, D. J. Stability Conditions and Nuclear Rotations in the Hartree-Fock Theory. *Nucl. Phys.* **1960**, *21*, 225−232.
(210) Brorsen, K. Quantifying Multireference Character in Multicomponent Systems with Heat-Bath Configuration Interaction. *J. Chem. Theory Comput.* **2020**, DOI: 10.1021/acs.jctc.9b01273.
(211) Johnson, B. G.; Gonzales, C. A.; Gill, P. M. W.; Pople, J. A. A Density Functional Study of the Simplest Hydrogen Abstraction Reaction. Effect of Self-Interaction Correction. *Chem. Phys. Lett.* **1994**, *221*, 100−108.
(212) Kristyán, S.; Pulay, P. Can (Semi) Local Density Functional Theory Account for the London Dispersion Forces? *Chem. Phys. Lett.* **1994**, *229*, 175−180.
(213) Stanton, J. F.; Bartlett, R. J. The Equation of Motion Coupled-Cluster Method. A Systematic Biorthogonal Approach to Molecular Excitation Energies, Transition Probabilities, and Excited State Properties. *J. Chem. Phys.* **1993**, *98*, 7029−7039.
(214) Comeau, D. C.; Bartlett, R. J. The Equation-of-Motion Coupled-Cluster Method. Applications to Open-and Closed-Shell Reference States. *Chem. Phys. Lett.* **1993**, *207*, 414−423.
(215) Levchenko, S. V.; Krylov, A. I. Equation-of-Motion Spin-Flip Coupled-Cluster Model with Single and Double Substitutions: Theory and Application to Cyclobutadiene. *J. Chem. Phys.* **2004**, *120*, 175−185.
(216) Krylov, A. I. Spin-Flip Configuration Interaction: An Electronic Structure Model That Is Both Variational and Size-Consistent. *Chem. Phys. Lett.* **2001**, *350*, 522−530.
(217) Matthews, D. A.; Stanton, J. F. A New Approach to Approximate Equation-of-Motion Coupled Cluster with Triple Excitations. *J. Chem. Phys.* **2016**, *145*, 124102.
(218) Koch, H.; Jensen, H. J. A.; Jørgensen, P.; Helgaker, T. Excitation Energies from the Coupled Cluster Singles and Doubles Linear Response Function (CCSDLR). Applications to Be, CH^+, CO, and H_2O. *J. Chem. Phys.* **1990**, *93*, 3345−3350.
(219) Watson, M. A.; Chan, G. K.-L. Excited States of Butadiene to Chemical Accuracy: Reconciling Theory and Experiment. *J. Chem. Theory Comput.* **2012**, *8*, 4013−4018.
(220) Loos, P.-F.; Boggio-Pasqua, M.; Scemama, A.; Caffarel, M.; Jacquemin, D. Reference Energies for Double Excitations. *J. Chem. Theory Comput.* **2019**, *15*, 1939−1956.
(221) Ziegler, T.; Rauk, A.; Baerends, E. J. On the Calculation of Multiplet Energies by the Hartree-Fock-Slater Method. *Theor. Chim. Acta* **1977**, *43*, 261−271.
(222) Gilbert, A. T.; Besley, N. A.; Gill, P. M. Self-Consistent Field Calculations of Excited States Using the Maximum Overlap Method (MOM). *J. Phys. Chem. A* **2008**, *112*, 13164−13171.

https://dx.doi.org/10.1021/acs.chemrev.9b00798
Chem. Rev. XXXX, XXX, XXX−XXX

(223) Kowalczyk, T.; Yost, S. R.; Van Voorhis, T. Assessment of the ΔSCF Density Functional Theory Approach for Electronic Excitations in Organic Dyes. *J. Chem. Phys.* **2011**, *134*, 054128.
(224) Yost, S. R.; Kowalczyk, T.; Van Voorhis, T. A Multireference Perturbation Method Using Non-Orthogonal Hartree-Fock Determinants for Ground and Excited States. *J. Chem. Phys.* **2013**, *139*, 174104.
(225) Barca, G. M.; Gilbert, A. T.; Gill, P. M. Simple Models for Difficult Electronic Excitations. *J. Chem. Theory Comput.* **2018**, *14*, 1501−1509.
(226) Ramos, P.; Pavanello, M. Low-Lying Excited States by Constrained DFT. *J. Chem. Phys.* **2018**, *148*, 144103.
(227) Shao, Y.; Head-Gordon, M.; Krylov, A. I. The Spin-Flip Approach within Time-Dependent Density Functional Theory: Theory and Applications to Diradicals. *J. Chem. Phys.* **2003**, *118*, 4807−4818.
(228) Peach, M. J.; Williamson, M. J.; Tozer, D. J. Influence of Triplet Instabilities in TDDFT. *J. Chem. Theory Comput.* **2011**, *7*, 3578−3585.
(229) Hanson-Heine, M. W.; George, M. W.; Besley, N. A. Calculating Excited State Properties Using Kohn-Sham Density Functional Theory. *J. Chem. Phys.* **2013**, *138*, 064101.
(230) Pak, M. V.; Hammes-Schiffer, S. Electron-Proton Correlation for Hydrogen Tunneling Systems. *Phys. Rev. Lett.* **2004**, *92*, 103002.
(231) Wu, Q.; Van Voorhis, T. Extracting Electron Transfer Coupling Elements from Constrained Density Functional Theory. *J. Chem. Phys.* **2006**, *125*, 164105.
(232) Kaduk, B.; Kowalczyk, T.; Van Voorhis, T. Constrained Density Functional Theory. *Chem. Rev.* **2012**, *112*, 321−370.
(233) Gao, J.; Grofe, A.; Ren, H.; Bao, P. Beyond Kohn−Sham Approximation: Hybrid Multistate Wave Function and Density Functional Theory. *J. Phys. Chem. Lett.* **2016**, *7*, 5143−5149.
(234) Guo, X.; Qu, Z.; Gao, J. The Charger Transfer Electronic Coupling in Diabatic Perspective: A Multi-State Density Functional Theory Study. *Chem. Phys. Lett.* **2018**, *691*, 91−97.
(235) Hammer, T.; Coutinho-Neto, M. D.; Viel, A.; Manthe, U. Multiconfigurational Time-Dependent Hartree Calculations for Tunneling Splittings of Vibrational States: Theoretical Considerations and Application to Malonaldehyde. *J. Chem. Phys.* **2009**, *131*, 224109.
(236) Schröder, M.; Gatti, F.; Meyer, H.-D. Theoretical Studies of the Tunneling Splitting of Malonaldehyde Using the Multiconfiguration Time-Dependent Hartree Approach. *J. Chem. Phys.* **2011**, *134*, 234307.
(237) Coutinho-Neto, M. D.; Viel, A.; Manthe, U. The Ground State Tunneling Splitting of Malonaldehyde: Accurate Full Dimensional Quantum Dynamics Calculations. *J. Chem. Phys.* **2004**, *121*, 9207−9210.
(238) Viel, A.; Coutinho-Neto, M. D.; Manthe, U. The Ground State Tunneling Splitting and the Zero Point Energy of Malonaldehyde. *J. Chem. Phys.* **2007**, *126*, 024308.
(239) Wang, Y.; Braams, B. J.; Bowman, J. M.; Carter, S.; Tew, D. P. Full-Dimensional Quantum Calculations of Ground-State Tunneling Splitting of Malonaldehyde Using an Accurate Ab Initio Potential Energy Surface. *J. Chem. Phys.* **2008**, *128*, 224314.
(240) Lee, T. J.; Taylor, P. R. A Diagnostic for Determining the Quality of Single-Reference Electron Correlation Methods. *Int. J. Quantum Chem.* **1989**, *36*, 199−207.
(241) Szalay, P. G.; Muller, T.; Gidofalvi, G.; Lischka, H.; Shepard, R. Multiconfiguration Self-Consistent Field and Multireference Configuration Interaction Methods and Applications. *Chem. Rev.* **2012**, *112*, 108−181.
(242) Andersson, K.; Malmqvist, P.-A.; Roos, B. O.; Sadlej, A. J.; Wolinski, K. Second-Order Perturbation Theory with a CASSCF Reference Function. *J. Phys. Chem.* **1990**, *94*, 5483.
(243) Andersson, K.; Malmqvist, P.-A.; Roos, B. O. Second-Order Perturbation Theory with a Complete Active Space Self-Consistent Field Reference Function. *J. Chem. Phys.* **1992**, *96*, 1218.
(244) Liu, X.; Fatehi, S.; Shao, Y.; Veldkamp, B. S.; Subotnik, J. E. Communication: Adjusting Charge Transfer State Energies for Configuration Interaction Singles: Without Any Parameterization and with Minimal Cost. *J. Chem. Phys.* **2012**, *136*, 161101.
(245) Gordon, M. S.; Schmidt, M. W., Advances in Electronic Structure Theory: Gamess a Decade Later. In *Theory and Applications of Computational Chemistry: The First Forty Years*; Dykstra, C. E., Frenking, G., Kim, K. S., Scuseria, G. E., Eds.; Elsevier: Amsterdam, 2005.
(246) Shao, Y.; Gan, Z.; Epifanovsky, E.; Gilbert, A. T. B.; Wormit, M.; Kussmann, J.; Lange, A. W.; Behn, A.; Deng, J.; Feng, X.; al, e.; et al. Advances in Molecular Quantum Chemistry Contained in the Q-Chem 4 Program Package. *Mol. Phys.* **2015**, *113*, 184−215.
(247) Koster, A. M.; G, G.; Alvarez-Ibarra, A.; Calaminici, P.; Casida, M. E.; Carmona-Espindola, J.; Dominguez, V. D.; Flores-Moreno, R.; Gamboa, G. U.; Goursot, A.; Heine, T.; Ipatov, A.; de la Lande, A.; Janetzko, F.; del Campo, J. M.; Mejia-Rodriguez, D.; Reveles, J. U.; Vasquez-Perez, J.; Vela, A.; Zuniga-Gutierrez, B.; Salahub, D. R. *DeMon2k*, Version 6; 2018.
(248) Mejía-Rodríguez, D.; de la Lande, A. Multicomponent Density Functional Theory with Density Fitting. *J. Chem. Phys.* **2019**, *150*, 174115.
(249) Abedi, A.; Maitra, N. T.; Gross, E. K. Exact Factorization of the Time-Dependent Electron-Nuclear Wave Function. *Phys. Rev. Lett.* **2010**, *105*, 123002.
(250) Abedi, A.; Maitra, N. T.; Gross, E. Correlated Electron-Nuclear Dynamics: Exact Factorization of the Molecular Wavefunction. *J. Chem. Phys.* **2012**, *137*, 22A530.
(251) Khosravi, E.; Abedi, A.; Rubio, A.; Maitra, N. T. Electronic Non-Adiabatic Dynamics in Enhanced Ionization of Isotopologues of Hydrogen Molecular Ions from the Exact Factorization Perspective. *Phys. Chem. Chem. Phys.* **2017**, *19*, 8269−8281.
(252) Min, S. K.; Agostini, F.; Tavernelli, I.; Gross, E. K. Ab Initio Nonadiabatic Dynamics with Coupled Trajectories: A Rigorous Approach to Quantum (De)Coherence. *J. Phys. Chem. Lett.* **2017**, *8*, 3048−3055.
(253) Richings, G. W.; Habershon, S. MCTDH on-the-Fly: Efficient Grid-Based Quantum Dynamics without Pre-Computed Potential Energy Surfaces. *J. Chem. Phys.* **2018**, *148*, 134116.
(254) Richings, G. W.; Robertson, C.; Habershon, S. Improved on-the-Fly MCTDH Simulations with Many-Body-Potential Tensor Decomposition and Projection Diabatization. *J. Chem. Theory Comput.* **2019**, *15*, 857−870.
(255) Tully, J. Mixed Quantum−Classical Dynamics. *Faraday Discuss.* **1998**, *110*, 407−419.
(256) Sun, X.; Miller, W. H. Semiclassical Initial Value Representation for Electronically Nonadiabatic Molecular Dynamics. *J. Chem. Phys.* **1997**, *106*, 6346−6353.
(257) Miller, W. H. The Semiclassical Initial Value Representation: A Potentially Practical Way for Adding Quantum Effects to Classical Molecular Dynamics Simulations. *J. Phys. Chem. A* **2001**, *105*, 2942−2955.
(258) Miller, W. H. Electronically Nonadiabatic Dynamics Via Semiclassical Initial Value Methods. *J. Phys. Chem. A* **2009**, *113*, 1405−1415.
(259) Tully, J. C. Molecular Dynamics with Electronic Transitions. *J. Chem. Phys.* **1990**, *93*, 1061−1071.
(260) Ben-Nun, M.; Martínez, T. J. Nonadiabatic Molecular Dynamics: Validation of the Multiple Spawning Method for a Multidimensional Problem. *J. Chem. Phys.* **1998**, *108*, 7244−7257.
(261) Ben-Nun, M.; Martinez, T. J. A Multiple Spawning Approach to Tunneling Dynamics. *J. Chem. Phys.* **2000**, *112*, 6113−6121.
(262) Ben-Nun, M.; Quenneville, J.; Martínez, T. J. Ab Initio Multiple Spawning: Photochemistry from First Principles Quantum Molecular Dynamics. *J. Phys. Chem. A* **2000**, *104*, 5161−5175.
(263) Tao, H.; Levine, B. G.; Martínez, T. J. Ab Initio Multiple Spawning Dynamics Using Multi-State Second-Order Perturbation Theory. *J. Phys. Chem. A* **2009**, *113*, 13656−13662.
(264) Mignolet, B.; Curchod, B. F. E. A Walk through the Approximations of Ab Initio Multiple Spawning. *J. Chem. Phys.* **2018**, *148*, 134110.

https://dx.doi.org/10.1021/acs.chemrev.9b00798
Chem. Rev. XXXX, XXX, XXX−XXX

(265) Auer, B.; Pak, M. V.; Hammes-Schiffer, S. Nuclear-Electronic Orbital Method within the Fragment Molecular Orbital Approach. *J. Phys. Chem. C* **2010**, *114*, 5582−5588.
(266) Cossi, M.; Rega, N.; Scalmani, G.; Barone, V. Energies, Structures, and Electronic Properties of Molecules in Solution with the C-PCM Solvation Model. *J. Comput. Chem.* **2003**, *24*, 669−681.
(267) Levine, B. G.; Ko, C.; Quenneville, J.; Martínez, T. J. Conical Intersections and Double Excitations in Time-Dependent Density Functional Theory. *Mol. Phys.* **2006**, *104*, 1039−1051.
(268) Goings, J. J.; Kasper, J. M.; Egidi, F.; Sun, S.; Li, X. Real Time Propagation of the Exact Two Component Time-Dependent Density Functional Theory. *J. Chem. Phys.* **2016**, *145*, 104107.
(269) Goings, J. J.; Lestrange, P. J.; Li, X. Real-Time Time-Dependent Electronic Structure Theory. *Wiley Interdiscip. Rev.: Comput. Mol. Sci.* **2018**, *8*, No. e1341.
(270) Zhao, L.; Tao, Z.; Pavošević, F.; Wildman, A.; Hammes-Schiffer, S.; Li, X. Real-Time Time-Dependent Nuclear-Electronic Orbital Approach: Dynamics Beyond the Born-Oppenheimer Approximation. *J. Phys. Chem. Lett.* **2020**, DOI: 10.1021/acs.jpclett.0c00701, in press.
(271) Li, X.; Tully, J. C.; Schlegel, H. B.; Frisch, M. J. Ab Initio Ehrenfest Dynamics. *J. Chem. Phys.* **2005**, *123*, 084106.

https://dx.doi.org/10.1021/acs.chemrev.9b00798
Chem. Rev. XXXX, XXX, XXX−XXX